PREPARATION OF MEDIUM-CHAIN-LENGTH POLY-3-HYDROXYALKANOATES – BASED POLYMERIC NANOPARTICLE THROUGH PHASE INVERSION EMULSIFICATION AND ITS APPARENT FORMATION MECHANISM

KHAIRUL ANWAR BIN ISHAK

THESIS SUBMITTED IN FULFILMENT OF THE
REQUIREMENTS FOR THE DEGREE OF
DOCTOR OF PHILOSOPHY

INSTITUTE OF BIOLOGICAL SCIENCES
FACULTY OF SCIENCE
UNIVERSITY OF MALAYA
KUALA LUMPUR

2017

UNIVERSITI MALAYA

ORIGINAL LITERARY WORK DECLARATION

Name of Candidate: KHAIRUL ANWAR ISHAK

Registration/Matric No: SHC 150003

Name of Degree: DOCTOR OF PHILOSOPHY

Title of Project Paper/Research Report/Dissertation/Thesis ("this Work"):

PREPARATION OF MEDIUM-CHAIN-LENGTH POLY-3-HYDROXYALKANOATES–BASED POLYMERIC NANOPARTICLE THROUGH PHASE INVERSION EMULSIFICATION AND ITS APPARENT FORMATION MECHANISM

Field of Study: BIOTECHNOLOGY

I do solemnly and sincerely declare that:

(1) I am the sole author/writer of this Work;
(2) This Work is original;
(3) Any use of any work in which copyright exists was done by way of fair dealing and for permitted purposes and any excerpt or extract from, or reference to or reproduction of any copyright work has been disclosed expressly and sufficiently and the title of the Work and its authorship have been acknowledged in this Work;
(4) I do not have any actual knowledge nor do I ought reasonably to know that the making of this work constitutes an infringement of any copyright work;
(5) I hereby assign all and every rights in the copyright to this Work to the University of Malaya ("UM"), who henceforth shall be owner of the copyright in this Work and that any reproduction or use in any form or by any means whatsoever is prohibited without the written consent of UM having been first had and obtained;
(6) I am fully aware that if in the course of making this Work I have infringed any copyright whether intentionally or otherwise, I may be subject to legal action or any other action as may be determined by UM.

Candidate's Signature Date:

Subscribed and solemnly declared before,

Witness's Signature Date:

Name:

Designation:

ABSTRACT

Development of biodegradable polymeric nanoparticle for active compounds delivery into human body has gained a widespread interest in nutraceutical and pharmaceutical industries. It is frequently used as active compounds delivery vehicle due to its better encapsulation capability and controlled release, compound bioavailability improvement as well as non-toxic properties. However, common methods for polymeric nanoparticle production involve the application of polymerizing/crosslinking initiator and organic solvent, which are usually toxic and pose removal, disposal and recycling issues in the scaling up of polymeric nanoparticle production. This study demonstrated for the first time, a greener alternative for the production of polymeric nanoparticle by using medium-chain-length poly-3-hydroxyalkanoates (mcl-PHA) as part of component materials through phase inversion emulsification (PIE) method. It is a facile route to obtain polymeric nanoparticles whereby mcl-PHA serves as the integral component in the construction of protective encapsulating matrix in the nanoparticle. Emulsification process of mcl-PHA-incorporated emulsion system involved the formation of bi-continuous or lamellar structure phase at emulsion inversion point (EIP) before dispersion of oil phase into nanometer-sized particles. However, incorporating mcl-PHA into the emulsion system at inappropriate molecular weight and amount would lead to an alternative phase inversion mechanism that involved the formation of multiple emulsions resulting in micrometer-sized particles with wider distribution. Temperature also showed an interaction effect with mcl-PHA molecular weight towards the formation of bi-continuous/lamellar structure phase. Apparent formation mechanism for mcl-PHA-incorporated nanoparticle is proposed based on the experimental findings.

ABSTRAK

Pembangunan nano-partikel berasakan polimer boleh-terurai sebagai sistem penghantaran sebatian aktif ke dalam badan manusia telah menarik minat yang meluas dalam industri nutraseutikal dan farmaseutikal. Ia telah digunakan dengan kerap kerana pengkapsulan yang lebih baik, pelepasan yang terkawal, peningkatan "bioavailability" sebatian serta bersifat tidak toksik. Walau bagaimanapun, kaedah yang sering kali diguna pakai melibatkan penggunaan bahan pempolimeran dan pelarut organik yang toksik. Ini menimbulkan isu-isu pelupusan dan kitar semula dalam penghasilannya terutama sekali pada skala besar. Buat kali pertama, kajian ini menunjukkan kaedah alternatif yang lebih hijau untuk penghasilan nano-partikel berasakan bio-polimer (mcl-PHA) melalui teknik fasa penyosangan emulsi. Mcl-PHA berfungsi sebagai komponen penting untuk pembentukkan matriks pepejal yang mengelilingi nano-partikel tersebut. Proses pengemulsian sistem emulsi yang mengandungi mcl-PHA melibatkan pembentukan fasa struktur "bi-continuous atau lamellar" pada titik penyongsangan emulsi sebelum pemecahan minyak ke partikel bersaiz nanometer bermula. Penggunaan mcl-PHA pada tahap berat molekul dan jumlah yang tidak sesuai akan membawa kepada mekanisma fasa penyongsangan alternatif yang melibatkan pembentukan emulsi pelbagai, akhirnya saiz partikel yang lebih besar terbentuk. Suhu juga menunjukkan kesan interaksi dengan berat molekul PHA dalam mempengaruhi pembentukkan fasa struktur "bi-continuous/lamellar" tersebut. Mekanisma pembentukan sistem nano-partikel yang mengandungi mcl-PHA dicadangkan dalam kajian ini berdasarkan data penemuan yang diperolehi.

ACKNOWLEDGEMENTS

Bismillahirrahmanirrahim,

In the name of the Almighty the Most Gracious and Most Merciful.

Alhamdulillah, I am very grateful to be one of the members in the BET and FSSA group, Faculty of Science. There, I have gained countless knowledge and priceless experience that benefit me in every aspects. I am also grateful to be blessed with fully supportive parents; En. Ishak Omar and Pn. Nor Hamidah Mahmud. The love given throughout the hardships in completing the research are trully priceless.

I would like to thank my supervisor Professor Dr. Mohamad Suffian Mohamad Annuar for the encouragment and guidance in conducting this research throughout my Ph.D study. Not forgotten to Mrs. Azilawati Mohamed, Dr. Malinda Salim, Dr. Idayu Zahid, Dr. Noraini Ahmad and my friends, the members of BET and FSSA group for giving me the supports, mentally and physically, in completing this research. Because of them, I was able to finish my Ph.D study within time as planned from the beginning. Thank you very much for the endless support given.

Last but no least, thanks to University of Malaya for assisting me financially through grant RP031C-15AET, RU015-2015 and UM.C/625/1/HIR/MOHE/05 to conduct the research and Malaysian Ministry of Higher Education for giving me the MyPhD scholarship that includes tuition fee and monthly allowance.

May God bless you all

TABLE OF CONTENTS

LIST OF FIGURES

LIST OF TABLES

LIST OF SYMBOLS AND ABBREVIATIONS

mcl-PHA	:	Medium-chain-length poly-3-hydroxyalkanoates
FESEM	:	Field Emission Scanning Electron Microscopy
FTIR	:	Fourier Transform Infra-Red spectroscopy
SAXS	:	Small Angle X-ray Scattering
OPM	:	Optical Polarizing Microscopy
DSC	:	Differential Scanning Calorimetry
^{1}H-NMR	:	Proton Nuclear Magnetic Resonance
ANOVA	:	Analysis of variance
F	:	*F*-value
P	:	*P*-value
PIE	:	Phase inversion emulsification
EIP	:	Emulsion inversion point
PIC	:	Phase inversion composition
PIT	:	Phase inversion temperature
CPI	:	Catastrophic phase inversion
HLB	:	Hydrophile-lipophile balance
HLD	:	Hydrophile-lipophile deviation
W/O	:	Water-in-oil emulsion system
O/W	:	Oil-in-water emulsion system
W:(S:O)	:	Water-to-organic phase ratio
S:O	:	Surfactant-to-oil ratio
Cremo:Sp 80	:	Cremophor EL-to-Span 80 ratio
M_w	:	Weight-averaged molecular weight
PDI	:	Polydispersity index

T_g	:	Glass transition temperature
T_d	:	Degradation temperature
T_m	:	Melting temperature
nm	:	nanometer
μm	:	micrometer
ml	:	mililitre
μl	:	microlitre
g	:	gram
mM	:	milimolar
rpm	:	round per minute
min	:	minute
(*w/w*)	:	weight per weight
(*w/v*)	:	weight per volume
(*v/v*)	:	volume per volume

LIST OF APPENDICES

CHAPTER 1: GENERAL INTRODUCTION

1.1 Mcl-PHA as the constructing material

Poly-3-hydroxyalkanoates (PHA) is a biopolymer synthesized by micro-organisms (producer) as a reserve material in response to imbalanced growth conditions, where a suitable carbon source is present in excess while other nutrients are limiting e.g. nitrogen, oxygen, phosphorus, *etc*. (Braunegg *et al.*, 1998). It can be divided into three classes, depending on their monomer carbon atom number. Short-chain-length PHA (scl-PHA) contains monomer with four or five carbon atoms, while medium-chain-length PHA (mcl-PHA) contains monomer with carbon atom number ranging from 6 to 18. On the other hand, PHA with monomer carbon atom number more than 18 is catagorized as long-chain-length PHA (lcl-PHA). In the family of PHA, mcl-PHA attracts wide attention due to its biodegradability alongside thermal and mechanical properties that are similar to petroleum-based plastics, such as polypropylene (Budde *et al.*, 2011; Sudesh *et al.*, 2000).

A number of bacteria are reported to accumulate mcl-PHA. Among them are the fluorescent pseudomonads, belonging to *r*RNA homology group 1. The first discovery of mcl-PHA was in 1983 with *Pseudomonas oleovorans* grown in *n*-octane as carbon source (De Smet *et al.*, 1983). Other species such as *Pseudomonas putida* and *Pseudomonas aeruginosa* are also well known for their mcl-PHA production (Ballistreri *et al.*, 2001; Eggink *et al.*, 1992; Lageveen *et al.*, 1988). The ability to utilize various carbon substrates, especially renewable carbon sources, for producing mcl-PHA is a major advantage for the *Pseudomonas* species. For instance, mcl-PHA can be produced from various renewable resources, such as palm kernel oil (Tan *et al.*, 1997), soy molases (Solaiman *et al.*, 2006), fatty acids (Razaif *et al.*, 2016) and etc. The chemical structure of the carbon substrate fed to the bacteria determines the monomeric

composition of mcl-PHA (Lageveen *et al.*, 1988). It is reported that more than 150 units of mcl-PHA monomer types have been produced through *Pseudomonas* strains cultivations in many different carbon sources (Kim *et al.*, 2007).

In this study, a simple fermentation was conducted to obtain mcl-PHA with high 3-hydroxyoctanoate monomer content by cultivating *P. putida* BET001 (Figure 1.1*a*) with octanoic acid as carbon source (Ishak *et al*., 2016). This bacterium was isolated from palm oil mill effluent (Gumel *et al.,* 2012) and able to produce an elastomeric mcl-PHA with glass transition, melting and decomposition temperatures at about -37 °C, 52 °C and 250 °C, respectively (Figure 1.1*b*). With general chemical structure as shown in Figure 1.1*c*, the monomer composition consisted of 90 mole % 3-hydroxyoctanote, 5 mole % 3-hydroxyhexanoate and 5 mole % 3-hydroxydecanoate. Its weight-average molecular weight (M_w) was determined at 77,435 g mol^{-1} (polystyrene standard equivalent).

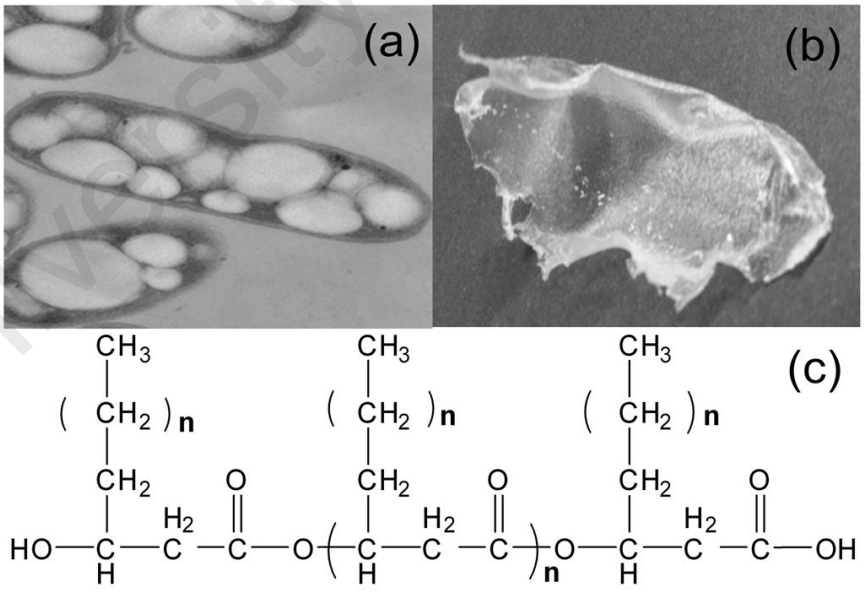

Figure 1.1: (*a*) Micrograph of PHA granules accumulated in *P. putida* (BET001) (*b*) Film of extracted mcl-PHA (*c*) General molecular structure of PHA

Mcl-PHA has gained much attention in various fields especially in medical-related applications. For instance, poly-3-hydroxyoctanoate and poly-3-hydroxyhexanoate (including their copolymers) have been intensively studied for applications such as surgical sutures, matrices for drug delivery and scaffold for tissue engineering (Philip *et al.*, 2007; Wang *et al.*, 2003; Xue *et al.*, 2003). However, the application of mcl-PHA in the development of polymeric nanoparticle-based delivery system has never been explored. Nanoparticle-based delivery system is one type of nanotechnology products that is useful in encapsulation of active compounds for targeted delivery applications within human body. Numerous types of nanoparticle-based delivery systems that have been developed for encapsulation and oral delivery are discussed in Chapter 2 – Literature Review.

1.2 Research outline and scope

In order to incorporate macromolecule like mcl-PHA into a nanoparticle, an efficient strategy is needed. There are several methods that can be used to produce polymeric nanoparticles such as nano-precipitation, solvent evaporation, coarcervation *etc*. However, all of them involve the use of organic solvent and/or chemical additives, which accrues toxicity concern. In addition, they require subsequent steps i.e. purification and solvent removal in order to obtain the polymeric nanoparticle (Vauthier & Bouchemal, 2009), which pose disposal and recycling issues in the scaling up of nanoparticle production. Therefore, a simple and greener approach has to be developed. It is hypothesized that mcl-PHA-based nanoparticle could be produced by using similar technique for producing solid lipid nanoparticle (a type of nanoparticle-based delivery system), whereby the solid lipid is melted at elevated temperature prior to emulsification (MuÈller *et al.*, 2000). The temperature-elevated emulsification technique provides a rational platform for incorporating the low melting temperature

mcl-PHA in a similar manner. It fulfills the simple and greener approach as organic solvents and downstream steps are absent in its preparation process compared to other polymeric nanoparticle production methods.

In this study, emulsification at elevated temperature to incorporate mcl-PHA into nanoparticle-based system has been implemented and the results are discussed in Chapter 3. The investigation detailed an oil droplet system made up of Span 80, Cremophor EL and jojoba oil that provide a template to build the mcl-PHA-based nanoparticle system. The ratio of jojoba oil, Span 80 and Cremophor EL mixture was first optimized using response surface methodology (RSM) to obtain nano-scale oil-in-water (O/W) emulsion before incorporating the mcl-PHA into the system. Similar to the re-crystallization of solid lipid within nanoparticle during cooling, melted mcl-PHA is hypothesized to form a solid-like polymeric network at low temperature thus imbuing the nanoparticle with a relatively rigid structure. The hypothesis is discussed further in subsequent chapters.

The low-energy emulsification technique that inverts the two phases i.e. from water-in-oil (W/O) emulsion to oil-in-water (O/W) emulsion used in this study is classified as phase inversion emulsification (PIE). It can be sub-categorized as catastrophic and transitional phase inversion (Salager *et al.,* 1983; Kumar *et al.,* 2015). In order to elucidate the type of phase inversion mechanism followed during the mcl-PHA-incorporated nanoparticle formation, a series of analyses using Fourier transform infrared (FTIR), small angle X-ray scattering (SAXS) and optical polarizing microscopy (OPM) were conducted. From interpretation of the data obtained, the mechanism of mcl-PHA-incorporated nanoparticle formation through PIE is proposed in Chapter 4. The pathway leading to the formation of mcl-PHA solid-like polymeric network within the nanoparticle as hypothesized previously is illustrated and discussed.

It is confirmed that more mcl-PHA can be incorporated into the nanoparticle when its molecular weight is reduced. However, there exists a limit in mcl-PHA amount for each different molecular weight that is favorable for the production of nano-scale particles. The application of inappropriate molecular weight and/or amount of mcl-PHA in the formulation will result in opaque solution due to micrometer-sized polymeric particle produced. The reason behind the observation is discussed in Chapter 5. In this chapter, the specific mechanism of phase inversion that plays crucial role in determining the final particle size and how mcl-PHA molecular weight and amount affect the mechanism is discussed. The effect of temperature during emulsification process was investigated and the results are discussed in Chapter 6. OPM images were used to study the *in-situ* formation of lamellar/bi-continuous phase in mcl-PHA-incorporated emulsion system at different temperatures.

1.3 Thesis composition and research objectives

In summary, all chapters are sequentially arranged to deliver a cohesive narrative of the thesis (Figure 1.2). They have been given specific title for publication purpose. Chapter 3 – 6 have their own aspect of study and objective as stated below, respectively:

1) To optimize the water, oil and surfactant ratio for production of mcl-PHA-incorporated nanoparticle *via* nanoemulsion templating;
2) To study the formation mechanism of mcl-PHA-incorporated nanoparticle through PIE;
3) To study the effects of mcl-PHA molecular weight and amount on the inversion mechanism of PIE;
4) To study the effects of emulsification temperature on the inversion mechanism of PIE.

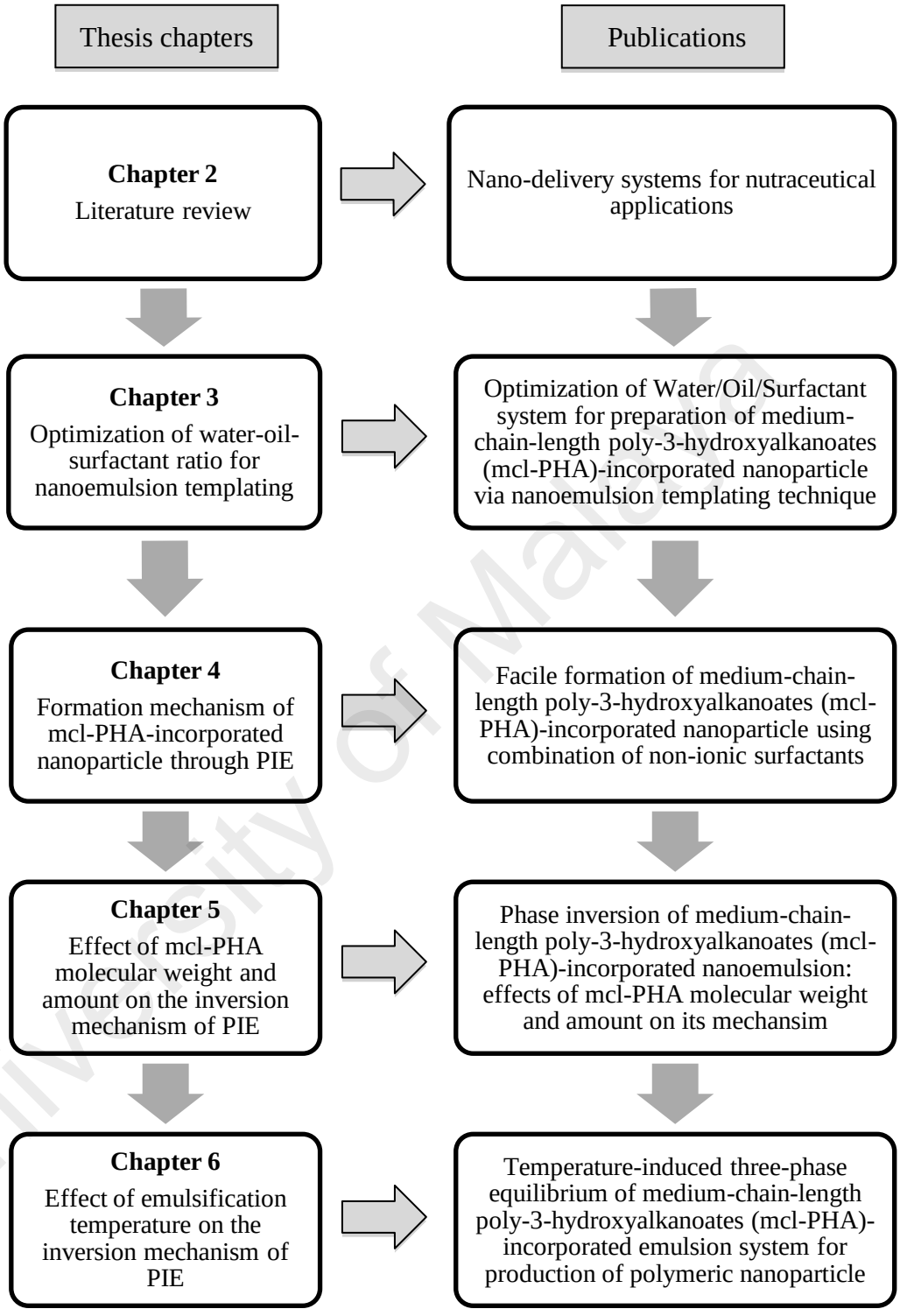

Figure 1.2: Flow chart of thematic thesis composition

CHAPTER 2: LITERATURE REVIEW

2.1 Nanotechnology in nutraceutical and pharmaceutical industry

Nanoscience is the study of nanoscale materials that exhibit remarkable properties, functionality and phenomena as the consequence of a very small dimension. Nanotechnology is the application of nanoscience with industrial and commercial objectives, that focuses on the fabrication, characterization and manipulation of organic and non-organic structures to form new materials, components and systems at the nanoscale level (usually smaller than 100 nm) (Poole Jr & Owens, 2003). Its benefits have been recognized by many industries and thus commercial products are already being manufactured. For instance, nanotechnology has been revolutionizing the food industry from production to processing lines, which includes storage and development of innovative products that offer a lot of benefits to the consumers as summarized in Table 2.1.

One of the nanotechnology applications in nutraceutical and pharmaceutical industry is the development of a nanoparticle-based delivery system that focuses on encapsulation of food bioactive components and drugs. For instances, compounds like metamizole, aspirin and acetaminophen have been commonly used to treat pain and fever (Oncel *et al.*, 2012; Devereaux *et al.*, 2014; Jasiecka *et al.*, 2014). Food bioactive like antioxidants, probiotic, polyunsaturated fatty acids and proteins are claimed to possess attributes such as anti-aging, anti-cancer, anti-diabetic and other diseases alongside health maintenance effects (Johnson & de Mejia, 2011; Kris-Etherton *et al*., 2002a,b). Encapsulating these compounds help to slow down or prevent the degradation processes until their delivery to the target sites where their functions are desired.

Table 2.1: Nanotechnology applications in the food industries

Applications and Benefits	Remarks	References
Nanodelivery system Improved bioavailability of nutrients and supplements and other health benefits without changing the taste and texture of food products.	Compounds are usually encapsulated in the form of liposome or nanoparticles.	(Salminen *et al*., 2013) (Qian *et al*., 2012a, 2012b) (Li *et al*., 2012) (Liang *et al*., 2013)
Nanotextured food products Offer healthier alternative and yet still tasteful products to the consumer.	Typical examples of food products are mayonnaise and ice cream that is low fat but as smooth as the original version. Surfactant is the key to successful production of these nanotextured foods (stable emulsion).	(Chandrapala *et al*., 2012) (Nitschke & Costa, 2007) (Neethirajan & Jayas, 2011)
Nanocoating Provide barrier or antimicrobial properties in food processing facilities. Development of edible nanocoating for food product helps to increase the shelf life of manufactured food even after opening of packaging.	Examples include nanosilica coating for self-cleaning surface and zinc oxide nanocoating for photocatalytic sterilization.	(Neethirajan & Jayas, 2011) (Currie *et al*., 2004) (Falguera *et al*., 2011)
Nanosized food additives Tastes and flavours enhancement due to greater surface areas compared to bulk forms. Improved solubility of hydrophobic additives in food product without the addition of fat or emulsifier.	The attribute of nanosized additives may range from colourings, preservatives, flavourings, anti-microbial properties and as additional supplements.	(Canham, 2007)

Table 2.1**,** continued.

Food packaging Plastic packaging with good flexibility, gas barrier properties and moisture stability. Anti-microbiotic plastic packaging to maintain the freshness of food product for a relatively long time.	Plastic polymer containing nanoclay as gas barrier and nanotitanium nitride for improving mechanical strength. The use of metal oxides in the plastic packaging is claimed to exhibit additional antimicrobial properties.	(Sothornvit *et al*., 2009) (Busolo *et al*., 2010) (BakoŠ, 2008)
Nanofiltration Removal of some undesired components in water.	Regenerated cellulose and has been used for aqueous-based filtration and clarification through reverse osmosis.	(Su *et al*., 2010)

Many encapsulation techniques have been reported but none of them can be considered as a universally ideal technique for a wide range of food bioactive and drugs. This is due to the fact that each compound exhibits different physico-chemical characteristics *viz*. molecular weight, polarity, solubility, etc. that originated from its molecular structure (Augustin & Hemar, 2009). This implies that different encapsulation techniques have to be engineered to accommodate specific physico-chemical requirements for a specific bioactive and drugs. However, the major requirement is that an encapsulation system has to be able to shield them from unwanted degradation e.g. hydrolysis and oxidation while at the same time functions to ensure their availability and functionality are at the best conditions as required (de Vos *et al*., 2010). Besides, it is necessary for the system to be able to transmit and release (i.e. delivery) the compound(s) to the intended target site(s) in the body (e.g. cells, tissues or organ) especially in a specific site of gastrointestinal tract (McClements *et al*., 2009). In addition, the encapsulation system should allow efficient package loads, which depend on the type of bioactive and drug compounds and should be easily incorporated into the supplements or medicinal products.

Nanoparticle-based encapsulation and/or delivery systems can be classified into two distinct classes namely liquid and solid (Borel & Sabliov, 2014). Between these two, solid nanoparticle delivery system has a better potential to be the delivery system for unstable bioactive and drugs. They exhibit several crucial traits including enhancement of chemical and physical stabilities of the incorporated compounds by protecting them from oxidants or other undesired agents. For instance, a solid matrix can protect sensitive the encapsulated compounds against chemical degradation by preventing their diffusion to the outer surface of nanoparticle (Helgason *et al*., 2009a; Salminen *et al*., 2013). Consequently, pre-mature exposure of the compounds at the

outer surface of nanoparticle where they could come into contact with oxidants is prevented.

Several literatures reviewed the application of nanotechnology in encapsulation and delivery technologies of food bioactive and drugs e.g. in common lipid-based nanoparticle delivery system such as nanoemulsion, solid lipid nanoparticle and liposome has been extensively studied and discussed (McClements & Rao, 2011; Qian & McClements, 2011; Sagalowicz & Leser, 2010; da Silva Malheiros *et al*., 2010). However, literature on compounds encapsulation within other types of nanoparticle-based delivery system is rather limited. Therefore, in this chapter, different types of nanoparticle-based delivery systems that have been engineered for encapsulation purposes will be discussed. With increasing interest in using nanoparticles for oral food-grade delivery of bioactive and drugs, the overview is concluded by addressing concisely on the ability of nanoparticle-based delivery systems in maintaining bioavailability of encapsulated compound upon ingestion.

2.2 Strategy for enhancing oral bioavailability of active compounds

Synthesis, isolation, characterization and identification of bioactive components and drugs (active compounds) from natural food sources and industrial manufacturing with high health benefits have been intensively conducted for the last few years (Simirgiotis *et al*., 2013; Udenigwe & Aluko, 2012; Fitzgerald *et al*., 2012; Sasidharan *et al*., 2011; Brusotti *et al*., 2014; Ahuja & Scypinski, 2010). However, the challenge does not lie in merely identifying their nutritional/therapeutic functions and incorporating them into commercial food products, but also the necessity to deliver them into consumer body at high oral bioavailability. This section highlights several strategies that could help to improve oral bioavailability of active compounds using food matrix design approaches.

2.2.1 Determination of active components category

Classifying active compounds according to the major factors limiting their oral bioavailability would facilitate the development of food matrices specifically designed to help increase their efficiency in promoting good health for consumer. Recently, a more comprehensive classification scheme has been proposed to characterize the major factors inhibiting the oral bioavailability of compounds.

The scheme is called Nutraceutical Bioavailability Classification Scheme (NuBACS) and categorizes nutraceuticals into three major classes: Bioaccesibility (*B**), Absorption (*A**) and Transformation (*T**) (Table 2.2 - McClements *et al*., 2015). Each major category is symbolized with '(+)' if it is non-limiting and '(–)' if it is limiting. For category with limiting designation, the sub-categories responsible for the poor bioavailability will be listed as subscript. For instances, a compound whose bioavailability is limited by low solubility in intestinal fluids and absorption due to inhibition of epithelial cell mucus layer would be classified as "$B^*(-)_S\ A^*(-)_{ML}\ T^*(+)$".

Categorizing compounds into different groups according to this classification scheme could prove useful in rapid identification of appropriate delivery strategy. For instance, encapsulating highly lipophilic compounds into lipid-based nanoparticle delivery systems that can be transformed into mixed micelles with a high solubilizing capacity during gastrointestinal tract digestion may be useful for compounds with a $B^*(-)_S$ designation (Qian *et al*., 2012a). Co-consumption of *A**(–) class compounds with food-grade cell membrane permeability enhancers is a great strategy to increase their bioavailability. Examples of cell membrane permeability enhancers are sucrose monoester (Yamamoto *et al*., 2013), rhamnolipids (Jiang *et al*., 2013) and piperine (Dudhatra *et al*., 2012), a natural constituent of black pepper. Researchers have shown that the metabolism of flavonoids (common natural constituent in tea) in gastrointestinal tract is influenced by food matrix composition such as carbohydrate or lipid content

(Clifford *et al*., 2013). Hence, specific food matrices that provide assistance in the metabolism of compound classified as *T**(–) class into more beneficial metabolites can possibly be designed in order to improve their oral bioavailability.

Table 2.2: The nutraceutical bioavailability classification scheme (NuBACS)

Major classes	Sub-classes
Bioaccessibilty (B*)	L : Liberation S : Solubilization I : Interaction
Absorption (A*)	ML : Mucosal layer TJ : Tight junction transport BP : Bilayer permeability AT : Active transporters ET : Efflux transporters
Transformation (T*)	C : Chemical degradation M : Metabolism

2.2.2 Designing food matrix for oral consumption

Active compounds may be delivered to consumers in several different forms. For instance, they may be part of fresh or minimally processed foods such as vegetables and fruits that naturally contain one or more bioactive components. This food is co-ingested with an excipient food which composition is specifically designed to increase the oral bioavailability of the active compound. For example, raw salad or cooked vegetable could be enjoyed with specially designed salad dressing or sauce to increase the carotenoid oral bioavailability. Examples of excipient foods can be found in a published review (McClements & Xiao, 2014).

Alternatively, they could be also synthesized or isolated from their natural source/environment, purified and incorporated into processed foods as extra beneficial ingredients to promote health. This type of food is called functional food. For instance, common processed food product that had been successfully incorporated with active compounds are beverages, yoghurt, sauces, salad dressing and desserts (Sagalowicz & Leser, 2010). However, before they can be successfully incorporated into food matrices, it is often advantageous to encapsulate them within an appropriate nanoparticle-based delivery system. An appropriate delivery system must be able to encapsulate the active compounds e.g. solubilizing them if they are lipophilic without interfering with the original physico-chemical properties of the food matrix. Hence, the type of active compound and matrix of final food product would define the suitable type of nanoparticle-based delivery system, which will be discussed in the next section.

2.2.3 Selection of nanoparticle-based delivery system

There have been rapid advances in the development of nanoparticle-based delivery system to encapsulate, protect and release active compounds over the past few years. Different kinds of nanoparticle-based delivery systems have been developed, including nanovesicle, nanoemulsion, lipid nanoparticle, polymeric nanoparticle and nanocrystal. If these nanoparticle-based delivery systems are going to find widespread applications within food industries, it is important for them to be able to overcome some constraints associated with delivering active compounds in food systems (McClements *et al*., 2009). Factors discussed below must be carefully considered at each stage of the design and development process.

Firstly, the delivery system should be formulated from legally acceptable ingredients (non-toxic) and processing methods. The cost of development should be economically viable as well. Asuitable delivery system must be able to render them

readily soluble in aqueous-based food product such beverages, desserts, dressing, sauce etc.

At the same time, it has to protect the functional compound that had been encapsulated within it from chemical degradation. Equally important is the delivery system itself must be compatible with the food medium. It should not cause any adverse effects or reduce the normal/commercial quality of the food products such as appearance, texture, flavour, rheology and stability (shelf-life).

In addition, the delivery system must be able to withstand different types of environmental stresses that food/food products would experience during production, storage and transportation. Examples of these stresses are pH changes, high ionic strengths, ingredient interaction, cooling, heating, dehydration and mechanical agitation.

Lastly, the delivery system must be able to survive the human digestive system to some extent in order to protect the active compound and maintaining their bioavailability until it reaches the target site(s)

2.3 Engineered nanoparticle-based delivery system

Numerous nanoparticles have been invented and tested for their potential to encapsulate, protect, controlled release and increase the oral bioavailability of encapsulated compounds. Depending on their structures, engineered nanoparticles can be categorized into different classes. As mentioned earlier, they can be classified into two main groups, which are liquid and solid nanoparticle-based delivery system (Borel & Sabliov, 2014) or as lipid-based and non-lipid-based (Yao *et al*., 2015). On the other hand, they are also categorized as lipid-based, surfactant-based and polymer-based delivery system (McClements *et al*., 2009). These different classifications from three different sources are shown in Table 2.3.

Table 2.3: Different classifications of nanoparticle-based delivery systems

Types	Classification criteria		
	(Borel & Sabliov, 2014)	(Yao *et al*., 2015)	(McClements *et al*., 2009)
Nanoemulsion	Liquid nanodelivery system	Lipid-based nanoparticle	Lipid-based delivery system
Solid lipid nanoparticle (SLN)	Solid nanodelivery system	Lipid-based nanoparticle	Lipid-based delivery system
Nanostructure lipid carrier (NLC)	Solid nanodelivery system	Lipid-based nanoparticle	Lipid-based delivery system
Nanocapsule	Solid nanodelivery system	Non-lipid-based nanoparticle	Polymer-based delivery system
Nanosphere	Solid nanodelivery system	Non-lipid-based nanoparticle	Polymer-based delivery system
Liposome	Liquid nanodelivery system	Lipid-based nanoparticle	Surfactant-based delivery system
Niosome	Liquid nanodelivery system	Lipid-based nanoparticle	Surfactant-based delivery system
Polymerosome	Liquid nanodelivery system	Non-lipid-based nanoparticle	Polymer-based delivery system
Nanocrystal	Solid nanodelivery system	Not applicable	Not applicable

2.3.1 Nanoemulsions

An emulsion is the mixture of immiscible liquids (usually water and oil) usually stabilized by surfactants or other types of stabilizing agents to form a solution with one of the liquids being dispersed as spherical droplets in the other (McClements, 2004). Nanoemulsion is typically light bluish transparent due to the droplets size measured in between 10 to 100 nm in diameter, the scale smaller than the ultra-violet light range. The substance that makes up the droplets in an emulsion is called the dispersed phase whereas the substance that makes up the surrounding liquid is called the continuous phase. Conventionally, emulsion can be classified into oil-in-water (O/W) and water-in-oil (W/O) emulsion types according to the organization of the oil and water. If the organic phase (oil) forms the droplets in the aqueous continuous phase it is called oil-in-water (O/W) emulsion and *vice versa*. In addition to conventional O/W and W/O emulsion, it is possible to formulate multiple emulsions, for instances oil-in-water-in-oil (O/W/O) and water-in-oil-in-water (W/O/W) (Garti & Benichou, 2004). Multiple emulsions are a double dispersion system whereby small droplets are dispersed within larger droplets, which are then dispersed in the continuous phase.

In food industry, emulsion whose continuous phase is aqueous (i.e., O/W and W/O/W as presented in Figure 2.1*a* and *b*, respectively) is the most commonly used as delivery system compared to other particle-based delivery systems. For instance, stabilized emulsion of olive oil with sodium caseinate was used to replace the animal fats in meat products (Cofrades *et al*., 2013) and lemon oil emulsion was developed for food and beverage flavourings (Rao & McClements, 2012). Conventional emulsion is employed when the hydrophobic compound is to be dissolved within the internal organic phase, whereas multiple emulsions is mainly employed for the delivery of hydrophilic compounds (Sapei *et al*., 2012) such as immunoglobins (Lee *et al*., 2004), proteins and amino acids (Su *et al*., 2006).

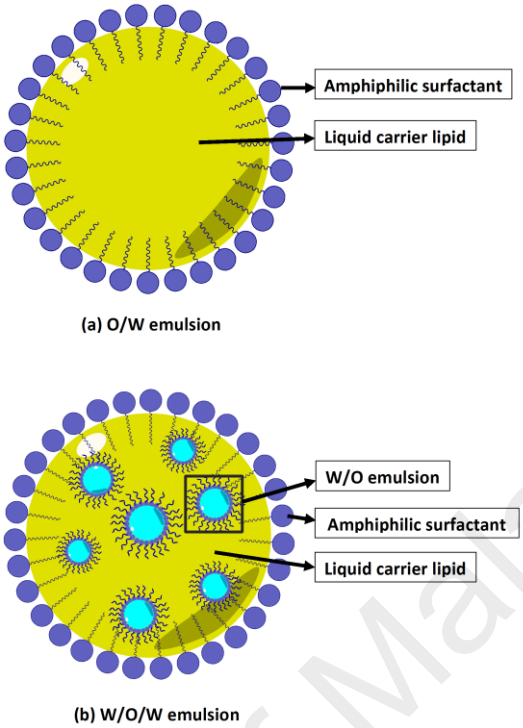

Figure 2.1: Emulsion system

Conventional nanoemulsion should usually be the first system to be considered when one is thinking of delivering lipophilic bioactive or drugs with a $B^*(-)_S$ designation owing to their relative ease of preparation and low cost compared to other more sophisticated nanoparticle-based delivery systems. In addition, by controlling their chemical composition, they can be created with different rheological properties (ranging from viscous liquids, plastic pastes to elastic solids) to accommodate a number of specific applications. In addition, they can be dried to form powders through spray- or freeze drying, which may increase their range of versatility for utilization in many applications.

2.3.2 Lipid nanoparticles

Solid lipid nanoparticles (SLN) and nanostructure lipid carriers (NLC) have emerged as potential delivery systems for unstable lipophilic compounds. The general structure for these two carriers is represented in Figure 2.2. They present several major advantages *viz.* enhanced chemical and physical stabilities of incorporated compounds, improved bioavailability, sustained release properties as well as amenable for large scale production (Müller *et al*., 2002).

SLNs are similar to nanoemulsion except that the lipids of the emulsion are fully crystallized into solid phase for encapsulating the lipophilic compounds. A major advantage of SLNs is that they provide means of incorporating lipophilic molecules in stable particles without the use of organic solvents. The solid matrix of SLNs restricts the mobility of lipophilic compounds, hence the ability to provide controlled-release of lipophilic compounds (MuÈller *et al*., 2000). However, this type of nanoparticles have a low loading efficiency because compounds might be expelled out during crystal structure transformation (i.e. lipid polymorphism) during storage (Helgason *et al*., 2008; Weiss *et al*., 2008). Polymorphic lipid transformation from α- to β-subcell can shift the shape of the spherical nanoparticles to a needle-shaped morphology, causing reduction of space availability for the bioactive/drug ingredients. Nevertheless, specific crystal structure can be designed by regulating the carrier lipid, surfactant composition, cooling step and storage temperature in order to sustain the performance of lipid nanoparticles (Weiss *et al*., 2008; Helgason *et al*., 2009b; Qian *et al*., 2012b; Paliwal *et al*., 2009). Triglycerides such as tristearin, tripalmitin, trimyristin and trilaurin are commonly used lipid for the development of solid lipid nanoparticles (Esposito *et al*., 2008; Bunjes *et al*., 1996; Westesen & Bunjes, 1995). These lipids have the main advantage of low toxicity due to their structural similarities to physiological lipids compared to other polymeric materials.

NLCs are lipid nanoparticles with both crystallized and liquid phases of lipid (partially solid matrix), which can be created by blending different lipid molecules i.e. solid lipid with carrier lipid (oil) (Müller *et al*., 2002). The inner liquid phase dissolves and entraps the compound to provide chemical stability, controlled release and higher loading capacity (Tamjidi *et al*., 2013). However, incorporation of liquid lipophilic active ingredients into NLCs is not as efficient as SLNs in terms of protecting them from oxidation as a consequence structural stability problem. For instance, NLC formulation with carnauba wax loaded with blackcurrant seed oil yielded high level of peroxides suggesting a high oxidation rate (Hommoss, 2009). Therefore, the aspect of physical stability must somehow be addressed fully to extend the shelf life of the NLC formulations.

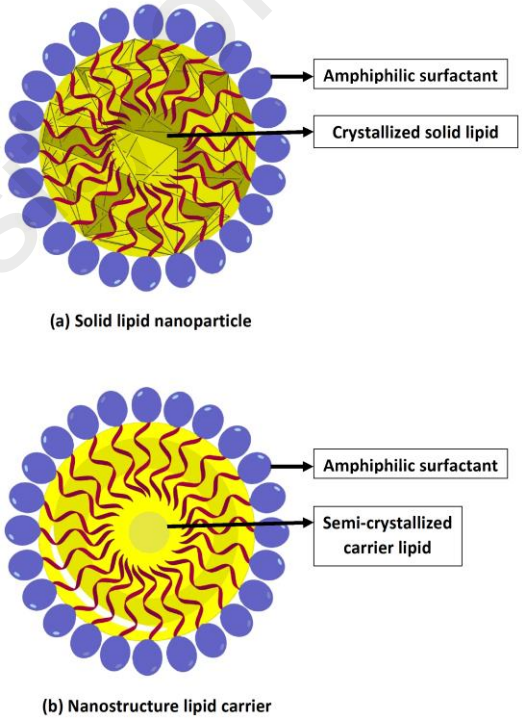

Figure 2.2: Lipid nanoparticles

2.3.3 Polymeric nanoparticles

Polymeric nanoparticles composed of matrices of polymer with entrapped molecules and surrounded by surfactant or emulsifier (Hunter *et al*., 2012). Like lipid nanoparticles, they are designed to protect the entrapped active components from degradation and to exhibit muco-adhesive properties or to enhance permeability (Chen *et al*., 2011). Based on the structural organization, polymeric nanoparticles can be classified as nanocapsule and nanosphere. These nanoparticles are widely used for the encapsulation of various useful compounds and to develop nanomedicine (Jeong *et al*., 2008; Joo *et al*., 2008).

Polymeric nanocapsules or nanoencapsulates are nanoparticles with colloidal size. The polymer forms a membrane-like wall that surrounds the compound-rich liquid core (vesicular system) (Figure 2.3a). Unlike polymerosome, nanocapsules are filled with hydrophobic liquid instead of aqueous phase core. Monomer composition of polymer, molecular geometry and relative monomer length exert important influences towards physico-chemical properties and morphologies of the nanocapsule (Letchford & Burt, 2007).

Polymeric nanosphere is formed when polymer aggregates to generate a solid central core in which active compounds are entrapped, encapsulated, chemically bound or adsorbed to the polymer matrix (Figure 2.3b). However, the central core may display more or less solid-like behaviour depending on the copolymer composition (Letchford & Burt, 2007).

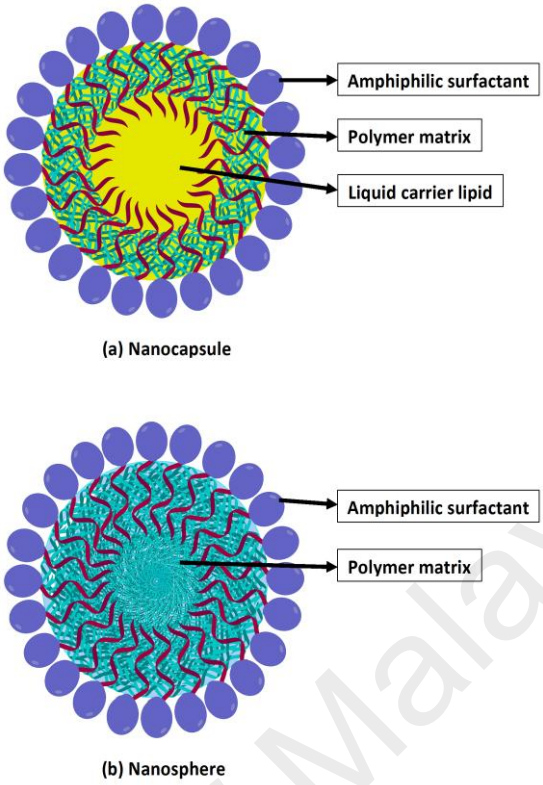

Figure 2.3: Polymeric nanoparticles

Natural carbohydrates are usually used to protect the active food/drug components from the harsh conditions in the stomach. They can be modified for optimal compatibility with the active components. The most commonly used polysaccharides are alginates, chitosan, pectins, dextran, starch and inulin. Chitosan is of special interest for targeted release of active components to living cells (Chen & Subirade, 2005). It is a derivative of naturally occurring chitin from alkaline deacetylation. Usually it is blended together with alginate to withstand the low pH in the stomach and to facilitate the release of active components in the ileum or colon (Marsich *et al*., 2008; Iyer *et al*., 2005). In addition, chitosan is a polycationic molecule making it a suitable candidate to be mixed together with pectin to form a slowly degrading complex (Yu *et al*., 2009). Starch and inulin are plant-derived macromolecules that merit further investigation for their potential in the delivery of active food/drug components owing to their inherent advantages such as economical, relative ease of handling and can be applied in

combination with almost all encapsulation techniques (Carr *et al*., 1991; Hinrichs *et al*., 2006). Both are difficult to hydrolyse which qualifies them as matrix molecules for nanoparticles targeted to reach the colon and survive the upper part of the gastrointestinal tract (Gibson *et al*., 2004; Macfarlane & Englyst, 1986). Unlike inulin and starch, dextran is a bacterial-derived polysaccharide abundantly present in *Bacteroides.* A beneficial feature of dextran is that by varying its structure in the capsules allows for the regulation of its degradation rate in the gut. Moreover, combination with other polymers have been shown to be an effective approach in modulating the kinetics of load release (Kosaraju, 2005).

Besides naturally produced polymer, other non-natural polymers are also used to develop biodegradable nanosystems. The most commonly used polymers are poly-*D,L*-lactide-*co*-glycolide (PLGA), polylactic acid (PLA) and polycaprolactone (PCL). In the body, PLGA is hydrolysed to produce biodegradable metabolite monomers (lauric acid and glycolic acid) (Jain, 2000), which can be effectively metabolized by human body negating systemic toxicity issue for PLGA as nanodelivery system. PLGA has been blended with other polymers such as alginate, chitosan and pectin in order to make it compatible with active compounds (Liu *et al*., 2004). Other compatible blend includes PLA (Ruan & Feng, 2003), a biocompatible and biodegradable material, which produces monomeric units of lactic acid upon natural hydrolysis of its ester linkages in the human body. Lactic acid is a natural intermediate in the carbohydrate metabolism. Owing to its slow and alterable drug release behaviour, PCL is a suitable matrix material to construct the solid phase of a nanodelivery system (Choi *et al*., 2006; Prabu *et al*., 2009).

To ensure that a designed polymer-based nano-delivery system is ideal as active compounds carrier for use in nutraceutical and pharmaceutical industry, better fundamental understanding of polymer-polymer and polymer-compound interaction at

the molecular level and their influence on functional properties of the delivery systems are required. The compounds are either bound on the surface or encapsulated inside of the nanoparticles. Various methods have been used to synthesize polymeric nanoparticles according to the pre-requisites of their applications and types of compounds to be encapsulated (*Section 2.4.2*). Biodegradable polymers are highly preferred to develop nanoparticles as they provide sustained release property and biocompatibility with tissues and cells (Letchford & Burt, 2007). Moreover, biopolymer-based nanoparticles are stable in blood, non-toxic, non-thrombogenic and most importantly applicable to various bioactive and drugs (Nitta & Numata, 2013).

2.3.4 Nanovesicles

Vesicular systems are colloidal particles in which concentric bilayer made-up of amphiphilic compounds surround an aqueous compartment (Negi *et al*., 2009). They are novel means for delivering both hydrophobic and hydrophilic active compounds, which are encapsulated within the lipid bilayer and in the interior aqueous compartment, respectively. There are three main types of nanovesicles, which are liposome, niosome and polymerosome.

Liposomes are nanovesicles formed by self-assembly of natural or synthetic phospholipids bilayer arrangement (Figure 2.4a). They are ideal for carrying hydrophilic bioactive or compounds entrapped within their aqueous-based core. For instances, liposomes have been used to formulate iron-enriched milk (Xia & Xu, 2005) and encapsulate ellagic acid for antioxidant delivery (Madrigal-Carballo *et al*., 2010). However, hydrophobic molecules can also be entrapped within the hydrophobic region of the bilayer shell. For instance, liposomes have been developed for food applications as a method of co-delivering vitamins E and C with orange juice (Marsanasco *et al*., 2011).

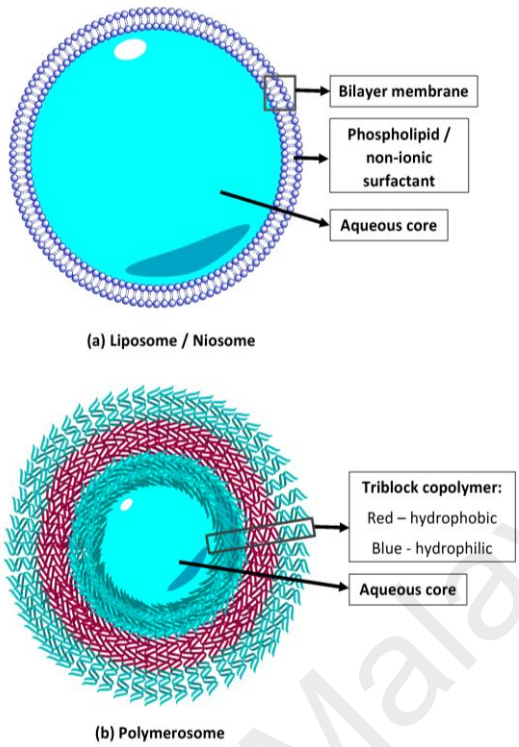

Figure 2.4: Nanovesicles

If vesicular systems are made up of non-ionic surfactants, it is called niosomes. They share similar structure and function as liposome, which made them useful for active compound delivery with enhanced oral bioavailability in addition to providing therapeutic activity in a controlled manner for a prolonged period of time (Mahale *et al*., 2012). Non-ionic surfactants are commonly used in preparing nanovesicles due to the biological system associated benefits like less toxic, less irritating to cellular surfaces and tend to maintain their structure near physiological pH in solution as compared to their anionic, cationic and amphoteric counterparts (Sahin, 2007). Examples of non-ionic surfactants are sorbitan fatty acid esters (Span 20, 60 and 80), polyoxyethylene fatty acid esters (Tween 28 and 80), polyoxyethylene stearyl ethers (Brij 72 and 76), polyoxyethylene cetyl ethers (Brij 52, 56 and 58), polyoxyethylene 4 lauryl ether (Brij 30). The encapsulation efficiency is influenced by the hydrophilic-lipophilic balance (HLB) value and phase transition (T_C) of non-ionic surfactants that are used to develop

niosomes. Apart from these two parameters, the chain length of hydrophobic tail and size of the hydrophilic head group of the non-ionic surfactant also influence the encapsulation efficiency (Uchegbu & Vyas, 1998).

Polymerosomes are nanoparticles that exhibit similar general structure and function as liposomes and niosomes (Figure 2.4b). They can be used to entrap both hydrophilic and hydrophobic compounds. However, unlike liposome and niosome, instead of phospholipids or any amphiphilic surfactants, amphiphilic block copolymers i.e. polymers consisting of covalently linked hydrophilic and hydrophobic chains are used to form the shell. An example of block copolymer is tri-block copolymers of poly(caprolactone)-poly(ethylene-glycol)-poly(caprolactone). Constructing vesicle by using polymer as opposed to lipid-based imparts several advantages including controlled-release of compounds and increased stability of shell (Rastogi *et al*., 2009). Furthermore, a molecular dynamic study has shown that amphiphilic block copolymer is also able to form cell-like membranes and vesicles (Srinivas *et al*., 2004). Polymerosomes can be synthesized using methods similar to those used for polymeric nanoparticles.

2.3.5 Nanocrystals

Nanocrystal consists of crystallized drug or bioactive surrounded by a surfactant or polymeric stabilizer (Junghanns & Müller, 2008). They are developed in order to attain adequate bioavailability of poorly soluble bioactive or drugs in aqueous medium. Unlike lipid and polymeric nanoparticles where a compound is encapsulated in, the compound itself serves as the solid matrix of the nanoparticles. Hence, the major advantage of a nanocrystal is that they have 100 % bioactive/drug loading. However, this type of nanoencapsulation only works best with compounds that possess high melting temperature i.e. the ability to crystallize under ambient temperature e.g.

bioactive that belongs to carotenoid family and most type of drugs. Nanocrystals are also referred as nanosuspension because they are typically produced in a liquid dispersion medium where they are suspended in the liquid (Figure 2.5).

Nanocrystal has gained a great interest in the pharmaceutical industry because of their simple structure and composition (Müller & Keck, 2012). However, the study of bioactive nanocrystal is not as extensive as drug nanocrystal. Hence, most of the understanding came from the drug crystal literature. Nanocrystal has huge benefits to offer to the food and pharmaceutical industry including improvement in formulation performance i.e. enhanced saturation solubility and dissolution rate of active compound particles. In addition, their high loading capacities allow for a highly efficient transportation of active compounds to/into cells, thus enable them to possess a sufficiently high therapeutic concentration for the desired pharmacological effects.

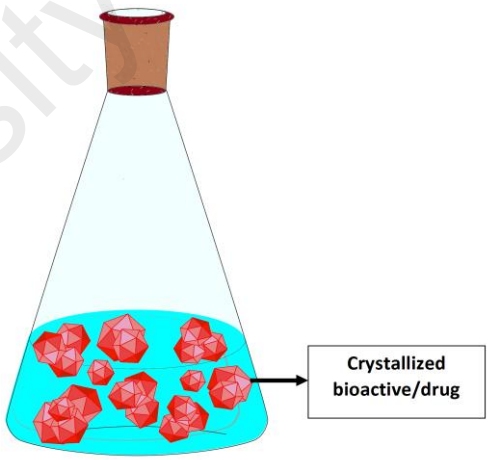

Figure 2.5: Suspension of nanocrystals

2.4 Development of a nanoparticle-based delivery system

Methods to be applied in the encapsulation of active compounds are dictated by the type of nanoparticles to be produced. The difference is primarily due to the chemical structure of matrix material and the variety of intended products. The different methodologies currently available to develop the nanoparticle delivery systems based on the main matrix material used are discussed in the subsequent paragraphs.

2.4.1 Formation of a lipid-based nanoparticle

Emulsification is the most common technique to produce lipid nanoparticles. It is defined as a process of dispersing one liquid in another immiscible liquid and can be categorized either as mechanical (high-energy method) or chemical process (low-energy method). High-energy methods including microfluidization and ultrasonication are often used to homogenize a big portion of lipid into nanoparticle size of SLNs and NLCs for food applications (McClements & Li, 2010; Tamjidi *et al*., 2013). The two basic homogenization techniques for SLNs as well as NLCs are the hot and cold homogenization (MuÈller *et al*., 2000; Tamjidi *et al*., 2013). For both techniques, the active compound is first dissolved in the lipid that is being melted at approximately about 5 to 10 °C above its melting point. For the hot homogenization technique, the compound-containing melt is homogenized in a hot aqueous surfactant solution. For cold homogenization technique, the solidified compound-containing melt obtained *via* cooling is dispersed and homogenized in an aqueous surfactant solution at below room temperature. Other widely used mechanical method is extrusion (Breitenbach, 2002), whereby small droplets of encapsulated material are produced by coercing the solution through small openings (nozzle) in a droplet-generating device. By changing the inner diameter of the nozzle or opening, the particle size can be varied.

Through phase inversion composition (PIC) and phase inversion temperature (PIT) methods, emulsion is formed as a result of spontaneous formation of emulsion droplets attributed to the hydrophobic effects of lipophilic molecules in the presence of emulsifier (McClements & Li, 2010). These low-energy emulsifications, commonly known as phase inversion emulsification (PIE), are often used to form conventional emulsion. Phase inversion can be initiated by changing the system composition i.e. PIC (water-to-oil ratio) through stepwise addition of intended continuous phase (Bouchama *et al.,* 2003). The critical volume fraction that induces this inversion is called emulsion inversion point (EIP). An emulsion system can also be inverted by altering its formulation *via* changing the strength of interaction between surfactants and fluid phases i.e. PIT. Temperature has been shown to modulate the affinity of surfactant toward water and oil phases (Shinoda & Saito, 1968; Sherman & Parkinson, 1978; Anton & Vandamme, 2009). The critical temperature that induces the transitional inversion is called hydrophile-lipohile balance (HLB) temperature.

Spray drying is another commonly used method for encapsulation. It is a fast, cheap and highly reproducible procedure that involved dissolving the active compound in a dispersion of a selected matrix material (Freitas & Müller, 1998b). Subsequently, water is removed from the dispersion by atomizing it in heated air. As a result, powdered particles are formed and can be harvested from the drying air at the outlet of lower temperature. Spray cooling shares similar principle with spray drying. Instead of heating, the dispersion is immobilized at low temperature. It is suitably applied for dry products like enzyme, minerals and proteins.

2.4.2 Formation of a polymer-based nanoparticle

Nanoprecipitation method produces nanocapsules that consist of a central oily core surrounded by a thin polymer wall (Guterres *et al*., 1995). This involves adding together polymer solution (in acetone or other water miscible solvent) with active compounds (in lipophilic solvent like oil) to be encapsulated into a stirred aqueous solution containing a surfactant. Consequently, the water miscible solvent will diffuse into aqueous phase resulting in the formation of lipophilic compound-containing nanocapsules. The water insoluble polymer will slowly adsorb to interface of the nanocapsules.

The preparation of nanospheres or polymerosome using solvent evaporation method involves emulsification of polymer solution containing dissolved compounds into an aqueous phase followed by evaporating of the polymer solvent. This consequently induces the formation of polymer precipitation as nanospheres with the compound finely dispersed in the inner polymer matrix network (Pinto Reis *et al*., 2006). If amphiphilic copolymers were used as the matrix material, polymerosomes would be formed instead of nanospheres.

Another commonly applied technology is coacervation. The technique is based on forming a nanoparticle complex by mixing active compounds with a matrix material of opposite charge. Varying the ratio between compound-matrix, pH, ion concentration and type of matrix allow for modulation of the size of nanoparticles. This technique is driven mainly by electrostatic attraction and hydrophobic interactions (Augustin & Hemar, 2009). The emulsion-coacervation technique (Lertsutthiwong *et al*., 2008; Lertsutthiwong *et al*., 2009) engages the emulsification of an organic phase (oil and active compound) with an aqueous phase (water and stabilizing agent). Subsequently, a coacervation process is conducted by depositing a single or a mixture of polyelectrolyte(s) (e.g. sodium alginate) solution (coacervate phase) into the emulsion

system. It is possible for additional complementation with cross-linked steps to be carried out so as to obtain a rigid nanocapsule shell structure by the addition of an appropriate chemical or enzymatic cross-linker such as glutaraldehyde or transglutaminase.

Polymer-coating method entails the adsorption of the polymer onto pre-formed uncoated emulsion droplets. It begins with the formation of an emulsion template and then incubating it with the polymer solution under pre-determined stirring and contact time conditions (Prego *et al*., 2006; Calvo *et al*., 1997). Unlike emulsion-coacervation method, the polymer deposition and precipitation onto the emulsion droplets is induced by solvent evaporation without the need for chemical additive.

2.4.3 Formation of a nanovesicle

The general method for preparing nanovesicles requires evaporation of solvent to produce a thin layer of lipid film followed by hydrating process with a hydration medium (usually phosphate buffer at various pHs). There are four common methods usually used to develop nanovesicle *viz.* transmembrane pH gradient method, lipid layer hydration, reversed-phase evaporation and microfluidization.

Developing nanovesicle by using transmembrane pH gradient method involves dissolving surfactant and cholesterol in a solvent (usually chloroform) followed by evaporation under reduced pressure (Alyane *et al*., 2015; Bhaskaran & Lakshmi, 2009). The resulting lipid film is then hydrated with acidic solution e.g. citric acid accomplished by vortex mixing. The resulting product is subjected to freeze-thaw cycles alternating with the addition of aqueous solution of active compound and vortexing of the mixture. The pH of the solution is then raised to 7 using disodium hydrogen phosphate solution.

Lipid layer hydration method entails the hydration of the lipid film, as described above, with an aqueous solution of active compound at temperature slightly above the phase transition temperature (T_C) of the surfactant for a certain time with mild shaking (Bhaskaran & Lakshmi, 2009).

Reversed-phase evaporation comprises of adding surfactant solution (in a mixture of chloroform and ether) into an aqueous solution containing active compounds. The resulting two-phase system is then homogenized and the organic phase evaporated to obtain nanovesicles dispersed in the aqueous phase (Guinedi *et al*., 2005).

Microfluidization is a process to produce nanovesicle whereby a solution of surfactant and active compounds is pumped under high pressure through an interaction chamber and cooling loop to remove the generated heat. This process can be repeated until the desired size of nanovesicle is obtained (Sorgi & Huang, 1996).

2.4.4 Formation of a nanocrystal

There are two basic approaches to produce nanocrystals involving the bottom-up and top-down methods. The basic principle of bottom-up approach is the creation of small particles of active compound molecules through precipitation in the presence of an agent or condition that induces nucleation of the molecules in an organic solution. There are various techniques for bottom-up approach e.g. sono-crystallization, confined impinging liquid jet precipitation and multi-inlet vortex mixing (Chan & Kwok, 2011).

On the other hand, top-down approach is based on two basic size reduction methods, which are wet milling (Merisko-Liversidge & Liversidge, 2011) and high-pressure homogenization (Keck & Müller, 2006). The wet milling method involves application of shear stress through grinding of an aqueous suspension that contains large compound particles and stabilizer using beads in a milling chamber. As for high-pressure homogenization, it involves the application of shear force, turbulent flow and

cavitation of fluid streams of large compound particles suspension to reduce the particle size to nanometer range. Some examples of this procedure are microfluidization and piston-gap homogenization.

2.5 Characterization of a nanoparticle-based delivery system

Characterization of an aqueous dispersion of nanoparticles is necessary in order to better control the products quality. Determining the properties of the nanoparticles poses an even greater challenge due to the minute size of the particles and the complexity of the colloidal suspension. Parameters that have direct impact on the system stability are discussed in the following section.

2.5.1 Particle surface charge and size

The electrical potential at a shear plane is called zeta potential. A shear plane is an imaginary surface separating the thin layer of liquid and solid phase in motion (Kirby & Hasselbrink, 2004). Zeta potential is a useful indicator for particle surface charge, which can be used to predict the stability of a colloidal suspension. The greater the zeta potential, the more stable the suspension because the charged particles repel one another and hence circumvent coagulation issues (Heurtault *et al*., 2003). Zetasizer is commonly used to determine zeta potential and size of the nanoparticle dispersion in many studies (Freitas & Müller, 1998a; Ahmad *et al*., 2012).

Photon Correlation Spectroscopy, PCS (also known as Dynamic Light Scattering) and Laser Diffraction (LD) are the most common techniques to determine particle size (Filella *et al*., 1997). Both techniques do not directly measure particle size but rather relatively detect the light scattering effects, which are used to calculate particle size. PCS measures the relative particle size based on intensity fluctuation of the scattered light, which is caused by the particle movement (the Brownian motion).

On the other hand, LD measures the particle size based on the dependency of the diffraction angle on the particle radius. Larger particles cause less intense scattering at high angles compared to smaller ones. One advantage of LD over PCS is the broad coverage of size from nanometer to millimeter range.

2.5.2 Crystallinity and phase modification

Thermoanalysis of the solid colloidal dispersion provides information about the liquid crystal properties, degree of crystallinity, enthalpy, polymorphic transition and fusion temperature. Evaluation on the degree of lipid, polymer and surfactant crystallinity and polymorphic modification must be made carefully since these parameters strongly affect the efficiency of drug incorporation and its release rate.

Combination of Differential Scanning Calorimetry (DSC) and Small Angle X-ray Scattering (SAXS) analyses are widely used to investigate the status of the solid phase of lipid, polymer and surfactant-compound nanocrystal in colloidal suspension (Bunjes *et al*., 1996; Siekmann & Westesen, 1994; Westesen *et al*., 1993; Lukowski *et al*., 2000). DSC analysis is based on the fact that different states of solid modification possess different melting points and melting enthalpies. By means of X-ray scattering, one can assess the distance of various planes of the crystal lattice. Hence, this technique is frequently used to study crystallization tendency and polymorphic transition of lipid nanoparticles (Lukowski *et al*., 2000; Bunjes *et al*., 1996).

Another technique supporting crystallographic analysis is Fourier transform infrared spectroscopy (FTIR). The basic principle that governs this technique is the bonds and groups of bonds vibrate at certain frequencies by absorbing the wavelength energy at that particular frequency. Different molecules will give different IR spectra or absorption plot which are the characteristic to those molecules (Berthomieu & Hienerwadel, 2009). Measured IR spectra usually will be analysed and matched with

known signatures of identified materials in the FTIR library. Besides that, it can also be used to characterize intermolecular interaction within a colloidal system (Vieira *et al.,* 2002; Silva *et al.,* 2011).

2.5.3 Homogeneity in colloidal suspension

Possible artefacts arising during sample preparation may complicate characterization of the nanoparticle dispersion. For example, the use of surfactant or processing temperature may change solid phase modification that will influence the nanoparticle shape (Garti & Zour, 1997). Furthermore, it is almost impossible to completely obtain the desired well-shaped nanoparticles. For instance, the co-existence of additional colloidal structures such as micelles, liposomes, supercooled melts, polymer coagulates and drug-nanoparticles may occur during processing culminating in a heterogeneous dispersion. Hence, there is a need to characterize the type of nanoparticles in colloidal dispersion in order to control the quality of the formulation product.

One of the techniques to identify the state of nanoparticle is ^{1}H-NMR spectroscopy. Simple ^{1}H-NMR analysis permits an easy and rapid detection of supercooled melts (Jores *et al*., 2003; Wissing *et al*., 2004). Supercooled melts formed when the solid lipid nanoparticles do not undergo polymorphic transformation to form more stable β-subcell crystal (Kulkarni, 2012; Sato, 2001). Moreover, ^{1}H-NMR also permits the characterization of liquid compartments of developed nanoparticles in a system (Jenning *et al*., 2000). For example, in an attempt to develop a solid nanoparticle-based delivery system by homogenizing an aqueous dispersion of emulsifiers and a blend of solid and liquid lipids, one can determine the structural stability of the resulting nanostructure lipid carriers (NLCs). This method is based on the different proton relaxation time in the liquid and semisolid or solid state. The

mobility of the molecules is related to the width of the signal. Protons in the liquid state will give a strong signal with sharp amplitudes, while semisolid or solid will give weak and broad signal. Jores and colleagues have performed physico-chemical investigations of different formulations of SLNs and NLCs by using NMR (Jores *et al*., 2003).

Difficulties may arise in ^{1}H-NMR measurement for samples that contain several populations of different types and sizes of nanoparticles. Therefore, additional techniques might be useful to complement ^{1}H-NMR analysis e.g. optical polarized microscopy (OPM) and electron microscopy (EM). Even though OPM is not particularly sensitive to nanometer size range, it assists to give a fast indication about the presence and the character of microparticles (i.e. aggregate of small particles). In addition, OPM can also be used to investigate the crystal-packing pattern of solid lipids and their liquid crystalline properties (Zhao *et al*., 2005). Electron Microscopy (EM) is used to obtain images of nanometer size of nanoparticles (Jores *et al*., 2004; Regev *et al*., 2004).

2.6 Evaluating oral bioavailability of encapsulated compounds

In this section, ingestion, absorption, distribution, metabolism and excretion characteristics of nanoparticle-based delivery systems are discussed. The passage and metabolism of compound-loaded nanoparticles following various exposure routes have been reviewed (Hagens *et al*., 2007). In the current review, only oral exposure will be considered as presented in Figure 2.6. Ingestion/digestion refers to chemical modification of nanoparticles by enzymes present in saliva while absorption refers to the interaction between compound-loaded nanoparticles with the intestinal mucosa and epithelial cells. After the compound-loaded nanoparticles passed through these barriers, distribution occurs through systemic circulation whereby they are distributed to organs such as lungs, heart, kidneys, spleen, liver and brain (Hagens *et al*., 2007). Metabolism

describes the biotransformation of the bioactive and drugs through interaction with proteins and lipids in those tissues. Organs that are primarily responsible for body excretory system will dispose any unnecessary metabolites out of the body. From absorption to excretion, there are some impediments that nanoparticles need to overcome in order to deliver the encapsulated compound to the target tissues. These comprised of enzymes, low pH of stomach, lining mucus of gastrointestinal tract, gastrointestinal epithelium, interaction with blood components, natural barrier, liver metabolism as well as bile excretion (Borel & Sabliov, 2014; Bouwmeester *et al*., 2009).

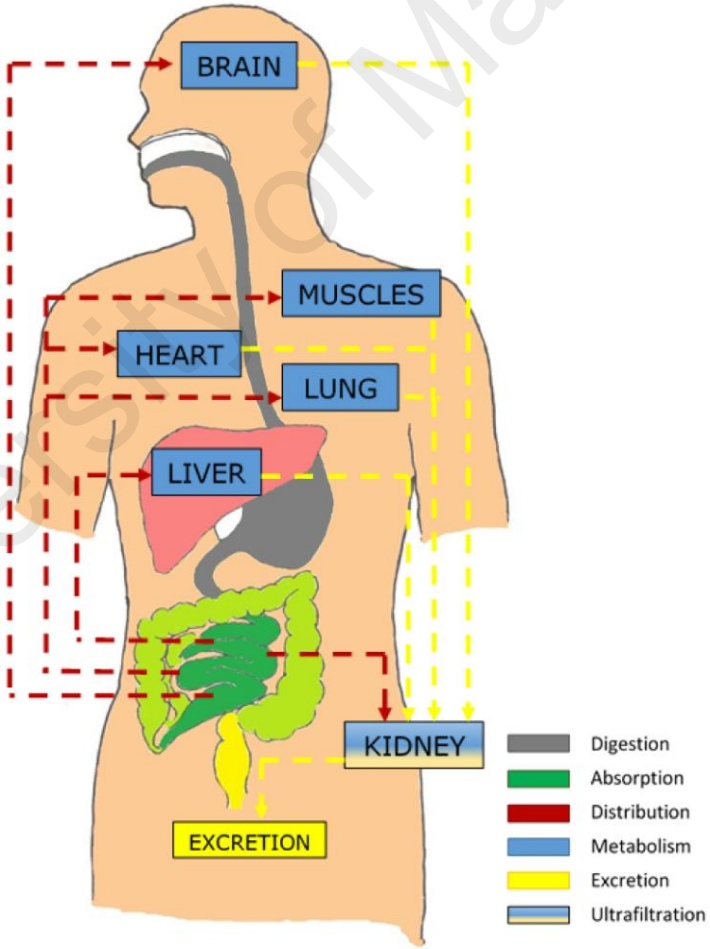

Figure 2.6: Nanoparticles pathway upon ingestion

Oral bioavailability of compounds defines the efficiency of engineered nanoparticle-based delivery systems in enhancing their bioavailability. It is greatly influenced by nanoparticles properties e.g. size, charge, hydrophobicity, targeting properties and type of loaded compound. The oral bioavailability of a compound (F) is defined as the fraction of the ingested compound that reaches the systemic (blood) circulation to be distributed to the tissues and organs in active form where it can exert its beneficial health effects. It can be estimated by the following equation (Yao *et al*., 2015; Yao *et al*., 2014):

$$F = F_B \times F_A \times F_M \quad \textbf{E.q. 2.1}$$

where F_B is the fraction of ingested compounds that got through the upper gastrointestinal tract and released from the nanoparticles into the gastrointestinal fluids, thereby made accessible for absorption by enterocytes. F_A is the fraction of accessible compounds that got absorbed and transported throughout the systemic circulation. F_M is the fraction of absorbed compound present in an active form after first-pass metabolism in the gastrointestinal tract, liver and any other forms of metabolism. In the following sections, the effects of nanoparticle-based delivery systems on bio-accessibility (F_B), absorption (F_A) and first-pass metabolism (F_M) of encapsulated compounds are discussed.

2.6.1 Gastrointestinal ingestion

Ingestion of nanoparticles begins when they are partially digested by enzymes present in saliva at pH between 5 to 7 (McClements & Li, 2010). Nanoparticles will enter stomach through oesophagus and will remain there for 30 minutes to 4 hours, depending upon whether the stomach is in fasting or fed state. If nanoparticles are made

of glycolipid and protein, degradation of the nanoparticles will be significant because the acidic pH of the stomach together with its enzymes will digest the carbohydrates and proteins. Subsequently, the breakdown products and undigested nanoparticles will enter the small intestines through duodenum and will remain there for about 3 to 6 hours before passing through large intestine or colon.

During the passage through the upper gastrointestinal tract, active compounds are exposed to substantial chemical reactions that may cause changes in their physical state and chemistry, therefore decreasing their bio-accessibility. By encapsulating compounds in a specially designed nanoparticle-based delivery system, protection for the compounds from premature degradation along with their stability improvement in gastrointestinal tract could be provided (Xu *et al*., 2013). For example, encapsulation of epigallocatechin gallate (EGCG), a green tea polyphenol, in nanoliposome decreased its degradation in simulated intestinal fluids up to ten-fold (Zou *et al*., 2014).

To be accessible to enterocyte absorption, a compound needs to be solubilized within the gastrointestinal tract fluid. This occurs when compounds are encapsulated in complex "mixed micelles" which are formed by the interaction of digested lipid with bile salts and phospholipids. Therefore, encapsulation of compound in engineered nanoparticles has a significant impact on its accessibility as the nanoparticles could provide digestible components (protein, lipid and surfactant) to form complex "mixed micelles" later on in the lumen of small intestine. The type of carrier lipids used in the development of nanoparticles is critical for the accessibility of encapsulated compounds. It has been shown that nanoemulsions containing primarily long chain triglycerides helped to increase the bio-accessibility of vitamin E, β-carotene and co-enzyme Q10 (Qian *et al*., 2012a; Yang & McClements, 2013; Cho *et al*., 2014) while medium chain triglycerides have been shown to produce higher bio-accessibility of curcumin (Ahmed *et al*., 2012). Besides carrier lipids, the type of surfactant used to

develop the nanoparticle may also have an impact on the bio-accessibility of encapsulated compounds. It was reported that the degree of lipid digestion in a simulated gastrointestinal tract was positively correlated with the hydrophilic/lipophilic balance (HLB) of the surfactant (Speranza *et al*., 2013). Besides that, the size of nanoparticle can also influence compound bio-accessibility. For instances, nanoemulsion with smaller particles have been reported to give higher bio-accessibility of β-carotene as they can promote the generation of mixed micelles more rapidly than larger particles during lipid digestion (Salvia-Trujillo *et al*., 2013).

2.6.2 Absorption

Absorption of nanoparticles or released compounds occurs mainly in small intestine. The inner surface of small intestine is covered with epithelial cells with mucosal layer to facilitate absorption of various nutrients and prevent uptake of harmful substances. Further penetration of nanoparticles (including mixed micelles) in the gastrointestinal tract depends on diffusion process through mucosal layer and permeability of gut epithelial cells membrane.

The first barrier for nanoparticles to pass through into the internal body system would be the mucosal layer. The diffusion rate of nanoparticles through mucosal layer depends largely on their size. Thus, nanoparticles with relatively smaller size are assumed to diffuse faster than the larger ones. However, a study has shown that nanoparticles with 200 nm size exhibit three times diffusion coefficient over 100 nm nanoparticles (Lai *et al*., 2007). Lai and colleagues proposed that the principle of size exclusion chromatography (SEC) could be used to explain the slower diffusion of 100 nm particles through mucosal layer. The extended retention time of small particles is attributed to multiple paths that they could have taken when moving through a reticulated gel media. Nanoparticles with approximate size of 500 nm usually will be

easily blocked for mucus transfer (Norris et al., 1998). Moreover, diffusion rate of nanoparticles also depends on the pore size of the mucosal layer. Average pore size of human mucosal layer is about 100 μm (Lai *et al*., 2009). However, digestive activity and daily diet may influence the thickness of the gastrointestinal tract mucus. For instance, deficiency of dietary fibre reduced the mucosal thickness in rats (Brownlee *et al*., 2003). Surface charge of nanoparticles also appears to be an important determinant of the extent of absorption. Anionic nanoparticles have been shown to reach the epithelial surface while cationic nanoparticles were trapped in the mucosal layer (Szentkuti, 1997).

After passing the mucosal layer, nanoparticles will have to pass through gastrointestinal epithelium (enterocytes), which acts as the second barrier. Inside enterocytes, lipophilic compounds could be absorbed and transported to the lymphatic circulation system *via* a chyclomicron-mediated pathway (Yao *et al*., 2015). Chyclomicrons are lipid particles endogenously produced by enterocytes using lipid components supplied by mixed micelles. It is also possible for compound to remain entrapped inside non-digested nanoparticles rather than being released (Harde *et al*., 2011). Hence compound-loaded nanoparticles could be taken up *via* para-cellular route, a passage between epithelial cells that are attached to each other *via* tight junctions. The integrity of this tight junction can be altered by specific polymers like chitosan, which causes separation of tight junction seals (Kondoh *et al*., 2012). Another possible uptake route is trans-cellular route whereby particles of approximately 100 nm to 1 μm in size are transported through M-cells in Peyer's patches and subsequently released at the basolateral side of the intestinal epithelium (Aprahamian *et al*., 1987; Carr *et al*., 1996; Hoet *et al*., 2004). Particles may enter M-cells through endocytosis such as clathrin-mediated endocytosis or fluid-phase endocytosis (Sahay *et al*., 2010). Specific nanoparticles characteristics such as size, surface charge and surfactant coating may

influence the trans-cellular uptake of nanoparticles in the gastrointestinal tract (Russell-Jones *et al*., 1999; Hoet *et al*., 2004).

2.6.3 Distribution and Metabolism

If the nanoparticles survive local degradation or metabolism within gastrointestinal tract, they will pass through the gastrointestinal epithelium and then enter both blood and lymphatic circulations. Hydrophobic nanoparticles are taken up in the gut-associated lymphoid tissue and transported to lymphoid circulation (Bouwmeester *et al*., 2009). If they are transported through this path, they will reach systematic circulation without being metabolized in the liver (Hunter *et al*., 2012). Hence, nanoparticles are able to bypass first-pass metabolism and increase the concentration of active compounds in the bloodstream. First-pass metabolism is a process where a compound is metabolized by a number of enzymes present mainly in the gut and liver. As previously mentioned, compounds that have been transported *via* chyclomicron-mediated pathway are be able to avoid this first-pass metabolism (Yao *et al*., 2014). Alternatively, nanoparticles are transported to the liver *via* the hepatic portal vein to be processed and delivered to systemic blood circulation (Chen *et al*., 2011).

Upon reaching systemic circulation, compound-loaded nanoparticles (also free compounds) are transported to various organs such as heart, lungs, spleen kidneys, liver and brain (Aillon *et al*., 2009). During the transportation, interaction between nanoparticles (including free compounds) with various blood components such as plasma-proteins, platelets, coagulation factors, red and white blood cells may occur (Nemmar *et al*., 2002). Interaction with these blood components may substantially influence the distribution and excretion of the nanoparticles. Aforementioned organs are exposed to higher concentration of nanoparticles by the virtue of higher blood flow (Faraji & Wipf, 2009). The metabolism of nanoparticles depends primarily on the type

of material used to construct them. However, little is known on the metabolic processes of nanoparticles and their components within systemic circulation.

When nanoparticles in systemic circulation have reached the targeted organs, the entrapped compounds are eventually released and then diffuse into the cells or tissue of the organs (Chen *et al*., 2011). However, the nanoparticles are restricted from passing through natural barriers like the cellular-, blood-brain-, blood-milk- and placental barriers (Bouwmeester *et al*., 2009). These barriers present a rigorous defence mechanism from blood borne particle exposure. Release of active compounds can be stabilized through the use of polymer like alginate and chitosan whereby a layer-by-layer technique is applied to prevent burst release. In addition, the mechanism of release could also be controlled through the use of polymers that are sensitive to a specific condition. For instance, polyethylene glycol (PEG) has been shown to increase pH-stimulated lysozyme release (Quintanilla-Carvajal *et al*., 2010).

The location where active compounds are released will determine their fate inside the body. If the compounds are released into the intestine, they are either transported into lymphatic system or portal vein routing them to the liver (Hunter *et al*., 2012; Markovsky *et al*., 2012). In systemic circulation, the properties of the compounds will determine how they interact with blood components. A hydrophilic non-ionic compound will remain in circulation longer than a hydrophobic ones (Sheng *et al*., 2009). If the compounds are released into the cells of organ tissues, they may follow the pathways of typical water-soluble or fat-soluble bio-macromolecules depending on their chemical and physical properties (Sahay *et al*., 2010). Different compounds will provide different bioactivities in the cells and tissues of the organ depending on their metabolism and the potential function of the metabolites. For example γ-tocopherol, which is an active form of vitamin E, appears to be highly effective in preventing cancer-related processes (Brigelius-Flohé, 2006).

2.6.4 Excretion

Excretion of nanoparticles occurs when they are not able to pass through epithelial cells or when they are degraded by liver metabolism. Nanoparticles can also pass by the epithelial cells and mucus without being absorbed and eventually enter the colon for excretion. Eventhough they are able to pass through the epithelial cells, they are exposed to the liver metabolism; if this happens, they may re-enter the intestines and subsequently excreted (Bertrand & Leroux, 2012). Hydrophilic nanoparticles may be excreted by kidney through urinary tract if their average dimension is smaller than 10 nm.

2.7 Concluding remarks

Nanoparticle-based delivery system offers a multitude of physical and chemical advantages in enhancing bioavailability and stability of bioactive and drugs. A specific type of the system offers distinct benefits for bioactive and drugs with different properties and applications. The physical-chemical characteristics, behaviour of the nanoparticle-based delivery system and also its morphological properties will determine the manner of its interaction with human body and absorption-distribution-metabolism-excretion (ADME) profile. Currently, the potential risks of nanoparticles to the human health are not fully known and understood. Detailed investigation should be conducted in this aspect.

CHAPTER 3: OPTIMIZATION OF WATER-OIL-SURFACTANT RATIO FOR NANOEMULSION TEMPLATING

3.1 Summary

Polymeric nanoparticles gain a widespread interest in food and pharmaceutical industries as delivery systems that encapsulate, protect and release lipophilic compounds such as omega-3 fatty acids, fat-soluble vitamins, carotenoids, carvedilol, cyclosporine, ketoprofen etc. In this study, medium-chain-length poly-3-hydroxyalkanoates (mcl-PHA)-incorporated nanoparticle was developed *via* facile organic solvent-free nanoemulsion templating technique. The ratio of non-ionic surfactants (polyethoxylated castor oil - Cremophor EL and sorbitan oleate – Span 80) and Jojoba oil (O) were first optimized by using response surface methodology (RSM) to obtain nanoemulsion template prior to incorporation of mcl-PHA. The effects of water content (W:(S:O)), surfactant-to-oil ratio (S:O) and Cremophor EL-to-Span 80 ratio (Cremo:Sp80) on nanoparticle formation were investigated. The polymeric nanoparticle system showed a good preservation capability of ß-carotene and prolonged storage stability.

3.2 Introduction and literature review

The incorporation of bioactives into food and beverage products for the prevention of diet-related chronic diseases such as heart disease, diabetes, hypertension and cancer is the focus of many advanced researches (Stan *et al*., 2008; Omara *et al*., 2010; Udenigwe & Aluko, 2012; Huang *et al*., 2013). However, many bioactive compounds showed poor water solubility and stability, which significantly reduce their efficiency as disease-preventing and health promoter agent in nutraceuticals. Likewise, it is reported that inadequacy of water solubility among new drug candidates is

common, which cause major problem in terms of poor bioavailability and therapeutic index in pharmaceutical industry (Lipinski, 2002). In order to circumvent this problem thence improves bioavailability of the lipophilic bioactives and drugs, the use of lipid-based nanodelivery system like nanoemulsion is considered as the most promising route for oral delivery (McClements *et al*.,, 2009; Kuentz, 2012). In addition, it is flexible in terms of compatibility with many food matrices (McClements, 2011). Furthermore, incorporation of drugs or medicines into the nanoparticle has also made it possible to prolong their circulation in bloodstream hence increase their therapeutic index *via* intravenous means and reduce the risks of embolism (Ganta & Amiji, 2009; Couvreur, 2013).

Oil-in-water (O/W) nanoemulsion can be prepared mechanically *via* high-energy or low-energy input method. The former requires mechanical equipment that generates intense force to disrupt and intermingle water and oil phases e.g. ultrasonicator, high-pressure homogenizer and microfluidizer (Yang *et al*., 2012). Conversely, low-energy approach such as emulsion inversion point (EIP) or phase inversion composition (PIC) (Maestro *et al*., 2008; Ostertag *et al*., 2012), phase inversion temperature (PIT) (Anton & Vandamme, 2009) and spontaneous emulsification (Saberi *et al*., 2013) methods rely on the formation of oil droplets in surfactant-oil-water mixture system under favorable conditions. The O/W nanoemulsion can be utilized as a template to produce polymeric nanoparticle. For instances, polymeric nanoparticles can be engineered *via* nanoemulsion templating by *in situ* polymerization in the dispersed phase of the nanoemulsion (Vauthier & Bouchemal, 2009) or using preformed polymer, which is initially dissolved in volatile organic solvent as dispersed phase of the nanoemulsion and followed by solvent evaporation (Calderó *et al*., 2011; Fornaguera *et al*., 2015a). The later method is more biocompatible than the former as it circumvents the use of reactive substances (polymerizing/crosslinking initiator) and generation of byproducts.

Nevertheless, residual solvent accrues toxicity concern. In addition, both methods require subsequent steps i.e. purification and solvent removal in order to obtain the polymeric nanoparticle (Vauthier &Bouchemal, 2009), which could pose disposal and recycling issues in scaling up of the nanoparticle production.

Development of biodegradable polymeric nanoparticles for active compounds delivery into human body has gained a major interest in nutraceutical and pharmaceutical industries. For instance, oral delivery of bioactive curcumin encapsulated in polymeric nanoparticle for human cancer therapy has been reported (Bisht *et al*., 2007). Biopolymer nanoparticle has also been used to deliver galantamine and loperamide for neurodegenerative diseases treatment (Fornaguera *et al*., 2015a,b). Natural polymers possess specific characteristics that make them extremely useful in the production of polymeric nanoparticle (Mora-Huertas *et al*., 2010). Polysaccharides of plant and microbial origins (starch, gum arabic, carrageenan, xanthan gum, dextran etc.) and proteins (soy proteins, gelatin, casein etc.) have been used to construct delivery systems (Sundar *et al*., 2010). However, to the best of our knowledge, the application of medium-chain-length poly-3-hydroxyalkanoates (mcl-PHA) as raw material to construct polymeric nanoparticles has never been explored. Mcl-PHA is a biocompatible and biodegradable polymer produced intracellular by bacteria such as *Pseudomonas sp.* under nutrient stress conditions (Gumel *et al*., 2012).

The objective of this study is to develop mcl-PHA-incorporated nanoparticles through nanoemulsion templating using standard EIP method as a novel delivery system. A nanoemulsion system made up of Span 80, Cremophor EL, jojoba oil and water provides a basis or template to build the nanoparticle system. Response surface methodology was utilized to investigate the effects of key process variables and to optimize the formulation ratio in order to obtain the desired range of mean oil droplet size. β-carotene was used as the model compound for the encapsulation and

preservation studies. The study demonstrates the potential of mcl-PHA-incorporated nanoparticle as a nanodelivery system with enhanced protection for labile compounds.

3.3 Methodology

3.3.1 Materials

Oil phase: Jojoba oil (Sigma-Aldrich) was used as carrier oils. Mcl-PHA and *β*-carotene (Sigma-Aldrich) were used as additive and model compound, respectively, in the emulsion system.

Surfactants: Cremophor EL (polyethoxylated castor oil) and Span 80 (sorbitan oleate) were purchased from Sigma-Aldrich. The *HLB* value for Cremophor EL and Span 80 are 14 and 4.3, respectively.

Water phase: Ultrapure water (Easy, Heal Force, China) was used to prepare all emulsions.

3.3.2 Methods

3.3.2.1 Mcl-PHA synthesis, purification and characterization

Medium-chain-length poly-3-hydroxyalkanoates (mcl-PHA) was biosynthesized by *Pseudomonas putida* Bet001 utilizing a two–stage culture system in shake flasks with octanoic acids (1 % *w/v*) as the sole carbon and energy source (Ishak *et al*., 2016). Bacterial cultivation was carried out at 30 °C and the shaker rotation speed was kept constant at 200 rpm in all experiments. Rich medium (200 ml) and E2 medium (200 ml) were used for the first and second stage of fermentations, respectively. After 24 hours of E2 medium cultivation, the cells were harvested and dried at 70 °C until constant weight. Mcl-PHA was extracted from the cells using acetone and purified repeatedly by cold methanol precipitation (Ishak *et al*., 2016). The extracted mcl-PHA showed glass transition, melting and decomposition temperatures at about -37 °C, 52 °C and 250 °C,

respectively. It consisted of 90 mole % 3-hydroxyoctanote, 5 mole % 3-hydroxyhexanoate and 5 mole % 3-hydroxydecanoate. Its weight average molecular weight (M_w) was determined at 77,435 $gmol^{-1}$ (polystyrene standard equivalent).

3.3.2.2 Formulation of nanoemulsion system

Preliminary experiments were conducted in screw-cap tubes (10.0 cm long × 1.0 cm internal diameter) at room temperature (25 ± 1 °C). Emulsion was obtained through emulsion-inversion-point (EIP) method i.e. by changing the compositon of water-to-oil ratio (W:O) to induce phase inversion. Ultrapure water (W) was added dropwise into the organic mixtures (surfactants [S] and oil [O]) with simultaneous vortexing at room temperature (25 ± 1 °C). The final weight for each suspension systems was 5.0 gram. The ratio of surfactant-to-oil (S:O) studied was more than 1.0 for each level of Cremophor EL-to-Span 80 ratio at 80 and 90 % of water content (W:(S:O)) as shown in Tables 3.1 and 3.2.

The effects of three selected independent variables *viz.* water-to-organic phase ratio or water content (W:(S:O)), surfactant-to-oil ratio (S:O) and Cremophor EL-to-Span 80 ratio (Cremo:Sp80) were studied using Box-Behnken Design (BBD). These effects were evaluated in terms of generated oil droplets size. The range of uncoded independent variables, which were determined from the preliminary experiment results are presented in Table 3.3. The emulsification were conducted in a similar manner to the preliminary experiments. Randomized run order was generated using Minitab 16.0 software with three replicates for each level.

Table 3.3: Range of uncoded independent variables for Box-Behnken design experiment

Independent variables	Levels		
	Lowest	**Middle**	**Highest**
W:(S:O) ($\boldsymbol{X_1}$)	80:20	85:15	90:10
S:O ($\boldsymbol{X_2}$)	60:40	70:30	80:20
Cremo:Sp80 ($\boldsymbol{X_3}$)	50:50	65:35	80:20

3.3.2.3 Hydrophilic-lipophilic balance (*HLB*) number for surfactant mixture

The *HLB* of a surfactant mixture is taken to be an algebraic mean of its components and calculated using Equation 3.1 (Myers, 1990):

$$HLB_{mix} = f_A \times HLB_A + (1 - f_A) \times HLB_B \quad \textbf{Eq. 3.1}$$

where f_A is the weight fraction of surfactant A in the surfactant mixture. The *HLB* values of Cremophor EL (HLB_A) and Span 80 (HLB_B) are 14 and 4.3, respectively.

3.3.2.4 Incorporation of mcl-PHA and β-carotene in nanoemulsion

Mcl-PHA was incorporated into the nanoemulsion system after the optimal ratio of other components (water, jojoba oil, Cremophor EL, Span 80) has been determined (*section 3.2.2.2*). Incorporating mcl-PHA into the O/W emulsion system was accomplished by pre-heating the polymer with organic mixture (optimal amount of surfactants and oil) overnight at 75 °C with intermittent vortexing to aid the dissolution of solid PHA. Subsequently, emulsification was carried out at 75 °C by using ultrapure water that has been pre-heated to the same temperature. Different mcl-PHA amounts (1 to 6 % *w/w* of oil fraction) for incorporation were investigated in this study.

For the encapsulation of β-carotene, half fraction of the jojoba oil was used to dissolve β-carotene (0.01 % *w/w*) while the other half was mixed with surfactants and heated to 75 °C. Jojoba oil fraction with dissolved β-carotene was added to the heated mixture prior to emulsification process. Addition of β-carotene was done in this manner in order to minimize thermal effects towards β-carotene.

It should be noted that the amount of mcl-PHA and β-carotene incorporated into the emulsion formulation determined the final jojoba oil fraction. Accordingly, the amount of jojoba oil was reduced with increased fraction of mcl-PHA and β-carotene (% *w/w* of total oil fraction) so as to keep the final weight of the emulsion system constant at 5.0 g.

3.3.2.5 Stability of mcl-PHA-incorporated nanoemulsion

The stability of standard nanoemulsion and mcl-PHA-incorporated nanoemulsion at different amounts of mcl-PHA (1, 1.5, 2, 2.5 % *w/w* of oil fraction) was investigated continuously for the duration of four months. Each suspension system sample was stored at three different temperatures (10, 25 and 40 °C) in a dark condition. Measurements of mean size and size distribution of nanoparticles were carried out once every fortnight. Experiments were conducted in triplicate for each sample under sterile condition to avoid contamination by microorganisms.

3.3.2.6 Characterization of particle size and size distribution

The size and distribution of nanoparticles were measured based on the mean particle diameter (Zeta average) and particle size distribution (polydispersity index-PDI) of the suspension system, respectively. They were measured through dynamic light scattering (DLS) technique using Zetasizer-nanoseries (ZEN3600, Malvern Instruments

Ltd, UK). The samples were diluted with ultrapure water (0.05 ml of sample in 0.95 ml H_2O) to avoid multiple scattering effects.

3.3.2.7 *β*-carotene degradation profile

Stability of *β*-carotene encapsulated in standard nanoemulsion (without mcl-PHA) and mcl-PHA-incorporated nanoemulsion with different amounts of mcl-PHA (1.0, 1.5, 2.0 and 2.5 % *w/w* of total oil fraction) was investigated. To this end, 0.5 ml sample of suspension system was diluted with 1.5 ml ultrapure water in a cuvette and sealed with parafilm to avoid evaporation. Then, its absorbance was taken at 466 nm using UV-Vis spectrophotometer (V630, Jasco, Japan). 0.5 ml sample of suspension system without *β*-carotene was used as blank after dilution with 1.5 ml ultrapure water. Subsequently, 20 µl 1 mM benzoyl peroxide solution in methanol was added into the diluted sample followed by gentle shaking. The sample solution was stored in the dark at 25 + 1 °C and its absorbance was taken periodically. Experiments were conducted in triplicate for each sample. The degradation percentage of *β*-carotene was calculated as shown below **(**Equation 3.2):

$$\beta - \text{carotene degradation } (\%) = \frac{Abs_0 - Abs_t}{Abs_0} \times 100 \qquad \textbf{Eq. 3.2}$$

where Abs_0 is initial absorbance and Abs_t is absorbance at a particular time interval, *t*.

3.4 Results and discussion

3.4.1 Preliminary experiment

The effects of water content (*w/w*), surfactant-to-oil ratio (S:O) and surfactant mixtures ratio (Cremo:Sp80) on the mean particle diameter of emulsion were investigated. The size of the oil droplets produced was highly depended on S:O and Cremo:Sp80 (Tables 3.1 and 3.2). In contrast, water content with 80 and 90 % (*w/w* of total weight) did not show any significant effects on the size of oil droplets. Thus, the following disccusions are relevant for emulsion with 80 and 90 % water content following its insignificant effect towards oil droplet size produced.

High surfactant-to-oil ratios (90:10 – 50:50) produced emulsion systems with submicrometer oil droplet sizes with the exception of emulsion at 25:75 of Cremophor EL-to-Span 80 ratio (will be discussed later). The results corresponded to other studies that reported a decrease in mean droplet size at high surfactant concentration for nanoemulsion prepared *via* EIP method (Fernandez *et al*., 2004; Jahanzad *et al*., 2009; Mayer *et al*., 2013). Fernandez and co-workers had proposed that high surfactant concentration allows for a complete solubilization of the oil phase near the EIP with the droplet size distribution primarily controlled by the bi-continuous or lamellar phase during the phase inversion (Fernandez *et al*., 2004). Meanwhile, other research groups had suggested that at a relatively high surfactant concentration, O/W/O emulsions are produced during titration and the final mean oil droplet size is determined by the size of the inner oil droplets in the intermediate multiple emulsions (Jahanzad *et al*., 2009; Mayer *et al*., 2013).

Table 3.1: Results of preliminary experiment at 90 % water content

S:O[a] / C:Sp[b]	90:10	80:20	70:30	60:40	50:50
75:25 HLB_{mix} **=11.58**	[c]O = 1.0 % [d]C = 6.75 % [e]Sp = 2.25%  Size (nm) = 36.8 ± 2.7	O = 2.0 % C = 6.0 % Sp = 2.0 %  Size (nm) = 13.3 ± 2.0	O = 3.0 % C = 5.25 % Sp = 1.75 %  Size (nm) = 85.2 ± 2.1	O = 4.0 % C = 4.5% Sp = 1.5%  Size (nm) = 214.1 ± 1.7	O = 5.0 % C = 3.75% Sp = 1.25%  Size (nm) = 259.1 ± 9.9
50:50 HLB_{mix} **=9.15**	O = 1.0 % C = 4.5 % Sp = 4.5 %  Size (nm) = 117.7 ± 3.7	O = 2.0 % C = 4.0 % Sp = 4.0 %  Size (nm) = 69.2 ± 4.9	O = 3.0 % C = 3.5 % Sp = 3.5 % 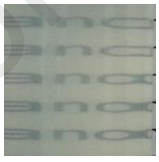 Size (nm) = 22.1 ± 2.5	O = 4.0 % C = 3.0 % Sp = 3.0 %  Size (nm) = 43.3 ± 4.2	O = 5.0 % C = 2.5 % Sp = 2.5 %  Size (nm) = 104.6 ± 5.1
25:75 HLB_{mix} **=6.73**	O = 1.0 % C = 2.25 % Sp = 6.75 %  Size = > 10 μm	O = 2.0 % C = 2.0 % Sp = 6.0 %  Size = > 10 μm	O = 3.0 % C = 1.75 % Sp = 5.25 %  Size = > 10 μm	O = 4.0 % C = 1.5 % Sp = 4.5 %  Size = > 10 μm	O = 5.0 % C = 1.25 % Sp = 3.75%  Size = > 10 μm

[a]S:O = Surfactant : oil, [b]C:Sp = Cremophor EL : Span 80, [c]O = oil, [d]C = Cremophor EL, [e]Sp = Span 80

Table 3.2: Results of preliminary experiment at 80 % water content

S:O[a] / C:Sp[b]	90:10	80:20	70:30	60:40	50:50
75:25 HLB_{mix} =11.58	[c]O = 2.0 % [d]C = 13.5 % [e]Sp = 4.5 %  Size (nm) = 43.3 ± 2.4	O = 4.0 % C = 12.0 % Sp = 4.0 %  Size (nm) = 16.5 ± 1.9	O = 6.0 % C = 10.5 % Sp = 3.5 %  Size (nm) = 102.5 ± 3.2	O = 8.0 % C = 9.0 % Sp = 3.0 %  Size (nm) = 252.3 ± 3.4	O = 10.0 % C = 7.5 % Sp = 2.5 %  Size (nm) = 291.8 ± 8.1
50:50 HLB_{mix} =9.15	O = 2.0 % C = 9.0 % Sp = 9.0 %  Size (nm) = 125.3 ± 4.7	O = 4.0 % C = 8.0 % Sp = 8.0 %  Size (nm) = 91.2 ± 2.8	O = 6.0 % C = 7.0 % Sp = 7.0 % 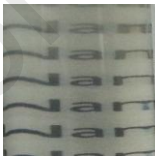 Size (nm) = 25.8 ± 3.5	O = 8.0 % C = 6.0 % Sp = 6.0 % 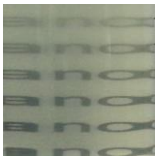 Size (nm) = 45.8 ± 6.5	O = 10.0 % C = 5.0 % Sp = 5.0 %  Size (nm) = 119.6 ± 4.7
25:75 HLB_{mix} =6.73	O = 2.0 % C = 4.5 % Sp = 13.5 %  Size = > 10 μm	O = 4.0 % C = 4.0 % Sp = 12.0 %  Size = > 10 μm	O = 6.0 % C = 3.5 % Sp = 10.5 %  Size = > 10 μm	O = 8.0 % C = 3.0 % Sp = 9.0 %  Size = > 10 μm	O = 10.0 % C = 2.5 % Sp = 7.5 %  Size = > 10 μm

[a]S:O = Surfactant : oil, [b]C:Sp = Cremophor EL : Span 80, [c]O = oil, [d]C = Cremophor EL, [e]Sp = Span 80

Besides S:O, Cremophor EL-to-Span 80 ratio was also a significant parameter in determining the mean oil droplet size in the emulsion. At 75:25 and 50:50 of surfactants mixture ratios, emulsion systems with submicrometer droplet sizes can be obtained (Tables 3.1 and 3.2). Apparently, all emulsions at the two surfactants mixture ratio levels exhibited transparent to mild turbidity with less viscous suspension. In contrast, at 25:75 of Cremophor EL-to-Span 80 ratio, all emulsions showed high viscosities and turbidities due to the presence of many large droplets (> 10 μm). In addition, the mixture showed tendency towards lipophilic property (HLB_{mix} = 6.73) due to the higher fraction of Span 80. Consequently, O/W emulsion could not be produced efficiently.

On the other hand, nanoemulsion with oil droplet size less than 50 nm can be obtained when S:O were in between 90:10 – 80:20 and 70:30 – 60:40 at Cremo:Sp80 of 75:25 and 50:50, respectively (Tables 3.1 and 3.2). From visual inspection, the nanoemulsion systems were transparent indicative of the formation of nano-scale oil droplets, which resulted in less light scattering. Besides *HLB* value, molecular geometry of a surfactant is one of the most important parameters that may influence its ability to form small droplets (Nagarajan, 2002). Even though both surfactants possess same length of hydrocarbon chain with one double bond (C18:1), Cremophor EL has bigger head group with higher number of oxyl groups (thus more hydrophilic) compared to Span 80. This makes Cremophor EL to be easily soluble in water than Span 80 due to more hydrogen bonding with water molecules. On the other hand, Span 80 is expected to have a higher packing parameter (*p*), which is the ratio of the tail group area to the head group area ($p = a_T/a_H$). Thus, Span 80 molecules can be easily adsorbed and arranged at high density onto the oil-water interfacial boundary. Span 80 and Chremophor EL would synergistically enhance the dispersion and solubilization of the oil phase into submicrometer oil droplet sizes. Other study has exploited the synergism effect to induce phase inversion where a couple of surfactants were used to lower the

interfacial tension with respect to a system applying only one type of surfactant (Strey, 1996). Minimum interfacial tension between oil and water phase at phase inversion point has been shown to be the essential state of emulsification in order to obtain emulsion with oil droplet size below than 50 nm (Morales *et al*., 2003; Solans & Solé, 2012).

From the preliminary screening, it can be concluded that S:O must be more than 1 in order to obtain mean oil droplet size less than 50 nm. In addition, the quantity of jojoba oil and Span 80 also played an important role in determining the mean oil droplet size. Oil droplet size was smaller when the ratio of Span 80-to-jojoba oil approximately equal (ratio ≈ 1).

3.4.2 Box-Behnken design experiment

3.4.2.1 Statistical analysis and model fitting

Experiments were conducted in order to optimize water content (W:(S:O)), surfactant mixture-to-jojoba oil ratio (S:O) and Cremophor EL-to-Span 80 ratio (Cremo:Sp80) formulation. The suitable ranges of S:O and Cremo:Sp80 determined for optimization experiments were 60:40 and 80:20 and 50:50 and 80:20, respectively. Meanwhile, the range of water of content was kept constant at 80:20 and 90:20. Table 3.4 shows the list of runs for the three independent variables and their corresponding response variables.

Table 3.4: Mean droplet size obtained at different experimental points in the Box-Behnken design

Condition	Water (g)	Oil (g)	Cremophor EL (g)	Span 80 (g)	Droplet size (nm)	Nano-emulsion
(X_1) 85:15 **(X_2) 70:30** **(X_3) 65:35**	4.25	0.225	0.341	0.184	20.4 ± 1.2	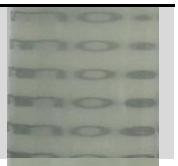
(X_1) 90:10 **(X_2) 60:40** **(X_3) 65:35**	4.50	0.200	0.195	0.105	62.2 ± 1.9	
(X_1) 90:10 **(X_2) 70:30** **(X_3) 50:50**	4.50	0.150	0.175	0.175	32.7 ± 1.9	
(X_1) 90:10 **(X_2) 80:20** **(X_3) 65:35**	4.50	0.100	0.260	0.140	17.1 ± 1.7	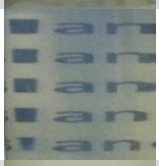
(X_1) 90:10 **(X_2) 70:30** **(X_3) 80:20**	4.50	0.150	0.280	0.070	298.7 ± 15.7	
(X_1) 80:20 **(X_2) 60:40** **(X_3) 65:35**	4.00	0.400	0.390	0.210	64.2 ± 4.7	
(X_1) 80:20 **(X_2) 70:30** **(X_3) 50:50**	4.00	0.300	0.350	0.350	38.4 ± 1.7	
(X_1) 80:20 **(X_2) 80:20** **(X_3) 65:35**	4.00	0.200	0.520	0.280	18.9 ± 1.8	
(X_1) 80:20 **(X_2) 70:30** **(X_3) 80:20**	4.00	0.300	0.560	0.140	348.5 ± 25.5	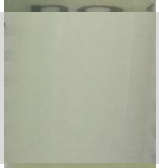
(X_1) 85:15 **(X_2) 80:20** **(X_3) 50:50**	4.25	0.150	0.300	0.300	94.2 ± 3.7	
(X_1) 85:15 **(X_2) 80:20** **(X_3) 80:20**	4.25	0.150	0.480	0.120	15.1 ± 0.5	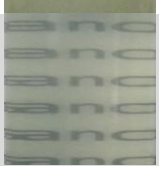

Table 3.4, continued.

(X_1) 85:15 **(X_2) 60:40** **(X_3) 50:50**	4.25	0.300	0.225	0.225	44.5 ± 1.2	
(X_1) 85:15 **(X_2) 60:40** **(X_3) 80:20**	4.25	0.300	0.360	0.090	351.8 ± 10.8	

From ANOVA, both S:O and Cremo:Sp80 showed significant influence (p < 0.05) towards the mean size of oil droplets produced. In addition, the two-way interaction between the two parameters was also significant (p < 0.05). In contrast, water content did not give significant effect on the mean oil droplet size (p = 0.45). Its interaction with the other two parameters was also insignificant (p > 0.05). Summary of ANOVA on these parameters and their interactions is shown in Table 3.5. Only significant factors (p < 0.05) were selected for model fitting.

Table 3.5: ANOVA of independent variables and their interactions

	Factors	***F*-value**	***p*-value**
Linear	X_1	0.65	0.425
	X_2	24.71	0.000
	X_3	111.6	0.000
Square	$X_1 X_1$	4.33	0.049
	$X_2 X_2$	0.89	0.353
	$X_3 X_3$	47.72	0.000
2-way interaction	$X_1 X_2$	0.00	0.911
	$X_1 X_3$	0.62	0.439
	$X_2 X_3$	51.79	0.000

By applying multiple regression analysis on the experimental data, the response surface variable (oil droplet size) and the test variables are related by the following second-order polynomial equation:

$$Y = -808 + (37.15\,X_2) + (-15.6\,X_3) + (0.5185\,X_3^2) + (-0.6442\,X_2X_3)$$

Eq. 3.3

where Y is the size of oil droplets (nm) while X_2 and X_3 are the independent variables for S:O and Cremo:Sp80, respectively. Statistical testing of the model was performed using ANOVA. The high determination cofficient (R^2 = 86.41) indicated that only 14 % of the total variation was not explained by the model. The value of the adjusted determination coefficient (adjusted R^2 = 84.81) also strongly indicated the model utility. High F-value (F = 54.03) and low p-value ($p < 0.0001$) supported the significance of the model.

3.4.2.2 Evaluation of independent variables and their interactions

2-D contour and 3-D response surface were plotted using Minitab 16 software to evaluate the effects of independent variables and their interactions on the mean size of oil droplet produced. The plots showed the effects of two factors on the response while the third factor was kept constant at midpoint level. The contour plots generated were used primarily for investigating the interaction effects between parameters. Water content parameter was included as a mandatory factor and the minimum diameter of the nanoemulsion that could be attained was assumed to be 5 nm (possible diameter for surfactant molecules aggregate – micelle).

Figure 3.1 shows the 2-D contour and 3-D response surface plots for different ranges of W:(S:O) and S:O at fixed Cremo:Sp80, which is 65:35. Varying water content at any level of S:O ratio do not result in significant change to the mean oil droplet size. In contrast, the mean droplet size become smaller as the S:O level increases indicating insignificant interaction between these parameters ($p \approx 0.9$).

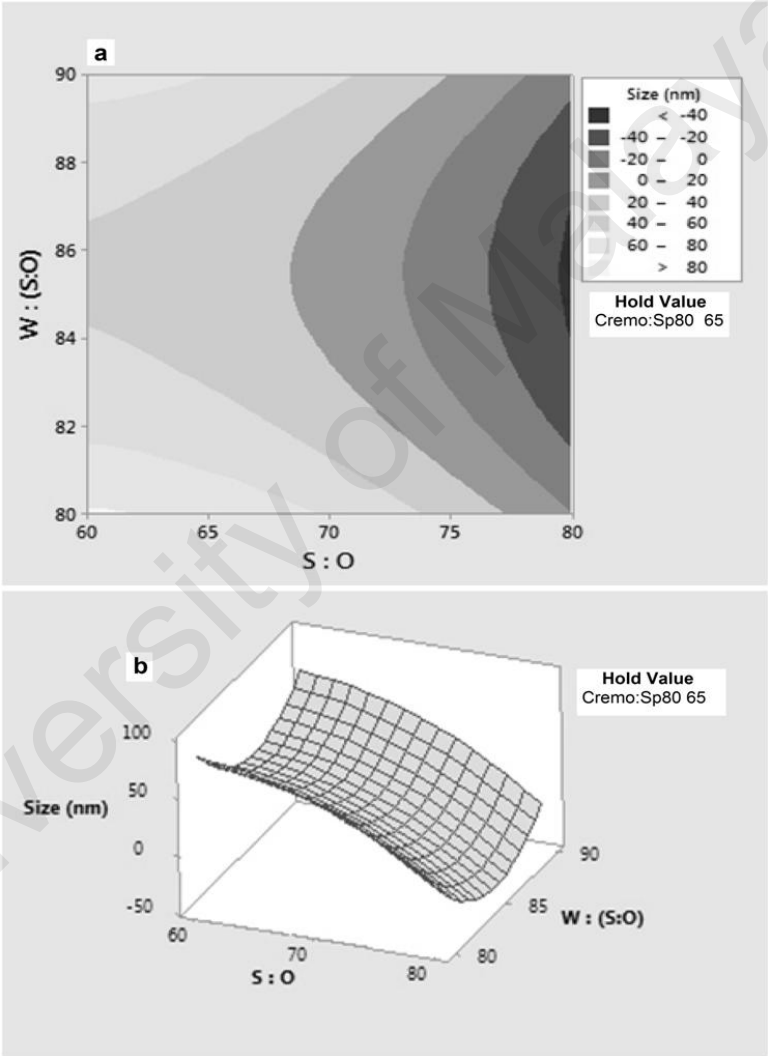

Figure 3.1: Contour (*a*) and surface (*b*) plots showing the effects of W:(S:O) and S:O ratios on the mean oil droplet size produced at constant Cremo:Sp80

In Figure 3.2, with S:O ratio held constant at 70:30, nanoemulsion with mean oil droplet size of 50 nm and below could be obtained when Cremo:Sp80 is approximately 68:32 and below. The mean droplet size increases at higher Cremo:Sp80 ratios indicating that the *HLB* value plays an important role in the EIP-based emulsification process. On the other hand, water content do not significantly influence the mean droplet size at any level of Cremo:Sp80 ratio indicating no interaction effect between these two parameters ($p \approx 0.5$).

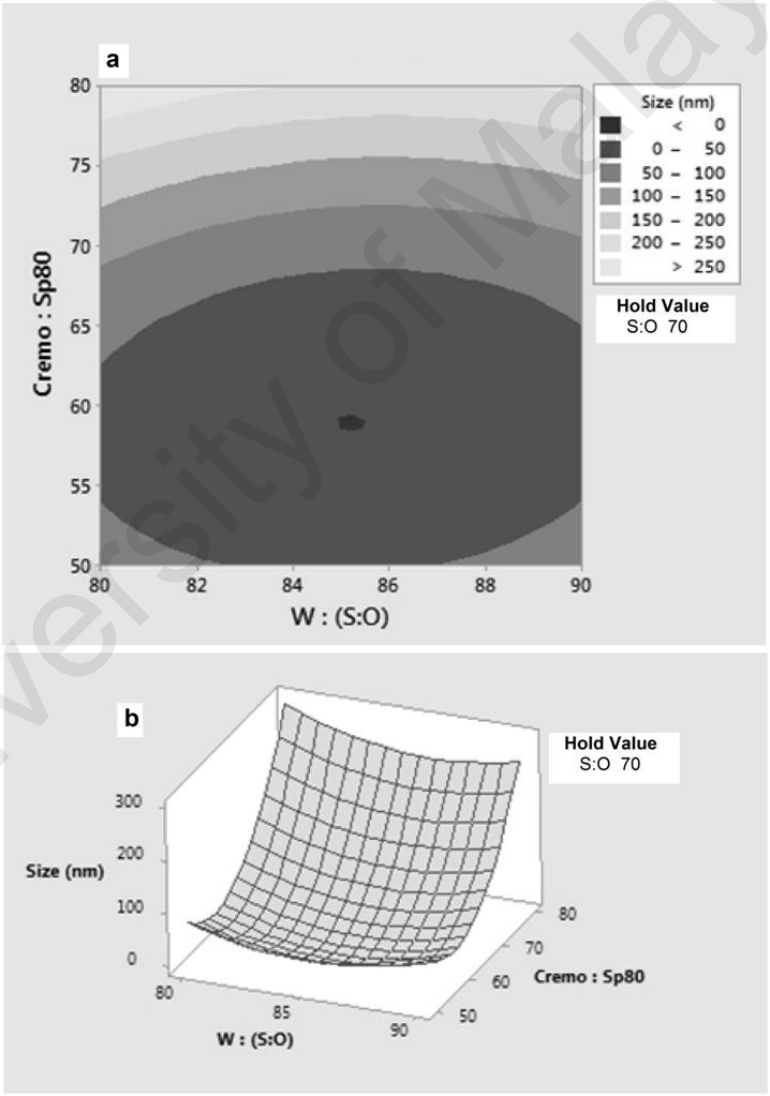

Figure 3.2: Contour (*a*) and surface (*b*) plots showing the effects of Cremo:Sp80 and W:(S:O) ratios on the mean oil droplet size produced at constant S:O

Figure 3.3 shows the 2-D contour and 3-D response surface plots for different ranges of Cremo:Sp80 and S:O at fixed W:(S:O), which is 85:25. The reduction in the mean size of oil droplets could be significantly obtained by lowering the Cremo:Sp80 ratio. The observation pointed to a significant interaction effect between these two parameters ($p < 0.05$) and is shown as butterfly-shaped surface plot (Figure 3*b*). This interaction effects could be attributed to two possible factors i.e. the *HLB* value and synergism effect between the surfactants as discussed earlier. Optimal ratio of Chremophor EL–Span 80–Oil may induce minimum interfacial tension of the water-oil-surfactant system at phase inversion point, which is imperative to obtain nanoemulsion with oil droplet size below than 50 nm (Morales *et al*., 2003; Solans & Solé, 2012).

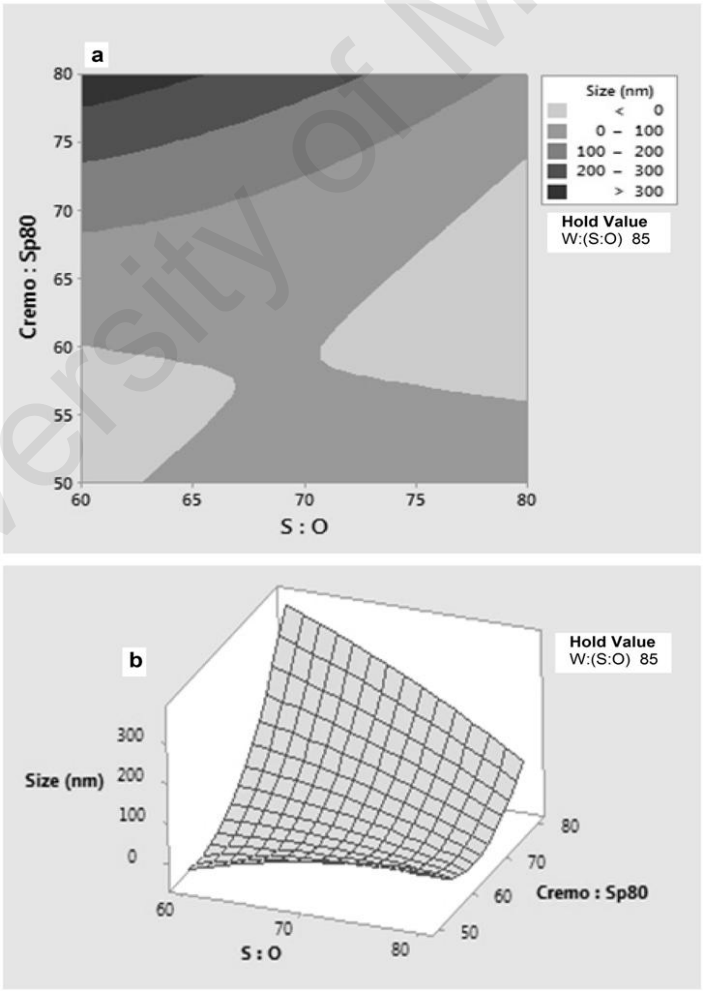

Figure 3.3: Contour (*a*) and surface (*b*) plots showing the effects of Cremo:Sp80 and S:O ratios on the mean oil droplet size produced at constant W:(S:O)

3.4.2.3 Optimization of nanoemulsion formulation

Figures 3.1-3.3 show the dynamic effects of the three studied factors (W:(S:O), S:O and Cremo:Sp80 on the mean droplet size of nanoemulsion produced. They also allows for the optimum trajectory to be rapidly assessed and determined. By setting the target of mean droplet size to be within 20 to 23 nm into the optimization routine, optimal ratios of W:(S:O), S:O and Cremo:Sp80 were determined at 86:14, 70:30 and 63:37, respectively. These ratios were verified and average oil droplet size of the nanoemulsion obtained was clearly within predicted size range (Figure 3.4 - *green line*). On the other hand, deviations from optimal ratio of Cremo:Sp80 (63:37) resulted in consistent shift of mean oil droplet size and size distribution plots to a larger size range (Figure 3.4 – *red, yellow, gray and blue lines*). The shift was attributed to the gradual change in terms of *HLB* value of the surfactants mixture towards lipophilic property. Thus, the oil phase could not be efficiently dispersed and solubilized into smaller size droplet to produce nanoemulsion.

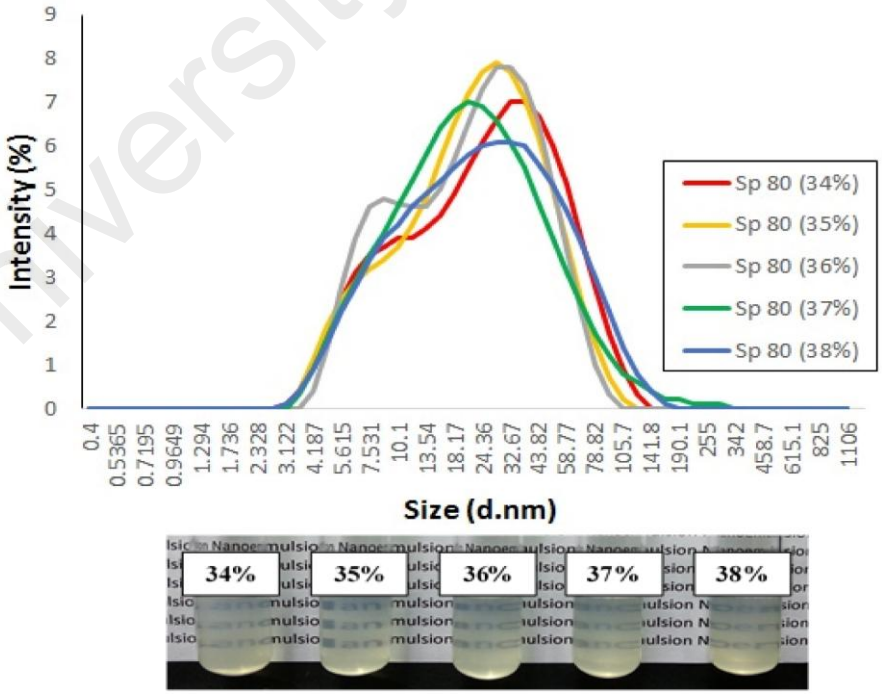

Figure 3.4: Particle size distribution of nanoemulsion at different concentrations of Span 80

3.4.3 Verification of the model

Table 3.6 shows the outcome of the verification experiments along with their predicted results (calculated using Equation 3.3) of mean oil droplet sizes. The model was able to predict the experimental results satisfactorily especially for emulsion system with narrow droplet size distribution (small PDI value) e.g. emulsion system W:(S:O) = 87:13, S:O = 75:35 and Cremo:Sp80 = 65:35 (Table 3.6).

Table 3.6: Verification results of seven different ratio formulations chosen randomly from the contour plot

Condition	Predicted size (nm)	Measured size (nm)	Polydispersity Index (PDI)	Nano-emulsion
W:(S:O) = 82:18 **S:O** = 65:35 **Cr:Sp80** = 65:35	61.60	30.42 ± 2.2	0.266 ± 0.06	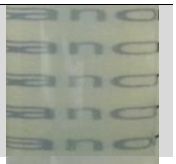
W:(S:O) = 85:15 **S:O** = 70:30 **Cr:Sp80** = 65:35	38.1	23.64 ± 1.2	0.313 ± 0.01	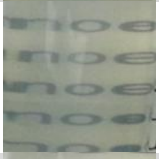
W:(S:O) = 87:13 **S:O** = 75:35 **Cr:Sp80** = 65:35	14.4	17.62 ± 2.5	0.236 ± 0.01	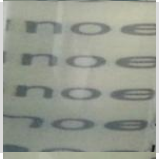
W:(S:O) = 80:20 **S:O** = 70:30 **Cr:Sp80** = 80:20	84.6	90.3 ± 3.8	0.640 ± 0.07	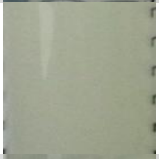
W:(S:O) = 85:15 **S:O** = 70:30 **Cr:Sp80** = 70:30	31.4	41.1 ± 2.7	0.377 ± 0.07	
W:(S:O) = 87:13 **S:O** = 75:25 **Cr:Sp80** = 55:45	17.5	20.3 ± 0.9	0.293 ± 0.01	
W:(S:O) = 85:15 **S:O** = 60:40 **Cr:Sp80** = 70:30	255.4	114.0 ± 1.7	0.862 ± 0.09	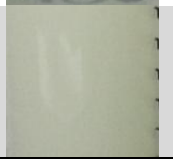

3.4.4 Incorporation of mcl-PHA and *β*-carotene into nanoemulsion

The mean size of nanoparticles was observed to be below than 50 nm when the mcl-PHA amount was 3 % (*w/w* of total oil fraction) and lower (Figure 3.5**)**. However, at higher mcl-PHA amount, nanoparticles with mean size about 190 nm were obtained. It has been shown that successful formation of O/W emulsion through EIP method is crucially dependent upon the formation of bi-continuous or lamellar structure at phase inversion point (Fernandez *et al*., 2004; Morales *et al*., 2003; Solans & Solé, 2012). The molecular composition of the water-oil-surfactant system influences the formation of bi-continuous or lamellar phase, which in turn dispersed into submicrometer oil droplets following the phase inversion point. Formation of these structures indicates minimum interfacial tension between oil and water phase. Adding more than 3 % (*w/w* of total oil fraction) of high molecular weight mcl-PHA (77,435 g mol^{-1}) increased the interfacial tension thus disturbed the formation of aforementioned structures. Consequently, nano-sized particles could not be produced efficiently. The result obtained in this study is comparable with other study i.e. ~ 45 nm of biopolymeric nanoemulsion was obtained by using 10,000 $gmol^{-1}$ of poly(lactic-*co*-glycolic acid) at 4 % (*w/w*) in ethanol/ethyl acetate mixture as dispersed phase (Fornaguera *et al*., 2015a).

Figure 3.6 shows nanoemulsion incorporated with mcl-PHA at different amount (1 – 2.5 % *w/w* of total oil fraction) and *β*-carotene at constant amount. Incorporation of *β*-carotene into the mcl-PHA-incorporated nanoemulsion shows negligible effects on the particle size and size distribution compared to standard nanoemulsion (without mcl-PHA). It is suggested that encapsulation of *β*-carotene within the mcl-PHA-incorporated nanoparticles did not compromise its structural integrity.

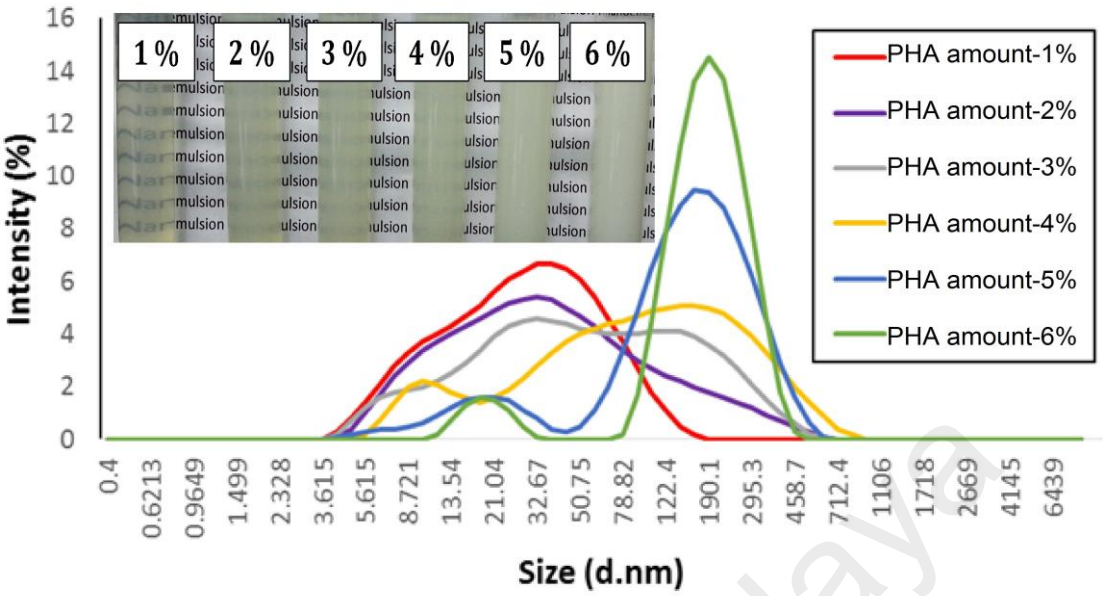

Figure 3.5: Particle size distribution of mcl-PHA-incorporated nanoemulsion at different mcl-PHA percentage of total oil fraction (*w/w*)

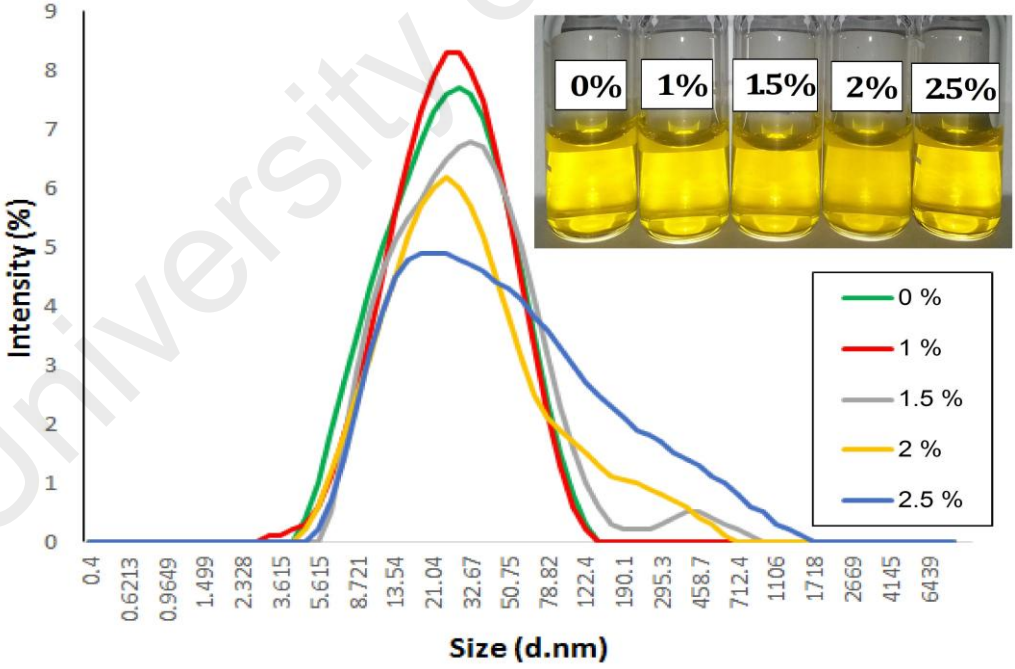

Figure 3.6: Particle size distribution of β-carotene-loaded nanoparticles at different mcl-PHA percentage of total oil fraction (*w/w*)

3.4.5 Stability of *β*-carotene encapsulated in mcl-PHA-incorporated nanoemulsion

β-carotene degradation rate was reduced significantly when mcl-PHA was incorporated into the nanoemulsion (Figure 3.7). Peroxide compounds encountered the polymer matrix of mcl-PHA-incorporated nanoemulsion before it could traverse to the internal *β*-carotene for oxidation reaction. Therefore, the mass transfer of oxidizing agent into the mcl-PHA-incorporated nanoemulsion was significantly curtailed compared to the standard nanoemulsion, resulting in lower degradation kinetic of *β*-carotene. Oxidation of *β*-carotene can be readily visualized from the alteration of color intensity in strong yellow-colored nanoemulsion, which gradually turning into faint yellow as oxidation proceeds with time (*see inserts in* Figure 3.7).

Structurally, the mcl-PHA-incorporated nanoparticle is expected to resemble a polymer-based encapsulation system called nanocapsule whereby a polymer forms an internal coating layer that surrounds the bioactive-rich liquid core (vesicular system) (Mora-Huertas *et al*., 2010).

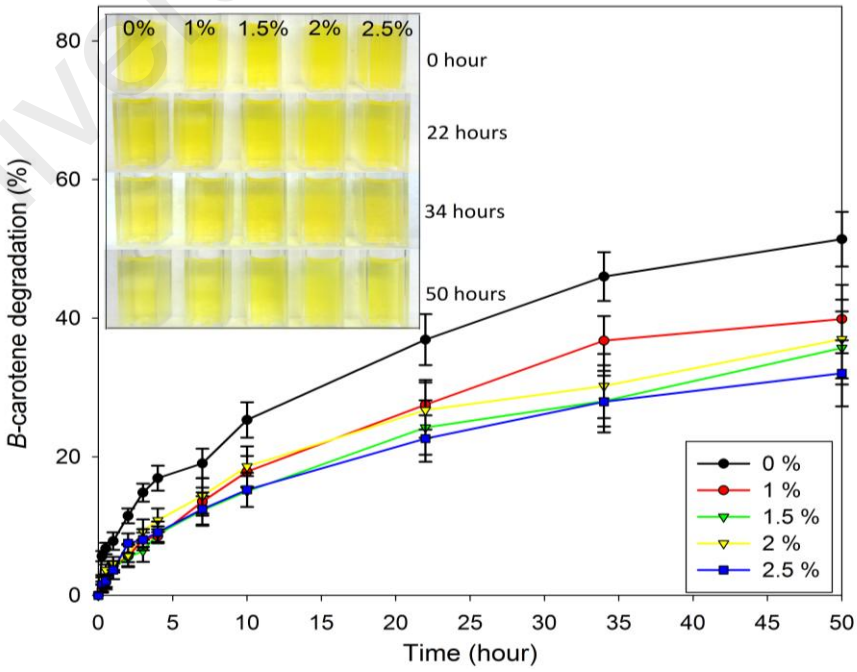

Figure 3.7: *β*-carotene degradation profiles for standard nanoemulsion and mcl-PHA-incorporated nanoemulsion

3.4.6 Storage stability of mcl-PHA-incorporated nanoemulsion

The thermostability of mcl-PHA-incorporated nanoemulsion was investigated and the results are shown in Figure 3.8. The incorporation of mcl-PHA (1 – 2.5 % *w/w*) into the nanoemulsion did not cause observable stability concern to the system (in terms of particle size and distribution) when stored at 10 (Fig. 3.8*a*, *b*), 25 (Fig. 3.8*c*, *d*) and 40 °C (Fig. 3.8*e*, *f*). The nanoparticle size and size distribution exhibited insignificant differences throughout the storage period (16 weeks) ($p > 0.05$). Similarly, nanoemulsion system without mcl-PHA incorporation also showed similar results indicating that combination of Cremophor EL and Span 80 was able to form stable interfacial complexes (i.e. film) to prevent coalescence, concurrent with effective lowering of the interfacial tension.

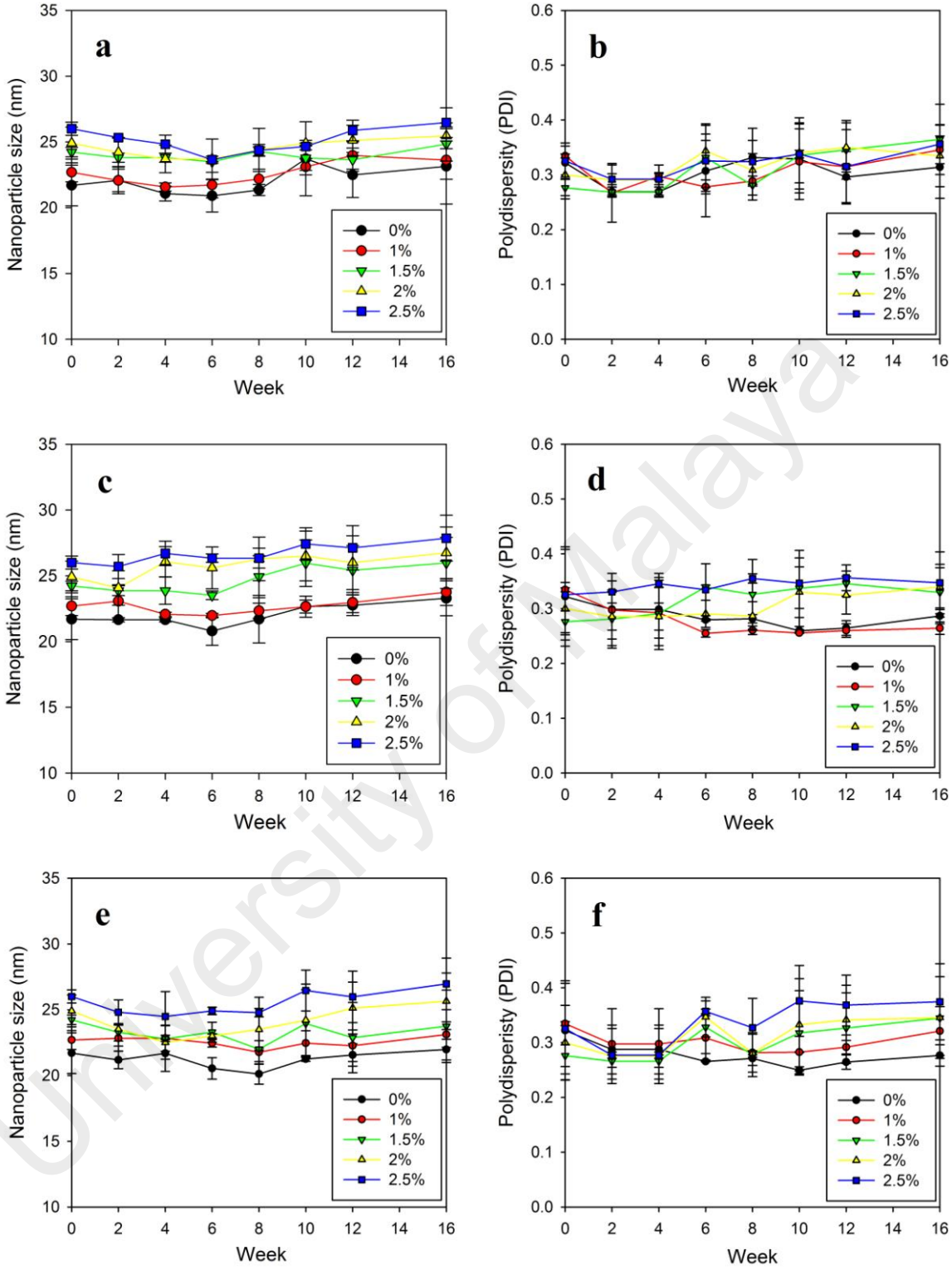

Figure 3.8: Storage stability of nanoparticles stored at 10 °C (*a*-*b*), 25 °C (*c*-*d*) and 40 °C (*e*-*f*). Particle size (*a*, *c* and *e*); size distribution (*b*, *d* and *f*)

3.5 Concluding remarks

The study contributes to the development of new biopolymer-based encapsulation system utilizing mcl-PHA through low-energy emulsification technology. It was demonstrated that the incorporation of mcl-PHA into the oil droplets could be accomplished via standard EIP method at elevated temperature. The facile method does not require subsequent purification step in the absence of cross-linking initiator usage. Moreover, the use of organic solvent, which is common in the production polymeric nanoparticle through solvent evaporation method, can be circumvented.

The optimal ratios of W/(S/O), S/O, and Cremo/Sp80 to obtain nanoemulsion with oil droplet size below than 50 nm were 86:14, 70:30, and 63:37, respectively. At M_W = 77,435 g mol^{-1}, 2.5% mcl-PHA (w/w of total oil fraction) was the amount limit of incorporation to produce nanosized particles. Nevertheless, it is expected that more mcl-PHA amount could be incorporated into the nanoemulsion if lower molecular weight mcl-PHA is used.

Significant amount of β-carotene preserved within the mcl-PHA-incorporated nanoemulsion after the addition of oxidizing agent indicated that mcl-PHA could offer a protective structure within the nanoparticle. Insignificant changes in particle size and size distribution throughout 4-month storage period at different temperatures testified to the excellent storage stability of mcl-PHA-incorporated nanoemulsion.

CHAPTER 4: FORMATION MECHANISM OF MCL-PHA-INCORPORATED NANOPARTICLE THROUGH PIE

4.1 Summary

The assembly of nanoparticle incorporating bacterial medium-chain-length poly-3-hydroxyalkanoates (mcl-PHA) *via* phase inversion emulsification (PIE) was investigated. Sequential addition of water into agitated mixture of carrier oil (jojoba oil), non-ionic surfactants (Cremophor EL and Span 80) and melted mcl-PHA triggered phase inversion of water-in-oil (W/O) to oil-in-water (O/W) emulsion. Emulsion inversion point (EIP) at 30 % *w/w* of water content was determined by abrupt changes in viscosity and conductivity of the suspension. Concurrently, infrared transmittance of O-H group of water, C-O-C group of surfactants and C-H group of alkane chain were practically identical while small-angle X-ray scattering indicated the presence of bi-continuous or lamellar structure. The morphology of the emulsion changed, with increasing water content, from W/O to bi-continuous or lamellar structure and finally to O/W. Mcl-PHA appears to form a bridging polymeric network, covering the nanoparticle with a protective layer for enhanced protection of the encapsulated compound. A hypothetical mechanism for the mcl-PHA-based nanoparticle assembly is also proposed.

4.2 Introduction and literature review

Emulsion is a mixture of two immiscible liquid phases, in which one phase is dispersed in the form of droplets (dispersed phase) in another phase (continuous phase). Typically, these liquids are water and oil-based phases. Emulsification technology has been widely used to produce emulsion in various fields especially in pharmaceutical, food and cosmetic industries (Salager *et al.*, 2004). Normally, emulsions with small

droplets (< 0.1 μm) and narrow size distribution are desired in those applications. For instances, nano-sized emulsion could help improving the delivery of active molecules through oral (Huang *et al.,* 2010), intranasal (Kumar *et al.,* 2008), intravenous (Fast & Mecozzi, 2009) and topical (Mou *et al.,* 2008) routes. Generating nanoemulsion using conventional emulsification, which involved vigorous agitation of an immiscible binary mixture, is strenuous, as it requires substantial energy to overcome a huge Laplace pressure. The use of surfactants helps to reduce the Laplace pressure considerably, where only a fraction of the energy required in direct emulsification is needed to form micro- and nanoemulsion (Maali & Mosavian, 2013).

One of the most common emulsification techniques is phase inversion emulsification (PIE), a low energy technique featuring a transition from a water-in-oil (W/O) emulsion to an oil-in-water (O/W) emulsion or *vice versa* (Solans & Solé, 2012; Maali & Mosavian, 2013). PIE is widely used in industry because of its ability to generate emulsion with nano-sized droplets. It can be sub-categorized as catastrophic and transitional (Kumar *et al.,* 2015). Catastrophic phase inversion is initiated by changing the system composition (water-to-oil ratio) through stepwise addition of intended continuous phase, which is known as phase inversion composition (PIC) or emulsion inversion point (EIP) method (Bouchama *et al.,* 2003). The critical volume fraction that induces this inversion is called emulsion inversion point (EIP). In contrast to catastrophic phase inversion, an emulsion system can also be inverted transitionally by altering its formulation *via* changing the strength of interaction between surfactants and fluid phases. Temperature has been shown to modulate the affinity of surfactant toward water and oil phases through phase inversion temperature (PIT) method (Shinoda & Saito, 1968; Sherman & Parkinson, 1978). The temperature that induces this transitional inversion with formation of bi-continuous (*D*) microemulsion or

lamellar liquid crystalline phase is called hydrophile-lipophile balance (*HLB*) temperature.

Catastrophic phase inversion (CPI) takes place during the continuous addition of dispersed phase. Drops of the dispersed phase merge together to form a bi-continous/lamellar structure phase, which is like to occur at high surfactant concentration (Fernandez *et al.,* 2004). In addition, it also could begin with an abnormal emulsion i.e. emulsion that exhibit a complex morphology i.e. double or multiple emulsion, in which the dispersed drops contain droplets of the continuous phase that somehow get inserted into the drops (Sajjadi *et al.,* 2004; Jahanzad *et al.,* 2009). It exhibits an interfacial curvature, against the normal condition forecasted by Bancroft's rule (Salager, 2000). During emulsification, the instability of an abnormal emulsion continuously increases until its inversion into a normal emulsion of the opposite morphology. The phase inversion is influenced by addition rate of the dispersed phase (Zambrano *et al.,* 2003) and stirring intensity of the emulsion (Mira *et al.,* 2003). Detailed discussions on CPI can be found in a number of literatures (Tyrode *et al.,* 2005; Rondón-Gonzaléz *et al.,* 2006, 2007, 2008, 2009).

For detection, observation and visualization of the phase inversion event, both indirect and direct methods can be used. Determination of phase inversion can be indirectly made by the measurement of the electrical conductivity of the emulsion (Lee *et al.,* 2003). For example, when W/O emulsion inverts into an O/W emulsion, the new continuous phase becomes conductive, making it possible to locate the phase inversion point *via* the observation of a rapid increase in electrical conductivity. Conductivity measurement is often used in conjunction with other complementary techniques, for example, the measurement of the emulsion viscosity whereby it depends on the volume fraction of dispersed phase as well as the formulation of the emulsion system (Tyrode *et al.,* 2005; Allouche *et al.,* 2004). The highest value of emulsion viscosity is expected at

the phase inversion point, which may be attributed to the formation of bi-continuous/lamellar structure phase and/or multiple emulsions with a high dispersed-phase volume fraction (Tyrode *et al.,* 2005; Fernandez *et al.,* 2004). The existence of this bi-continuous/lamellar structure can be evidenced by using Small Angle X-ray Scattering (SAXS) technique; the X-ray pattern produced can provide information on the aggregate structure (Merta *et al.,* 2001). Direct observation under optical polarizing microscope also provides important qualitative information on the changes of emulsion morphology (Kulkarni *et al.,* 2010). Illumination of the sample with polarized light enables the researchers to detect birefringence in the emulsion sample, which indicates the existence of well-ordered molecules. Other technique such as infrared (IR) spectroscopy is a useful tool for understanding the events of phase inversion process. The IR absorbance or emission technique has long been used to characterize colloidal suspensions such as polymer emulsions (Vieira *et al.,* 2002; Silva *et al.,* 2011).

The use of phase inversion as a rapid, practical route in obtaining polymer emulsions as well as the flexibility in modifying the properties of the emulsion system afterwards, could be the breakthrough the industry has been looking for. For instance, nanoemulsion templating has been used to produce polymeric nanoparticle *via* low-energy methods (Vauthier & Bouchemal, 2009) with desired properties for a broad range of applications (Zhang *et al.,* 2008). Polymeric nanoparticles can be engineered by *in situ* polymerization in the dispersed phase of the nanoemulsion (Vauthier & Bouchemal, 2009; Gaudin & Sintes-Zydowicz, 2008, 2011) or using preformed polymer, which is initially dissolved in volatile organic solvent as dispersed phase of the nanoemulsion and followed by solvent evaporation (Calderó *et al.,* 2011; Fornaguera *et al.,* 2015). However, both methods require downstream steps i.e. purification and solvent removal in order to obtain polymeric nanoparticle (Vauthier &

Bouchemal, 2009) which pose disposal and recycling issues in scaling up the nanoparticle production.

The use of medium-chain-length polyhydroxyalkanoates (mcl-PHA) in polymeric nanoparticle development can help to overcome the aforementioned problems. Mcl-PHA is a biopolyester of 3, 4, 5 and 6-hydroxyalkanoic acids synthesized by numerous microorganisms through fermentation of carbon source and serves as energy storage compounds (Rai *et al.,* 2011). It is a biodegradable polymer with melting (T_m) and glass transition (T_g) temperatures ranging between 40 to 65 °C and -50 to -25 °C, respectively. Consequently, the thermoelastomeric and malleable properties of mcl-PHA make it possible to be incorporated into nanoemulsion system (O/W) using the same technique of producing solid lipid particle, whereby a solid lipid is melted at elevated temperature prior to emulsification (MuÈller *et al.,* 2000). Melted mcl-PHA is hypothesized to form a solid-like polymeric network at lower temperature thus providing the nanoparticle with a relatively rigid structure and other interesting properties. More importantly, the common use of crosslinking initiator and organic solvent to produce polymeric nanoparticle can be circumvented.

To the best of our knowledge, the application of bacterial-originated mcl-PHA as raw material to construct a polymeric nanoparticle has never been explored. Therefore, the objective of this study is to demonstrate, for the first time, that mcl-PHA-incorporated polymeric nanoparticle can be fabricated by using phase inversion emulsification. Fourier transform infrared (FTIR), Small Angle X-ray Scattering (SAXS) and Optical Polarizing Microscopy (OPM) techniques were used to investigate the macromolecular changes in polymer emulsion morphology at different water contents. β-carotene was used as the model compound for encapsulation and preservation study in order to demonstrate that the mcl-PHA-based nanoparticle

protects labile β- carotene against pre-mature chemical degradation. A mechanism of mcl-PHA-based nanoparticle formation is proposed.

4.3 Methodology

4.3.1 Materials

Oil phase: Jojoba oil (Sigma-Aldrich) was used as carrier oils. Mcl-PHA and β-carotene (Sigma-Aldrich, C9750) were used as additive and model compound, respectively, in the emulsion system.

Surfactants: Cremophor EL (polyethoxylated castor oil) and Span 80 (sorbitan oleate) were purchased from Sigma-Aldrich.

Water phase: Ultrapure water (Easy, Heal Force, China) was used to prepare all emulsions.

4.3.2 Methods

4.3.2.1 Mcl-PHA synthesis, purification and characterization

Medium-chain-length poly-3-hydroxyalkanoates (mcl-PHA) was biosynthesized by *Pseudomonas putida* Bet001 utilizing a two–stage fermentation in shake flasks with octanoic acid (1 % *w/v*) as the sole carbon and energy source (Ishak *et al.,* 2016). Bacterial cultivation was carried out at 30 °C and the shaker rotation speed was kept constant at 200 rpm in all experiments. Rich medium (200 ml) and E2 medium (200 ml) were used for the first and second stage of fermentation, respectively. After 24 hours of E2 medium cultivation, the cells were harvested and dried at 70 °C until constant weight. Mcl-PHA was extracted from the cells using acetone and purified repeatedly by cold methanol precipitation (Ishak *et al.,* 2016). This extracted mcl-PHA showed glass transition, melting and decomposition temperatures at about -37 °C, 52 °C and 250 °C, respectively. It consisted of 90 mole % 3-hydroxyoctanote, 5 mole % 3-

hydroxyhexanoate and 5 mole % 3-hydroxydecanoate. Its weight average molecular weight (M_w) was determined at 77,435 g mol^{-1} (polystyrene standard equivalent).

4.3.2.2 Emulsion preparation

O/W emulsion was obtained through emulsion inversion point (EIP) method by changing the composition of water-to-oil ratio (W:O) to induce phase inversion. Ultrapure water (W) was added dropwise into organic mixtures (surfactants and oil) with simultaneous vortexing until the final weight of 5.0 gram was reached. The optimum formulation of water-to-organic and oil-to-surfactant ratio to obtain nano-sized emulsion was 86:14 and 30:70, respectively. The term "organic" refers to combination of jojoba oil and surfactant fractions. For surfactant fraction, mixture of Cremophor EL and Span 80 were used at 63:37, respectively. These parameters were optimized using response surface methodology (RSM) with the size of oil droplets produced as the response variable. The Hydrophile-Lipophile Balance (*HLB*) value of the Cremophor EL-Span 80 mixture (63:37) was determined at 10.4, calculated using the following equation (Myers, 1990):

$$HLB_{mix} = f_A \times HLB_A + (1 - f_A) \times HLB_B \qquad \textbf{Eq. 4.1}$$

where f_A is the weight fraction of surfactant A (Cremophor EL) in the surfactant mixture. The *HLB* value for both surfactants, Cremophor EL and Span 80 are 14 and 4.3, respectively.

4.3.2.3 Incorporation of mcl-PHA and β-carotene

By using the same method to prepare an emulsion as described in the previous section, a new derivative of nanoparticle system was developed with the incorporation of mcl-PHA. To this end, all emulsification was carried out at 75 °C and kept constant throughout the preparation process. It was accomplished by pre-heating the ultrapure water and organic mixture overnight (separately) at 75 °C to aid the dissolution of solid mcl-PHA. A fraction of jojoba oil with dissolved β-carotene (0.01 % *w/w*) was added to the heated organic mixture prior to emulsification process. Addition of β-carotene was done in this manner in order to minimize heat effects.

It should be noted that the amount of mcl-PHA and β-carotene incorporated into the emulsion formulation determined the final jojoba oil fraction. Accordingly, the amount of jojoba oil was reduced with increased fractions of these two substances so as to keep the final weight of the emulsion system constant at 5.0 grams. The same amount of β-carotene was used in each emulsion system.

4.3.2.4 Determination of emulsion inversion point (EIP)

Changes in viscosity and conductivity of emulsion system at different water contents were used to identify the EIP. To this end, standard emulsion (without mcl-PHA) and mcl-PHA-incorporated emulsion were separately prepared at different water-to-organic phase ratios. Only the water-to-organic ratio was changed while the oil-to-surfactant and Cremophor EL-to-Span 80 ratios were kept constant.

Shear viscosity measurement was performed using a viscometer (DV2T, Brookfield, USA) equipped with 3.5 to 2.5 cm diameter cone spindle (CPA-52Z). Approximately 0.5 gram of emulsion samples was loaded onto sample cup for

measurement. All measurements were conducted under a shear rate of 50 s^{-1} at 75 °C for 2 minutes.

Electrical conductivity was measured using a conductivity meter (S230, Mettler-Toledo, Switzerland). For this, 0.02 M of saline solution was used as aqueous phase. Conductivities of 5.0 ml emulsion samples at different water contents were measured at 25.0 ± 0.5 °C.

4.3.2.5 Emulsion morphology

Changes in the morphology of polymer emulsion at different water contents were studied using Fourier transform infrared (FTIR) spectroscopy, Small Angle X-ray scattering (SAXS) and Optical Polarizing Microscopy (OPM). To this end, all emulsion samples (with or without PHA) at different water contents were prepared as described in the previous sections.

FTIR analysis was conducted to investigate functional group interactions among different molecular compounds in the emulsion formulation. Measurement was done in a FTIR spectrophotometer (Spectrum 400, Perkin-Elmer, USA) in the wavenumber range of 450 – 4000 cm^{-1}.

SAX scattering was conducted to investigate the presence of ordered structure in emulsion sample using an X-ray instrument (SaxSpace, Anton Paar, Austria). All measurements were performed using line collimation with exposure time of 15 minutes. Approximately 50 µl of emulsion sample was loaded into a liquid cell holder for measurement. X-ray patterns following sample exposure were recorded using 1-D diode detector under vacuum at 25 °C. The spectral data were analyzed using SAXSquant software package and the lamellar structure phases were assigned using SGI software.

The morphology of emulsion samples was also directly observed under OPM (BX51, Olympus, Japan) to detect the presence of birefringence, which indicates the

existence of well-ordered molecular structure. Observation was done by illuminating emulsion sample on a glass slide, heated to 50 °C using a hot stage (FP82, Mettler-Toledo, Switzerland), with polarized light. All images were captured using a digital camera (DP26, Olympus, Japan) and analyzed using cellSens-standard software.

4.3.2.6 Field emission scanning electron microscopy (FESEM)

Nanoparticles were observed under field emission scanning electron microscope (Quanta FEG 450, FEI, Holland) in high vacuum atmosphere operated at an acceleration rate of 3 to 5 kV. Diluted sample solution (5 % v/v) was dropped 3 to 4 times onto mesh copper grids (CF300-Cu) on top of a filter paper to blot excess liquid. Then, phosphotungstic acid solution (1 % w/v) was dropped 3 to 4 times onto the same grid to make the nanoparticle conductive. The grid was air-dried in vacuum chamber filled with silica beads for 4 days prior to observation.

4.3.2.7 Characterization of particle size and distribution

The size and size distribution of nanoparticles were measured based on the mean particle diameter (Zeta average) and particle size distribution (polydispersity index-PDI) of the suspension system, respectively. They were measured by dynamic light scattering (DLS) technique using Zetasizer-nanoseries (ZEN3600, Malvern Instruments Ltd, UK). The samples were diluted with ultrapure water (0.05 ml of sample in 0.95 ml H_2O) to avoid multiple scattering effects.

4.3.2.8 Stability of β-carotene encapsulated in mcl-PHA-incorporated nanoemulsion

Stability of β-carotene encapsulated in standard nanoemulsion (without mcl-PHA) and mcl-PHA-incorporated nanoemulsion with different mcl-PHA M_w *viz*. 77435, 56365, 23578 and 7370 g mol^{-1}, was investigated. For each M_w, the mcl-PHA content was varied at 2, 5, 7 and 10 % *w/w* of total oil fraction, respectively. The different M_ws were obtained through ultrasound-mediated partial methanolysis of native mcl-PHA. This was achieved by controlling the amount of acidified methanol used (Ishak *et al.*, 2016)**.** To this end, 0.5 ml sample of suspension system was diluted with 1.5 ml ultrapure water in a cuvette and sealed with parafilm to avoid evaporation. Then, its absorbance was taken at 466 nm using UV-Vis spectrophotometer (V630, Jasco, Japan). 0.5 ml sample of suspension system without β-carotene was used as blank after dilution with 1.5 ml ultrapure water. Subsequently, 20 µl 1 mM benzoyl peroxide solution in methanol was added into the diluted sample followed by gentle shaking. The sample solution was stored in the dark at 25 °C and its absorbance was taken periodically. Experiments were conducted in triplicate for each sample. The degradation percentage of β-carotene was calculated using formula shown in previous chapter **(**Equation 3.2):

4.4 Results and discussion

4.4.1 Emulsion inversion point (EIP)

We examined the phase behavior of standard emulsion (without mcl-PHA) and mcl-PHA-incorporated emulsion at different mcl-PHA content (1, 1.5, 2, 2.5 and 3 % (*w/w*) of jojoba oil fraction). The viscosity, appearance and electrical conductivity of all samples were determined at different water contents of the emulsion systems (Figure 4.1). In general, all initial organic mixtures (surfactant-oil-mcl-PHA) showed a relatively low viscosity (≈ 40 mPa), with the viscosity increasing with mcl-PHA content, slightly opaque appearance and low electrical conductivity (≈ 0 μs/cm).

The shear viscosity of all samples steadily increased as the water content increased, due to an increase in water droplet volume fraction in the W/O emulsion, until 30 % *w/w* water content, whereby it reached a maximum value (Figure 4.1*a*). The highest viscosity obtained at this point was attributed to the formation of bi-continuous/lamellar structure and/or a multiple emulsion with maximum close-packing condition. Then, it decreased steeply with further increase in water content up to 60 % due to a decrease in oil drop volume fraction in the O/W emulsion. However, viscosities of all samples were slightly increased when the water content reached 70 % *w/w*. Plausible explanation probably due to high volume fraction of micro-sized dispersed phase within the emulsion. It has been reported that the emulsion viscosity increased with a decrease in the average droplet size and became more significant when the dispersed phase occupied larger volume fraction (Das *et al.,* 1992). Therefore, it was expected that the emulsion viscosity would decrease at a final water content of 86 % *w/w* as the oil droplets became less concentrated. High deviation of emulsion viscosity at 70 % *w/w* water content indicated the non-Newtonian behavior of emulsion solutions whereby their viscosities increased with shearing force. For emulsion sample with mcl-PHA content of 3 % (*w/w* of oil fraction), its viscosity profile showed a relatively higher

value than the rest after 30 % *w/w* water content, most likely due to larger size of oil droplets produced.

In general, all samples exhibited similar appearances with increasing amount of water content (Figure 4.1*b*). Visually, they became transparent at 10 % *w/w* water content, presumably due to formation of W/O microemulsion. The suspension became more turbid as the water content was increased to 20 % *w/w*, attributed to the increase in volume fraction of water drops. At 30 % *w/w* water content, the highly opaque and viscous samples observed at this point were ascribed to the formation of bi-continuous/lamellar structure and/or a multiple emulsion with maximum close-packing condition. The opaque samples showed shear-birefringence upon heating indicating the melting of rigid lamellar liquid crystalline to fluidic bi-continuous microemulsion. After this point, they exhibited less opaque appearance and became more transparent, due to formation of O/W nanoemulsion, which getting smaller with increasing amount of water added. The mean particle diameter in all emulsion samples at final water content (86 % *w/w*) was in the range of 20 – 50 nm.

The electrical conductivity remained relatively low when water content was below 30 % *w/w* in all emulsion samples indicating the continuous phase was oil (Figure 4.1*c*). Immediately after this point, there was a sharp increase in conductivity, indicating the phase transition of W/O to O/W whereby the continuous phase of oil was inverted to water and continued to increase steadily afterwards. From the results, it can be deduced that the best composition to induce phase inversion, i.e. emulsion inversion point (EIP) was at 30 % *w/w* water content.

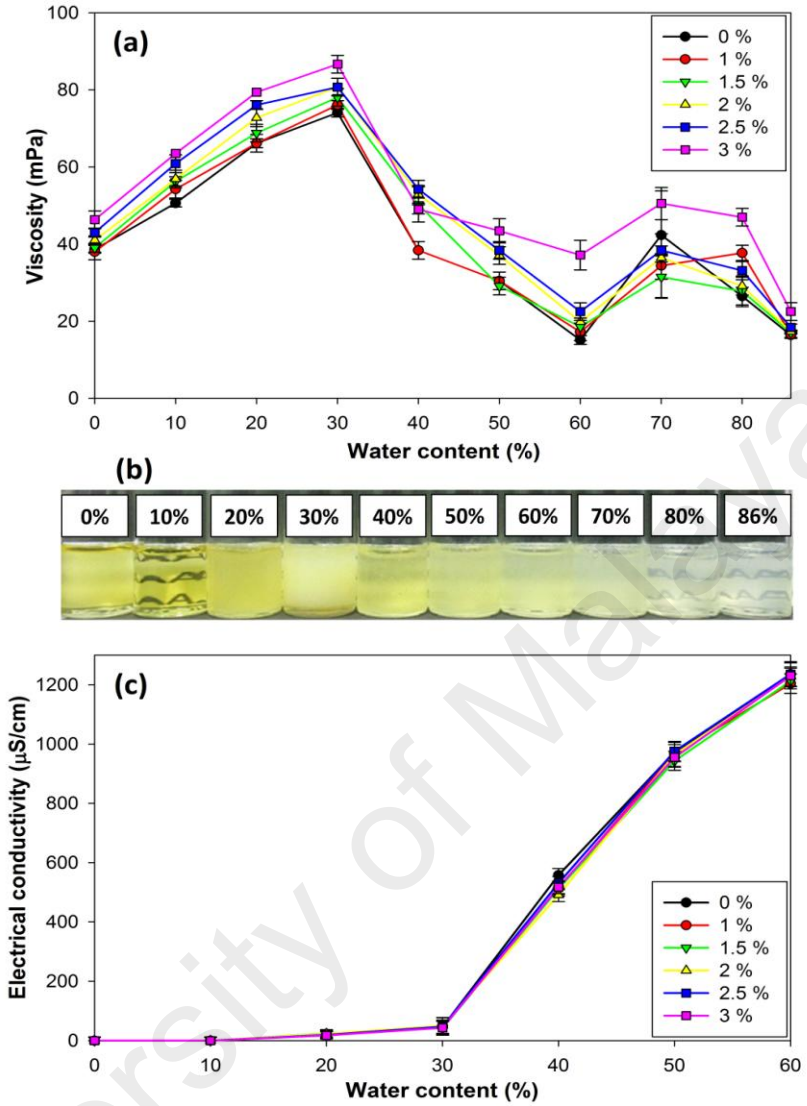

Figure 4.1: EIP determination - (*a*) Emulsion viscosity, (*b*) Emulsion appearance and (*c*) Emulsion conductivity

4.4.2 Fourier transform infrared (FTIR) analysis

The intermolecular interaction among emulsion components was studied from the observed changes in functional group spectra of emulsion samples at different water contents. Spectrum of individual starting materials utilized for mcl-PHA polymeric nanoparticle development was used as a reference (Figure 4.2**)**.

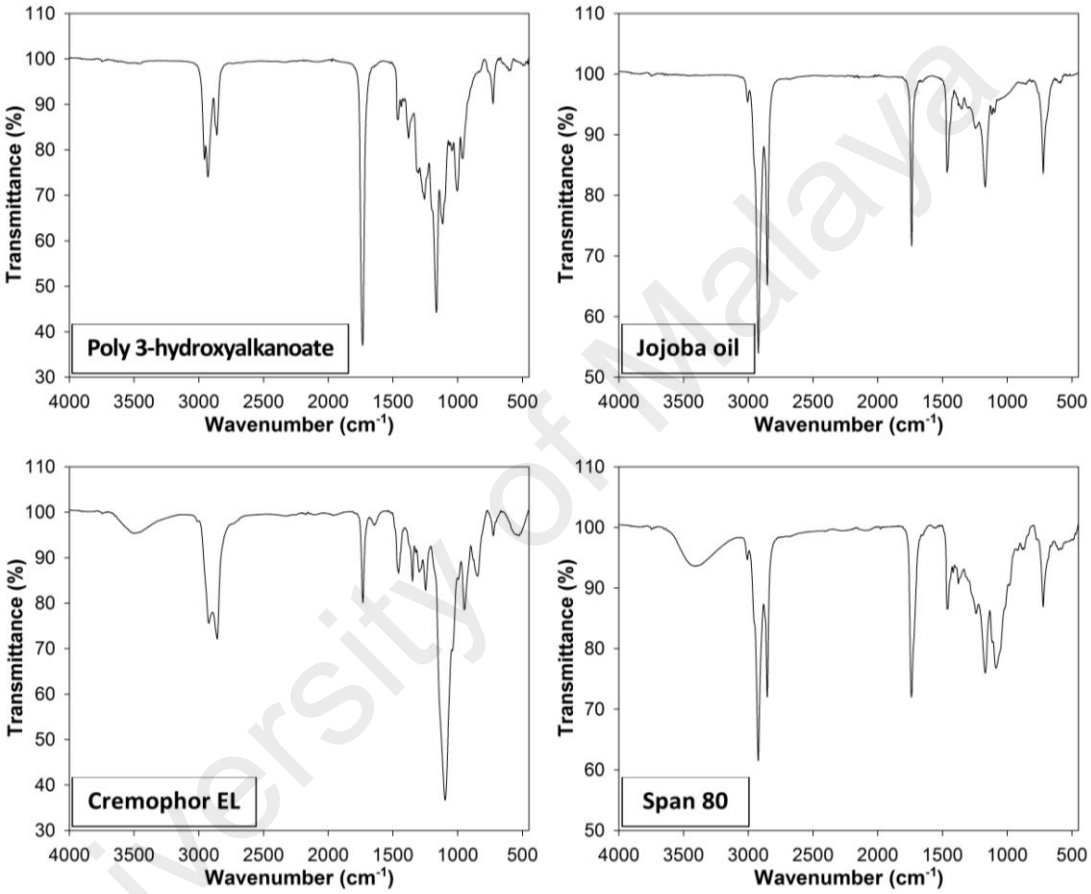

Figure 4.2: FTIR spectra of raw materials

In general, all four components shared similar peaks of chemical bonds representing C-H (≈ 2925 cm^{-1}) and C-H_3 (≈ 2855 cm^{-1}) of hydrocarbon chain, C=O (≈ 1735 cm^{-1}) and C-O-C (1080 – 1170 cm^{-1}) of ester bond as well as C-C and C-H (600 - 1500 cm^{-1}). For Cremophor EL and Span 80, two extra peaks were found at (≈ 3450 cm^{-1}) and (≈ 1600 cm^{-1}) representing O-H of their hydrophilic head and C=C of their

unsaturated hydrocarbon tail, respectively. Peak that represent C=C was not observed in jojoba oil spectrum probably due to domination by other major chemical bond peaks. Span 80 have two peaks of C-O-C (1170 and 1084 cm^{-1}), from ester bond and hydrophilic head while C-O-C from ester bond and hydrophilic head group of Cremophor EL was included in one peak at 1098 cm^{-1}.

Figure 4.3 (*a* – *f*) shows spectral information on intermolecular interaction among starting materials within the standard emulsion samples (without PHA) at different water contents. A peak is observed at 1600 cm^{-1} (*blue arrow* - Figure 4.3*a*), which becomes more significant as the water content in emulsion is increased. Three peaks at 600 – 850 cm^{-1} (*red arrow* - Figure 4.3*a*) gradually come together to form a single big broad peak as the water content in the emulsion is increased. These changes with water content are attributed to the assembly of Cremophor EL and Span 80 at the oil-water interface. In addition, those peaks have the same value of transmittance with C-O-C peak at 50 % *w/w* water content (Figure 4.3*f*), giving rise to the hypothesis that the two surfactants formed an interfacial film surrounding oil droplets after phase inversion. At 30 % *w/w* water content (Figure 4.3*d*), three peaks representing O-H (3450 cm^{-1}), C-H (2925 cm^{-1}) and C-O-C (1100 cm^{-1}) have the same value of transmittance indicating balanced intermolecular interactions among water, oil and surfactants. This lends support to the hypothesis of bi-continuous/lamellar structure formation at EIP, whereby surfactants would be aligned together to form separating film in-between oil and water phase as interfacial tension is minimized.

Figure 4.4 (*a* – *f*) shows FTIR spectra of mcl-PHA-incorporated emulsion samples at different water contents. The mcl-PHA content used in this emulsification was 10 % *w/w* of oil fraction with molecular weight of 7370 g mol^{-1}. Similar pattern of spectral peaks alterations is observed indicating that the emulsification process of mcl-PHA-incorporated emulsion was similar to the standard emulsification without mcl-

PHA (Figure 4.3). One additional peak (*green arrow* - Figure 4.4*d*) is identified at 1167 cm^{-1} to represent C-O-C of mcl-PHA ester bond showing that mcl-PHA molecules formed a part of the bi-continuous/lamellar structure.

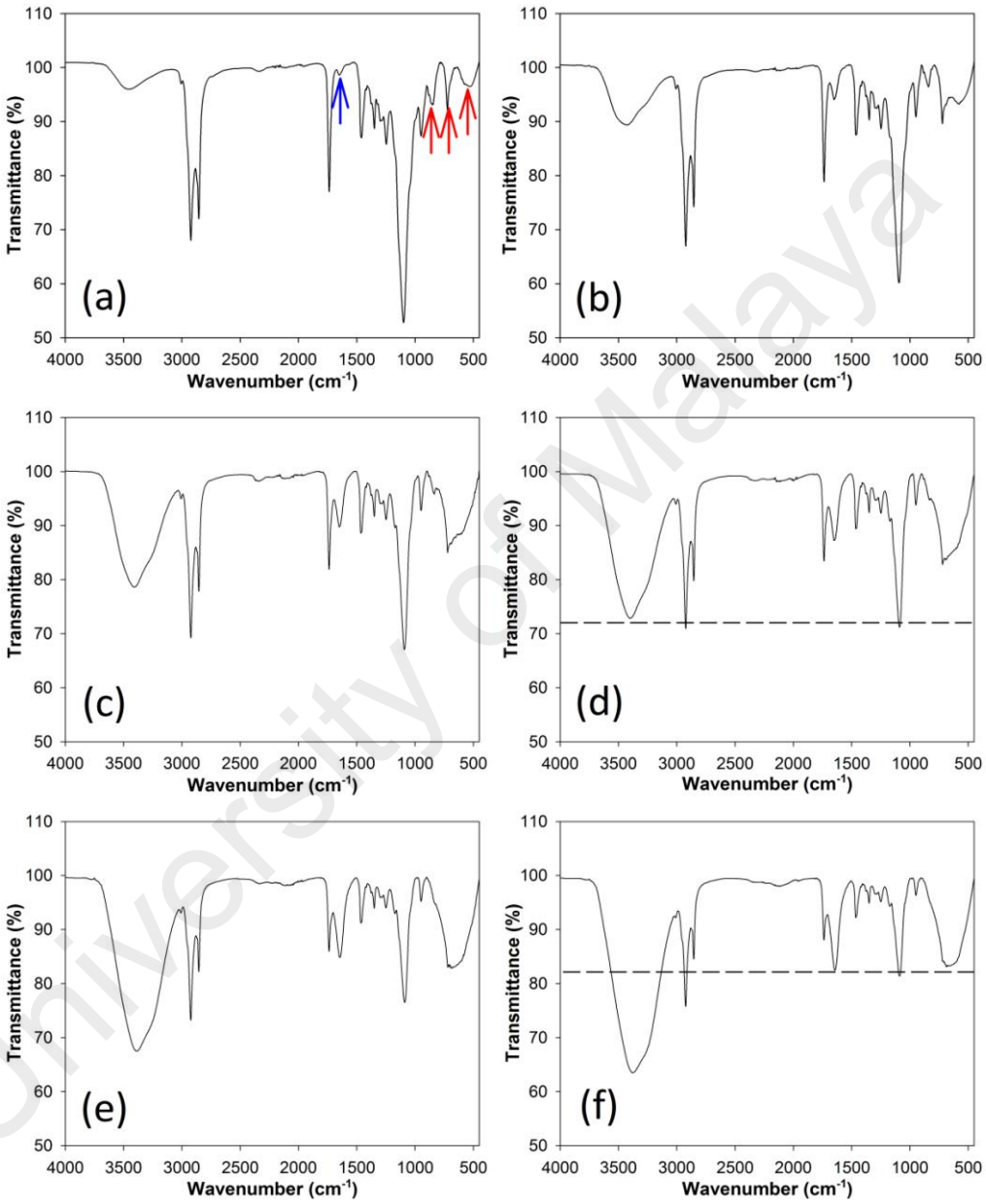

Figure 4.3: FTIR spectra of standard emulsion at (*a*) 0 %, (*b*) 10 %, (*c*) 20 %, (*d*) 30 %, (*e*) 40 % and (*f*) 50 % *w/w* water content

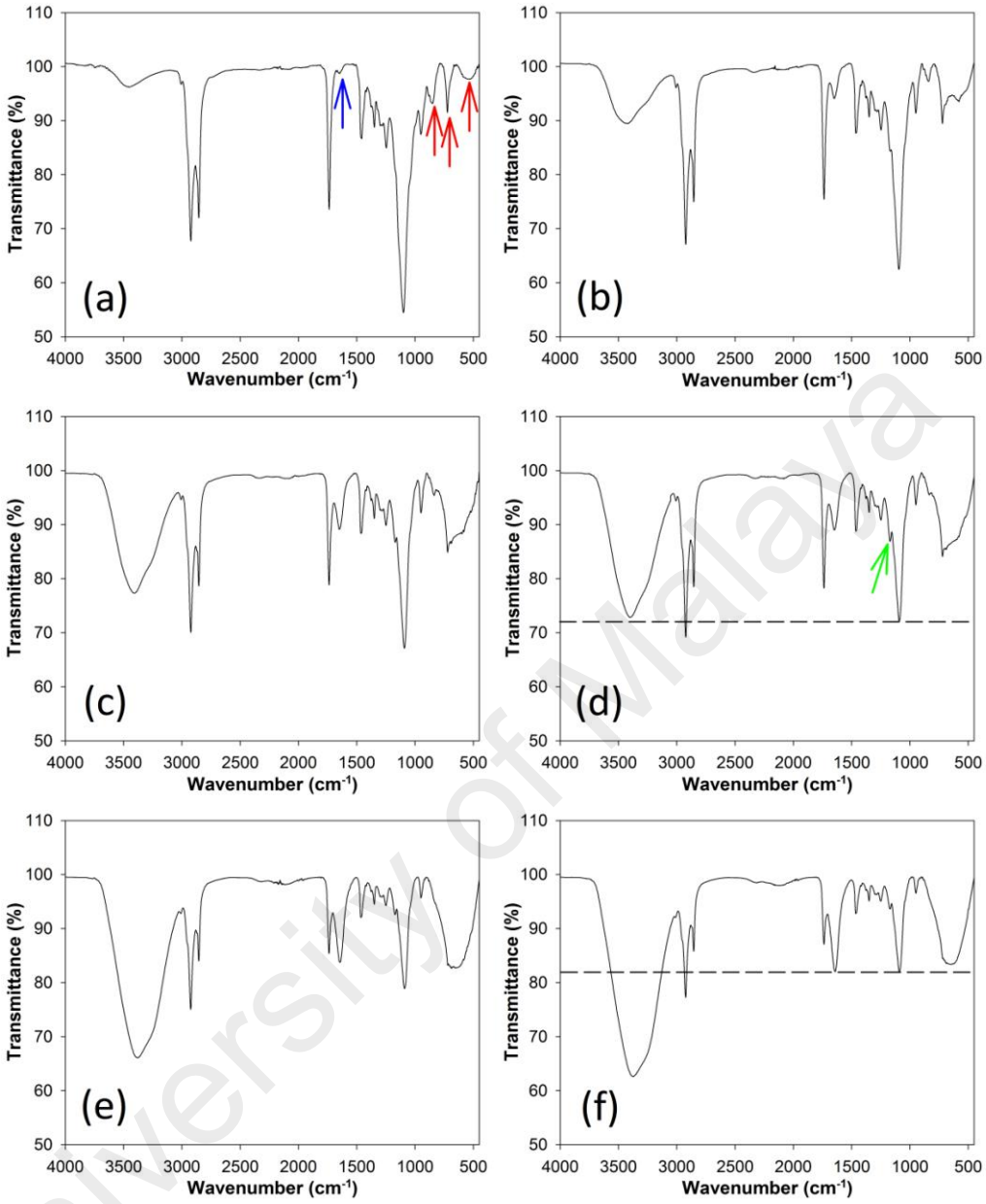

Figure 4.4: FTIR spectra of polymer emulsion at (*a*) 0 %, (*b*) 10 %, (*c*) 20 %, (*d*) 30 %, (*e*) 40 % and (*f*) 50 % *w/w* water content

4.4.3 SAX scattering and OPM analysis

The existence of lamellar structure in emulsion at EIP, as discussed earlier, was also indirectly supported by the interpretation of X-ray scattering patterns obtained. From Figure 4.5*a*, it can be seen that two peaks start to appear at 20 % *w/w* water content and become more prominent at 30 % *w/w* water content. This is ascribed to the water droplets (dispersed phase) starting to coalesce and elongate to form streamlines, which eventually stack together into bi-continuous/lamellar structure phase. This phenomenon is possible due to the minimization of interfacial tension of water and oil phases. In this phase, it is hypothesized that the surfactants are partially ordered, forming a separating linear film along the water-oil streamline interface. It should be noted that the two peaks become less prominent upon heating due to formation of bi-continuous microemulsion phase (*D*), which is the melted state of the lamellar liquid crystal. When water content is more than 30 % *w/w*, the peaks start to disappear indicating the surfactants are no longer closely packed together in a film formation. Instead, the interfacial film of surfactants is likely to have come apart and dispersion of oil phase starts to occur. Similar results were obtained with mcl-PHA-incorporated emulsion (Figure 4.5*b*), signifying that the events in emulsification process of polymer emulsion are not dissimilar to the standard emulsion.

Direct observation of emulsion morphology using OPM is shown in Figure 4.6. It can be seen that the emulsification process starts with formation of water droplets (*black arrow*) in oil phase that eventually become larger water drops as the water content increases (Figure 4.6*a* and *b*). As discussed earlier, these water drops coalesced to form streamlines, which eventually became stacked together into bi-continuous/lamellar structure phase. Figure 4.6*c* shows the oil and water phases that are structurally arranged in a bi-continuous/lamellar order. Following EIP, the oil phase (Figure 4.6*d*) disperses gradually to form oil drops as water content increases (Figure

4.6*e*). Subsequently, the micrometer-sized oil drops disperse into smaller droplets, which eventually lead to the formation of nano-sized particles (*white arrow* - Figure 4.6*f*). For mcl-PHA-incorporated emulsion, the change in morphology was not dissimilar to standard emulsion discussed above (data not shown), which also eventually leads to the formation of polymeric nanoparticles (Figure 4.7). Apparently, when lower molecular weight mcl-PHA was used, more of it can be incorporated into the emulsion to give particles below 50 nm in diameter.

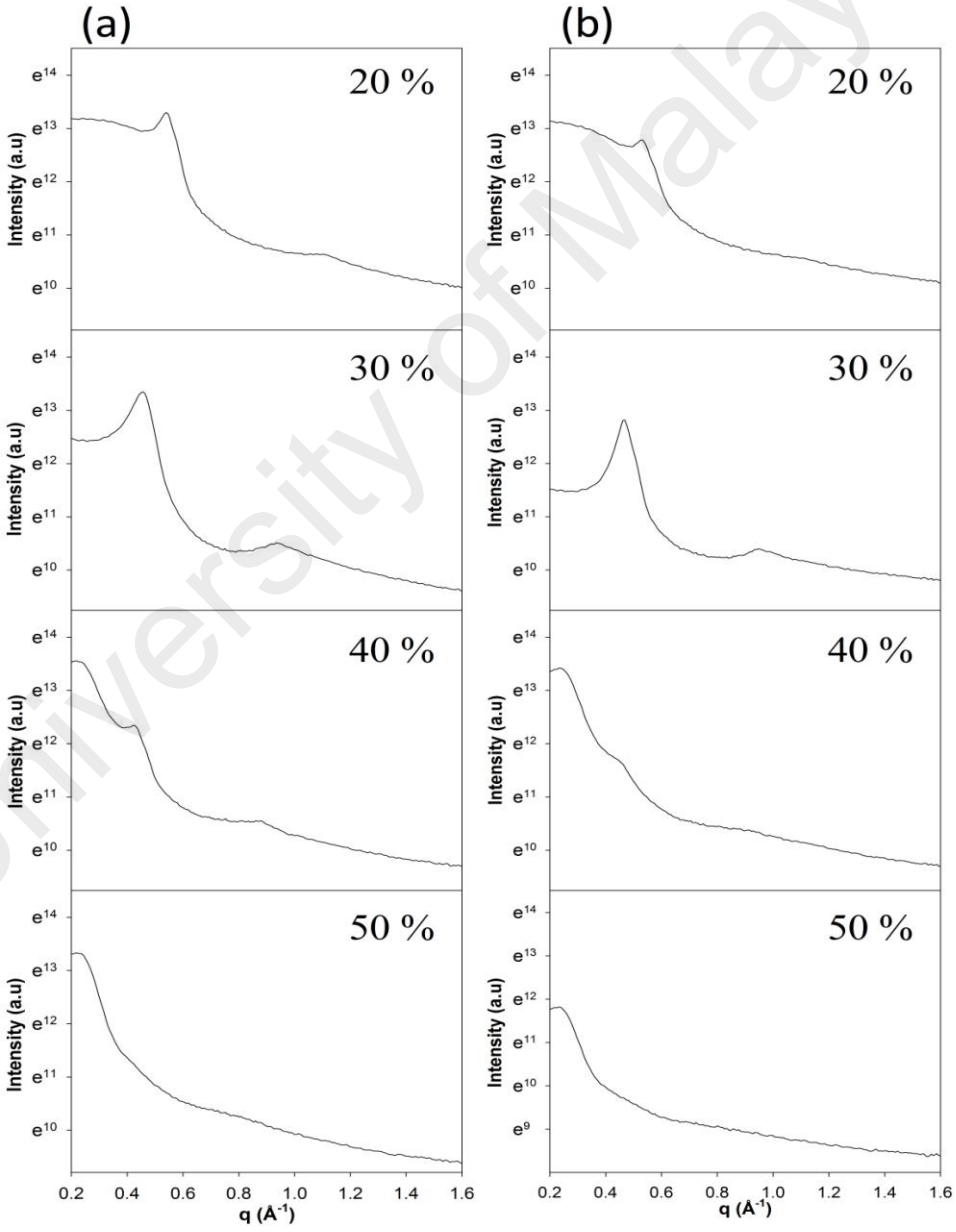

Figure 4.5: SAX scattering for (*a*) standard and (*b*) mcl-PHA–incorporated emulsions

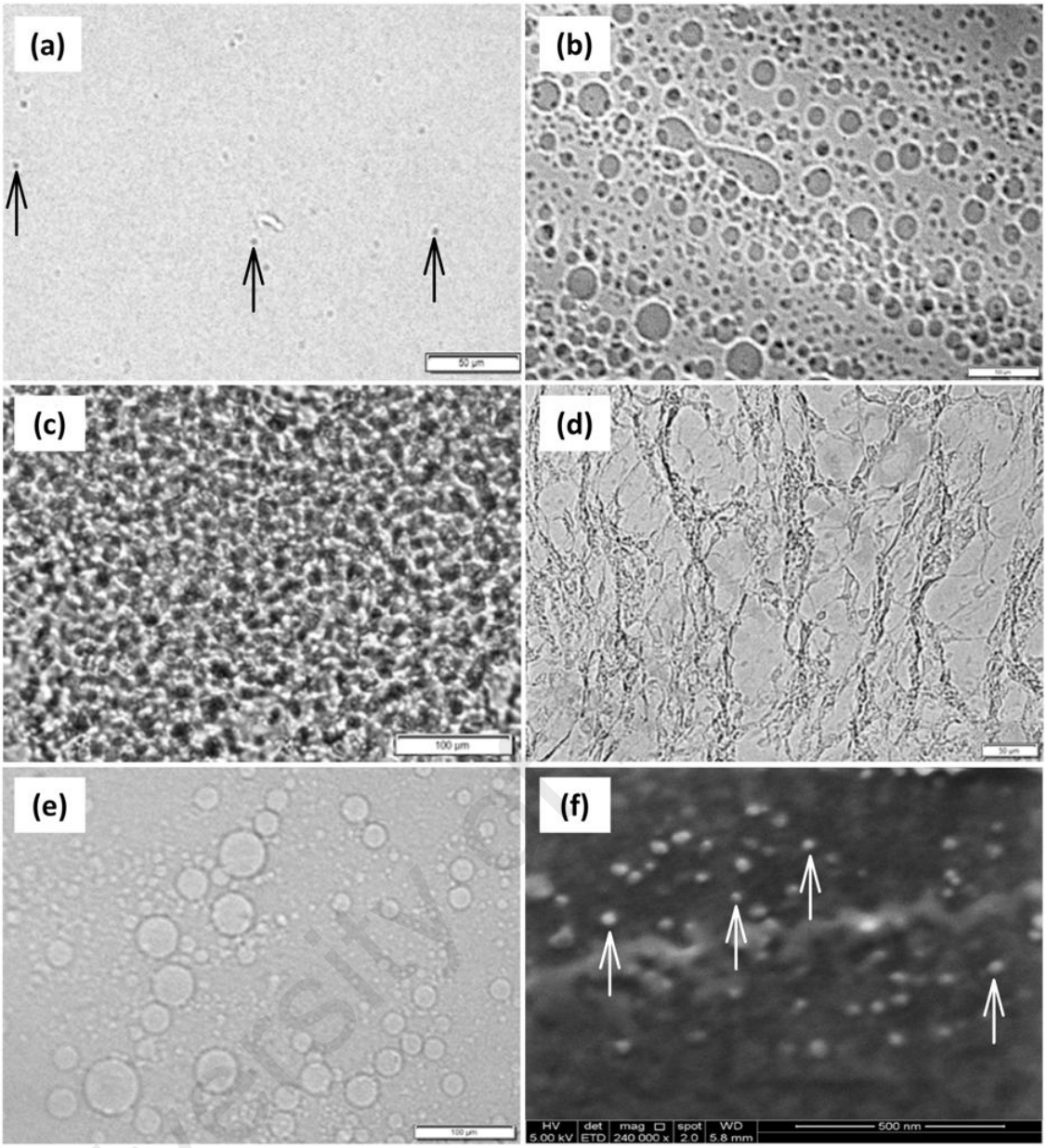

Figure 4.6: Morphology of standard emulsion at (*a*) 10 %, (*b*) 20 %, (*c*) 30 %, (*d*) 40 % and (*e*) 60 % *w/w* of water content; (*f*) FESEM image of O/W droplets

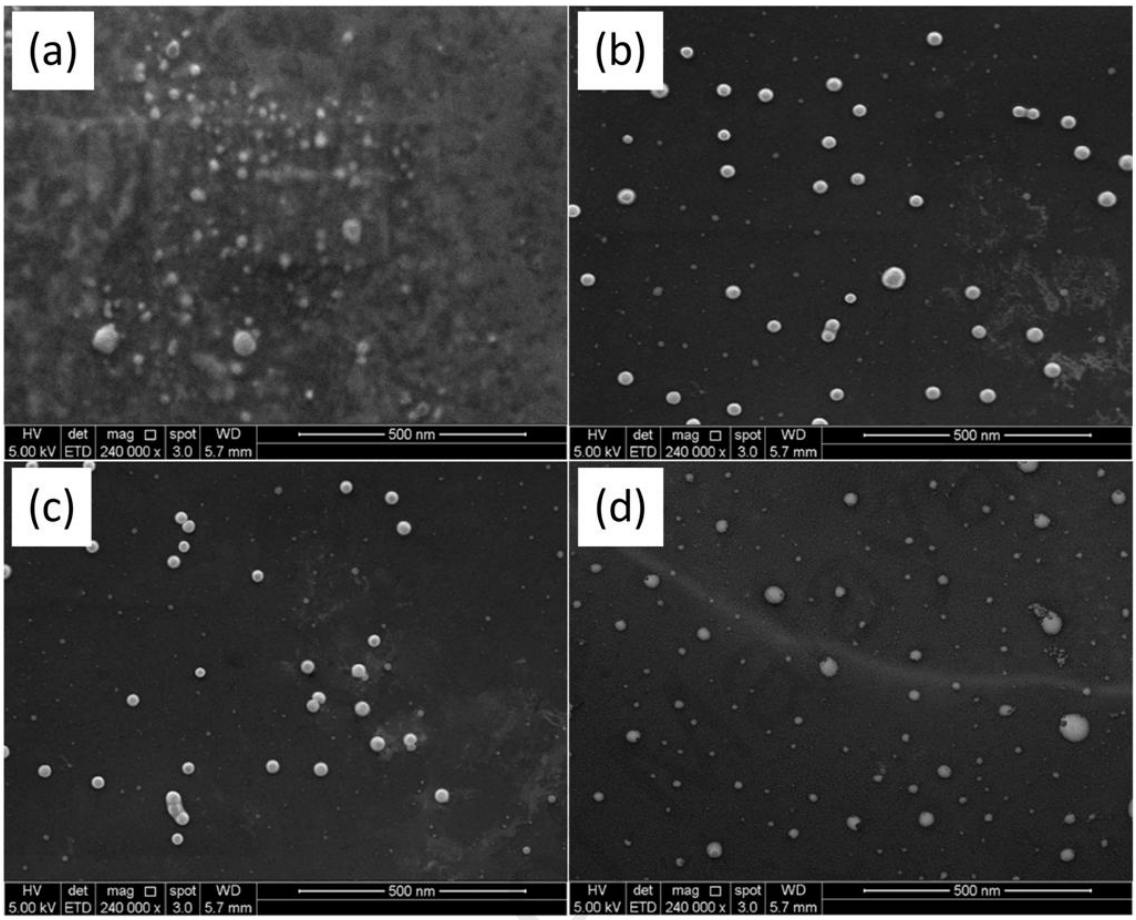

Figure 4.7: FESEM images of mcl-PHA-incorporated O/W droplets at (*a*) 2 %, (*b*) 5 %, (*c*) 7 % and (*d*) 10 % *w/w* of oil fraction

4.4.4 Encapsulation of *β*-carotene in mcl-PHA-incorporated nanoemulsion

To study the effects of *β*-carotene loading on the nanoparticles mean size, it was encapsulated into nanoemulsion with different mcl-PHA molecular weights *viz.* 77435, 56365, 23578 and 7370 g mol^{-1} at 2, 5, 7 and 10 % *w/w* of total oil fraction, respectively. The range of mcl-PHA amount was selected to obtain nanoparticles with average size less than 50 nm. The average size and size distribution of the mcl-PHA-incorporated nanoparticles loaded with *β*-carotene (Figure 4.8*b*) were similar to unloaded mcl-PHA-incorporated nanoparticles (Figure 4.8*a*). Generally, encapsulation of *β*-carotene in the mcl-PHA-incorporated nanoemulsion showed negligible effects on the particle size and size distribution when compared to standard nanoemulsion (without

mcl-PHA – 0 %) and did not compromise the integrity of nanoparticle structure in the emulsion system.

β-carotene degradation rate was significantly curtailed when mcl-PHA was incorporated into the nanoemulsion (Figure 4.8*c*). This lends support to the hypothesis that the mcl-PHA formed a protective coating layer surrounding the nanoparticle. Unlike standard nanoemulsion system, peroxide molecules encountered the polymer matrix of mcl-PHA-incorporated nanoemulsion before penetrating into the internal encapsulated β-carotene for oxidation reaction. Therefore, the mass transfer of oxidizing agent into the mcl-PHA-incorporated nanoemulsion was significantly limited compared to the standard nanoemulsion, resulting in lower degradation kinetic of β-carotene within the mcl-PHA-incorporated nanoemulsion.

However, β-carotene preservation was insignificant when low molecular weight mcl-PHA (7370 g mol^{-1}) was incorporated at 10 % *w/w* of total oil fraction within the polymeric nanoparticle. This indicates that low molecular weight mcl-PHA was deficient in bridging a continuous protective structure surrounding the nanoparticle. Hence, degradation rate of β-carotene loaded into this particular nanoparticles was similar to standard nanoemulsion (without mcl-PHA). Oxidation of β-carotene was readily visualized in the alteration of color intensity of bright yellow-coloured nanoemulsion, which was becoming less intense as oxidation time progressed (*see insert in* Figure 4.8*c*).

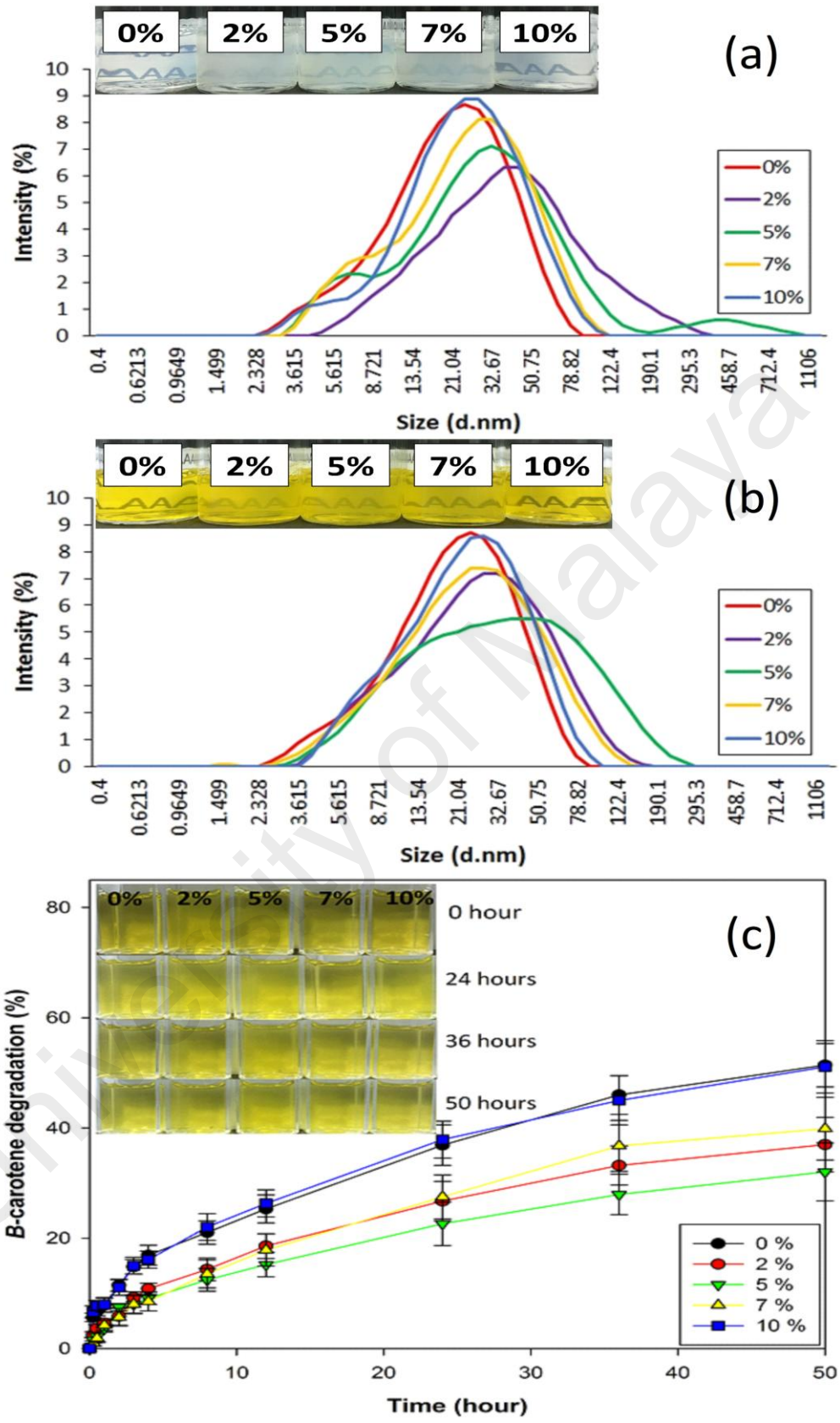

Figure 4.8: Mcl-PHA-incorporated nanoemulsion (*a*) without *β*-carotene and (*b*) with *β*-carotene; (*c*) *β*-carotene degradation profile

4.4.5 Hypothetical mechanism of mcl-PHA-based nanoparticle formation

From the results, it is clear that at optimum formulation, the phase inversion emulsification did not involve the formation of multiple emulsion (O/W/O) that would eventually lead to drops coalescence and release of internal oil droplets to form O/W emulsion. Instead, it involved the formation of bi-continuous/lamellar phase, which in turn dispersed into submicrometer-sized oil droplets following the EIP. Existence of lamellar liquid crystalline phase was also reported in a previous study whereby nanoemulsions were produced in composition showing phase equilibrium consisting of three phases of O/W microemulsion (W_m), lamellar liquid crystalline (L_a) and oil (O) (Forgiarini *et al.*, 2001). It was suggested that low value of equilibrium interfacial tension involving the lamellar liquid crystalline phase was likely to be the main reason for the smallest droplet size in nanoemulsion obtained through stepwise addition of water (Forgiarini *et al.*, 2001).

In this study, the emulsification process of mcl-PHA-incorporated emulsion is hypothesized to follow similar path as the standard emulsion (emulsion without mcl-PHA). Figure 4.9 shows the schematic of emulsification mechanism that leads to the production of mcl-PHA-based polymeric nanoparticle. The emulsification starts with the formation of water droplets in continuous oil phase i.e. W/O emulsion (Figure 4.9*b*) with gradual water addition into the organic phase mixture (Figure 4.9*a*). As the water content increases, liquid hydrodynamics due to mechanical stirring induce collision of water droplets leading to drops coalescence and elongation (Figure 4.9*c*), which eventually brings about the formation of bi-continuous/lamellar structure phase at EIP (Figure 4.9*d*). After the continuous oil phase is inverted into dispersed phase (Figure 4.9*e*), it is gradually dispersed in smaller droplets (Figure 4.9*f*) with the increase in water content. The drops dispersion proceeds until stable nano-sized particles are obtained.

It is during gradual cooling to ambience temperature (25 °C) that the melted mcl-PHA (Figure 4.9*g*) aggregates at the mixed surfactants layer (Cremophor EL and Span 80) forming a bridging, membrane-like lining around the oil droplet (Figure 4.9*h*). Structurally, the nanoparticle is expected to resemble a polymer-based encapsulation system called nanocapsule whereby a polymer forms membrane-like layer that surrounds the bioactive-rich liquid core i.e. vesicular system (Mora-Huertas *et al.*, 2010).

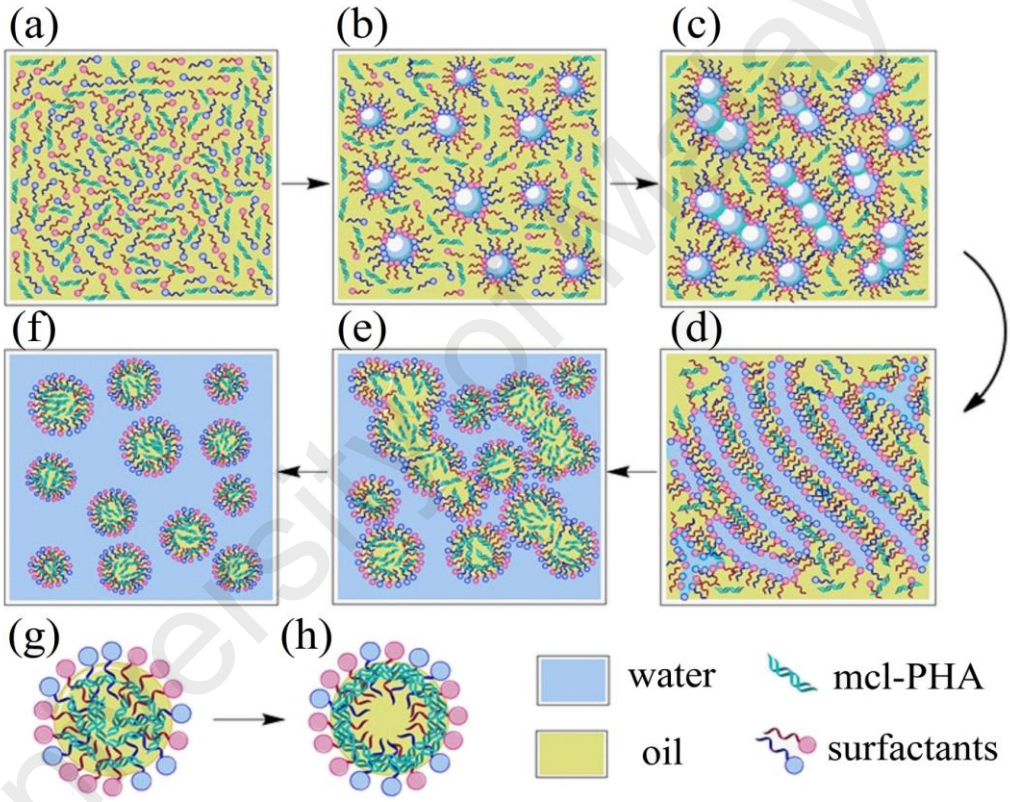

Figure 4.9: Hypothetical mechanism of mcl-PHA-incorporated nanoparticle formation

4.5 Concluding remarks

In this study, it was demonstrated that the incorporation of mcl-PHA into nanoemulsion could be accomplished through standard EIP method at elevated temperature without the need for using toxic solvents. The emulsification process of both standard emulsion and mcl-PHA-incorporated emulsion followed a similar path involving the formation of bi-continuous/lamellar structure phase at emulsion inversion point (EIP) before dispersion of oil fraction into submicrometer droplets.

A significant amount of β-carotene was preserved within the mcl-PHA-incorporated nanoemulsion compared to standard nanoemulsion after addition of an oxidizing agent, indicating that mcl-PHA incorporation could provide a protective coating structure to delay premature degradation of β-carotene. The study also highlighted a facile method to assemble biopolymer-based carrier system for encapsulation of lipophilic bioactive compounds.

CHAPTER 5: EFFECT OF MCL-PHA MOLECULAR WEIGHT AND AMOUNT ON THE INVERSION MECHANISM OF PIE

5.1 Summary

The study investigated the effects of molecular weight and amount of medium-chain-length poly-3-hydroxyalkanoates (mcl-PHA) on the formation of polymeric nanoparticle *via* phase inversion emulsification. Inversion from water-in-oil (W/O) to oil-in-water (O/W) emulsion through stepwise addition of water was affected by molecular weight and amount of incorporated mcl-PHA in the oil phase. The phase inversion mechanism depends upon molecular weight and amount of the incorporated mcl-PHA. It is hypothesized that at appropriate molecular weight and amount of mcl-PHA, the inversion occurs through the formation of bi-continuous/lamellar structure, in which the oil phase is gradually dispersed into the desired nano-sized droplets. Otherwise, it will lead to an alternative phase inversion mechanism involving multiple emulsions resulting in larger nanoparticles with wider distribution.

5.2 Introduction and literature review

Development of biodegradable polymeric nanoparticles for active compounds delivery into human body has gained a widespread interest in nutraceutical and pharmaceutical industries. It has been used frequently as active compounds delivery vehicles due to its better encapsulation, control release, compound bioavailability improvement as well as less toxic properties (Kumari *et al.*, 2010). For example, oral delivery of bioactive curcumin, a yellow polyphenol from *Curcuma sp*., in polymeric nanoparticle for human cancer therapy has been reported (Bisht *et al.*, 2007). Biopolymeric nanoparticle has also been used as nanocarrier for other active compounds delivery, such as galantamine and loperamide, to treat neurodegenerative

diseases (Fornaguera *et al.,* 2015a, b). The use of polymeric nanoparticle as innovative delivery system is a promising alternative as they are capable of reaching human organ due to their nanoscale size (Sahni *et al.,* 2011; Neha *et al.,* 2013), solubilizing huge amount of lipophilic compound and protecting them from pre-mature enzymatic degradation (Soppimath *et al.*, 2001; Todoroff & Vanbever, 2011). In addition, they can be easily prepared using scalable and cost-effective methods (Reis *et al.,* 2006; Vauthier & Bouchemal, 2009).

One of the effective and economical methods to produce polymeric nanoparticle is through phase inversion emulsification (PIE). Phase inversion is the process whereby a water-in-oil (W/O) emulsion system gets inverted into an oil-in-water (O/W) emulsion system, or *vice versa*. Initially, it is used to obtain polymer-based O/W emulsion and then modified to obtain different types of polymeric nanoparticles afterwards. This technique is known as nanoemulsion templating, which has been used to produce polymeric nanoparticle *via* low-energy methods (Vauthier & Bouchemal, 2009) with desired properties for a broad range of applications especially in biomedical field (Zhang *et al.,* 2008). For instance, polymeric nanoparticles can be engineered by *in situ* polymerization in the dispersed phase of the nanoemulsion (Vauthier & Bouchemal, 2009; Gaudin & Sintes-Zydowicz, 2008, 2011) or using preformed polymer, initially dissolved in volatile organic solvent as dispersed phase of the nanoemulsion followed by solvent evaporation (Fornaguera *et al.,* 2015a, b; Calderó *et al.,* 2011). However, both methods require downstream steps i.e purification and solvent removal in order to obtain polymeric nanoparticle (Vauthier & Bouchemal, 2009), which pose disposal and recycling issues in scaling up the nanoparticle production.

The use of medium-chain-length polyhydroxyalkanoate (mcl-PHA) in polymeric nanoparticle development through nanoemulsion templating could help to overcome the aforementioned problems. Mcl-PHA is a biopolyester composed of 3,4,5 and 6-

hydroxyalkanoic acids synthesized intracellular by numerous microorganisms through fermentation of excess carbon and serves as energy storage compounds (Rai *et al.*, 2011). It is a biodegradable polymer that has melting (T_m) and glass transition (T_g) temperature ranging between 40 to 65 °C and -50 to -25 °C, respectively. Therefore, mcl-PHA can be incorporated within oil droplet by using the same technique of producing solid lipid particle, whereby solid lipid is melted at elevated temperature prior to emulsification (MuÈller *et al.,* 2000). The melted solid lipid will eventually recrystallized within oil droplet as the system is cooled down. Similarly, it is hypothesized that the melted mcl-PHA would form a solid-like polymeric network within oil droplets at lower temperature thus forming relatively rigid nanoparticles that may possess equivalent desired properties as other developed polymeric nanoparticles. Consequently, the use of crosslinking initiator and organic solvent to produce polymeric nanoparticle can be circumvented.

Phase inversion emulsification can be classified into transitional and catastrophic phase inversion. A transitional inversion is triggered by alteration in surfactant affinity towards the two immiscible phases (i.e., the system formulation), which is influenced by the hydrophilic-lipophilic balance (*HLB*) of the surfactant (Brooks & Richmond, 1994), changing the system ionic balance (Maestro *et al.,* 2008) as well as the system temperature (Shinoda & Saito, 1968; Sherman & Parkinson, 1978). Meanwhile, catastrophic phase inversion (CPI) takes place due to continuous addition of dispersed phase (i.e., the system composition) until the dispersed-phase drops are close enough to coalesce upon contact forming bi-continuous/lamellar structure phase, which is likely to occur at high surfactant concentration (Fernandez *et al.,* 2004). In addition, it could also be induced through multiple/abnormal emulsion (i.e system that exists differently than predicted according to Bancroft's rule) by continuously stirring the emulsion system with or without changing the system

formulation and/or composition (Tyrode *et al.,* 2003). The stirring energy can cause the dispersed-phase drops become swollen with continuous-phase droplets, which eventually accommodate the close packing conditions, thus augmenting the rate of drop coalescence of dispersed phase. According to Ostwalds' phase volume theory, inversion occurs at maximum volume concentration of 74 %, which is the close packing upper limit for rigid sphere tessellation (Tyrode *et al.,* 2003, 2005). The effects of water fraction and surfactant concentration (Rondón-Gonzaléz *et al.,* 2006), hydrophile-lipophile balance (*HLB*) value of surfactants (Sajjadi *et al.,* 2004), water-to-oil ratio change rate (Zambrano *et al.,* 2003), stirring rate (Mira *et al.,* 2003) and phase viscosity (Rondón-Gonzaléz *et al.,* 2007) on the CPI have been reported previously.

To the best of our knowledge, the application of mcl-PHA as raw material to construct polymeric nanoparticle has never been explored. Therefore, the objective of this research is to investigate the effects of different molecular weights and amounts of mcl-PHA on the phase inversion emulsification process and final nanoparticle size and size distribution. Fourier transform infrared (FTIR), Small Angle X-ray Scattering (SAXS) and Optical Polarizing Microscopy (OPM) were used to study the polymer-incorporated nanoemulsion morphology at emulsion inversion point (EIP). Hypothetical inversion mechanism of mcl-PHA-incorporated emulsion with different mcl-PHA molecular weights and amounts is proposed.

5.3 Methodology

5.3.1 Materials

Oil phase: Jojoba oil (Sigma-Aldrich) was used as carrier oil. Mcl-PHA was used as additive compound in the emulsion system.

Surfactants: Cremophor EL (polyethoxylated castor oil) and Span 80 (sorbitan oleate) were purchased from Sigma-Aldrich.

Water phase: Ultrapure water (Easy, Heal Force, China) was used to prepare emulsion systems.

5.3.2 Methods

5.3.2.1 Mcl-PHA synthesis, purification and characterization

Medium-chain-length poly-3-hydroxyalkanoates (mcl-PHA) was biosynthesized by *Pseudomonas putida* Bet001 utilizing a two–stage fermentation in shake flasks with octanoic acids (1 % *w/v*) as the sole carbon and energy source (Ishak *et al.,* 2016). Bacterial cultivation was carried out at 30 °C and the shaker rotation speed was kept constant at 200 rpm in all experiments. Rich medium (200 ml) and E2 medium (200 ml) were used for the first and second stage of fermentation, respectively. After 24 hours of E2 medium cultivation, the cells were harvested and dried at 70 °C until constant weight. Mcl-PHA was extracted from the cells using acetone and purified repeatedly by cold methanol precipitation (Ishak *et al.,* 2016). This extracted mcl-PHA showed glass transition, melting and decomposition temperatures at about -37 °C, 52 °C and 250 °C, respectively. It consisted of 90 mole % 3-hydroxyoctanote (C_8), 5 mole % 3-hydroxyhexanoate (C_6) and 5 mole % 3-hydroxydecanoate (C_{10}). Its weight average molecular weight (M_w) was determined at 77,435 g mol^{-1} (polystyrene standard equivalent).

5.3.2.2 Emulsion preparation

O/W emulsion was obtained through emulsion-inversion-point (EIP) method by changing the compositon of water-to-oil ratio (W:O) to induce phase inversion. Ultrapure water (W) was added dropwise into a fixed ratio of organic mixtures (surfactants and oil) with simultaneous vortexing until the final weight of 5.0 gram was reached. The optimum formulation of water-to-organic and oil-to-surfactant ratio to obtain nano-sized emulsion was 86:14 and 30:70, respectively. The term "organic" refers to combination of jojoba oil and surfactant fractions. For surfactant fraction, mixture of Cremophor EL and Span 80 were used at 63:37, respectively. The Hydrophile-Lipophile Balance (*HLB*) value of this surfactant mixture was determined at 10.41, calculated using the same equation shown in chapter 3 (Equation 3.1). The *HLB* value of both surfactants, Cremophor EL and Span 80 are 14 and 4.3, respectively.

5.3.2.3 Incorporation of mcl-PHA

By applying the EIP method as described previously and optimal ratio of components, a new derivative of nanoparticle system was developed with the incorporation of mcl-PHA. To this end, all emulsification was carried out at 75 °C and kept constant throughout the preparation process. It was accomplished by pre-heating the ultrapure water and organic mixture overnight at 75 °C to aid the dissolution of solid PHA, prior to emulsification. It should be noted that the amount of mcl-PHA incorporated into the emulsion formulation determined the final jojoba oil fraction. Accordingly, the amount of jojoba oil was reduced with increased fraction of mcl-PHA so as to keep the final weight of the emulsion system constant at 5.0 grams.

5.3.2.4 Emulsion morphology and property at EIP

Morphology and property of polymer emulsion at emulsion inversion point (EIP) were studied by using Fourier transform infrared (FTIR) spectroscopy, Small Angle X-ray Scattering (SAXS) and Optical Polarizing Microscopy (OPM) and viscometer. EIP of the optimal formulation was determined at 30:70 of water-to-organic phase ratio. Therefore, all emulsion samples (with or without mcl-PHA) at 30 % of water content (*w/w*) were prepared similarly as described in previous section. Only water-to-organic ratio was altered while oil-to-surfactant and Cremophor EL-to-span 80 ratios were kept constant.

FTIR analysis was conducted to investigate functional group interactions among different molecular compounds in the emulsion formulation. Measurement was done using FTIR spectrophotometer (Spectrum 400, Perkin-Elmer, USA) at a range of 450 – 4000 cm^{-1}.

SAXS measurement was conducted to investigate the presence of ordered structure in the emulsion sample using an X-ray machine (SaxSpace, Anton Paar, Austria). All measurements were performed using line collimation with exposure time of 15 minutes. Approximately 50 µl of emulsion sample was loaded into a liquid cell holder for measurement. Scattered X-ray pattern following sample exposure was recorded using 1-D diode detector under vacuum at 25 °C. The spectral data were analyzed using SAXSquant software and the lamellar structure phases were assigned using SGI software.

Morphology of emulsion sample was also directly observed under OPM (BX51, Olympus, Japan) to detect the presence of birefringence, which indicates the existence of well-ordered phase structure. Observation was done by illuminating emulsion sample on a glass slide, heated to 50 °C using a hot stage (FP82, Mettler-Toledo, Switzerland)

with polarized light. All images were captured using digital camera (DP26, Olympus, Japan) and analyzed using cellSens-standard software.

Shear viscosity measurements were performed using a viscometer (DV2T, Brookfield, USA) equipped with 2.5 cm (in diameter) cone spindle (CPA-52Z). Approximately 0.5 gram of emulsion sample was loaded onto sample cup for measurement. All measurements were conducted at a shear rate of 50 s^{-1} at 75 °C for 2 minutes.

5.3.2.5 Field emission scanning electron microscopy (FESEM)

Nanoparticles were observed under field emission scanning electron microscope (Quanta FEG 450, FEI, Holland) in high vacuum atmosphere operated at an acceleration rate of 3 to 5 kV. Diluted sample solution (5 % *v/v*) was dropped 3 to 4 times onto mesh copper grids (CF300-Cu) on top of a filter paper to blot excess liquid. Then, phosphotungstic acid solution (1 % *w/v*) was dropped 3 to 4 times onto the same grid to make the nanoparticle conductive. The grid was air-dried in vacuum chamber filled with silica beads for four days prior to observation.

5.3.2.6 Characterization of particle size and distribution

The size and size distribution of nanoparticles were measured based on the mean particle diameter (Zeta average) and particle size distribution (polydispersity index-PDI) of the suspension system, respectively. They were measured by applying static light scattering (SLS) technique using Zetasizer-nanoseries (ZEN3600, Malvern Instruments Ltd, UK). The samples were diluted with ultrapure water (0.05 ml of sample in 0.95 ml H_2O) to avoid multiple scattering effects.

5.4 Results and discussion

5.4.1 Formulation-composition map

In this section, some of the fundamental concepts that are essential in comprehending phase inversion emulsification are firstly expounded. Figure 5.1 shows a schematic presentation of a simplified formulation-composition map that has been widely used as reference for studying and preparing emulsion (Tyrode *et al.*, 2003; Sajjadi *et al.*, 2004; Thakur *et al.*, 2007; Paruta-Tuarez *et al.*, 2011).

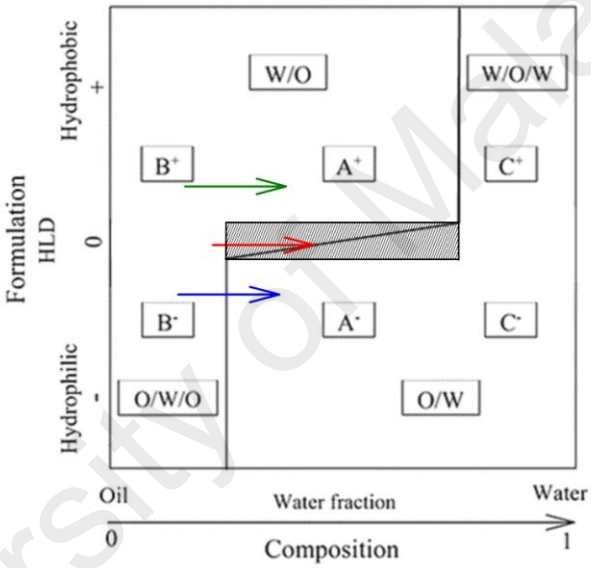

Figure 5.1: Standard Formulation-Composition map

The abscissa in this figure indicates the water content, generally plotted as water volume fraction (f_w). System with large excess of oil ($f_w \approx 0$) is labeled as *B* while *C* for system with large excess of water. The central region of the map located at intermediate water-oil content is labeled as *A*. The -/+ signs indicate the hydrophilic-lipophilic deviation (*HLD*) value, i.e., the formulation with respect to hydrophilic-lipophilic tendency. For instance, at + region (*HLD* > 0), the surfactant exhibits a stronger affinity for the oil and *vice versa* (Kabalnov & Wennerström, 1996). It has been reported that, balanced hydrophilicity and lipophilicty of the surfactant (*HLD* = 0) is attained with a

surfactant mixture corresponding to *HLB* value of 10 to 11 (Sajjadi *et al.*, 2004; Zambrano *et al.*, 2003). Hence, *HLD* > 0 (respectively, *HLD* < 0) is equivalent to *HLB* < 10 (respectively, *HLB* > 11).

HLD is a generalized numerical expression of the deviation from optimum formulation, a concept that includes not only surfactant characteristic of Hydrophile-Lipophile Balance (*HLB*), but also taking into account of other variables such as water-phase salinity, oil nature, the presence of alcohol and temperature (Salager *et al.*, 2000; Queste *et al.*, 2007). According to the definition, *HLD* = 0 is the point of optimum formulation, at which the free energy for transferring the surfactant from the oil to water phase is zero (Salager *et al.*, 1996). It can be expressed in mathematical equation as below (Salager *et al.*, 1996; Perazzo *et al*., 2015):

$$HLD = a - EON - k(ACN) + t(T - 25) + bS + \emptyset(A) \quad \textbf{Eq. 5.1}$$

where α, *k* and *t* are surfactant parameters, ϕ is constant that characterize alcohol/co-surfactant property, *EON* is the average degree of ethoxylation of the surfactant, *ACN* is the number of carbon atom in the alkane (oil phase), *T* is temperature of the system in °C, while *S* and *A* are salt and alcohol/co-surfactant concentration, respectively. From the linear equation, it can be deduced that any changes in system properties such as temperature, type of oil phase and surfactant and the presence of salt or alcohol/co-surfactant will lead to departure from the optimum formulation.

The stair-like line that zigzags the map is called standard inversion line. Emulsion systems on left side of the inversion line are oil continuous (e.g. A^+, B^+ and B^-), whereas on the right side are water continuous (e.g. A^-, C^- and C^+). The systems located in the A^-, A^+, B^+ and C^- regions are termed "normal" emulsion (e.g. W/O and O/W) because they obey Bancroft's rule of natural interfacial curvature (Salager *et al.*,

1983). These emulsions are found to be stable because the surfactant does favor the occurrence of the curvature. On the contrary, the systems located in *B*- and *C*+ regions are termed "abnormal" because they exhibit an interface curvature that against the Bancroft's rule. Abnormal emulsions exhibit a complex morphology called multiple emulsions (e.g. W/O/W and O/W/O), in which the dispersed drops contain droplets of continuous phase that got inserted inside the drops depending on the preparation process (Salager *et al.,* 1983). These types of emulsion reflect the compromise to resolve the incongruity that exists between formulation and water-oil composition, whereby the inner droplets favor the natural interfacial curvature and the outer drops favor the phase in the highest amount as the continuous phase. On the other hand, system that exists in the shaded region of the map (near the locus of optimum formulation i.e. $HLD = 0$) is associated with the three-phase behavior of the surfactant-oil-water system (Salager *et al.,* 1982). It exists when the interfacial tension of water-oil phase is minimum and the system spontaneous curvature is about zero, due to balance affinity of surfactant towards water and oil phase. A variety of phase equilibria such as "water (W) + bi-continuous microemulsion (*D*) + oil (O)", "W + *D* + lamellar liquid crystal (L_a)", "O + $D + L_a$", etc., occur in the surfactant-oil-water system (Kunieda & Shinoda, 1982).

Solid horizontal line in the shaded region is called transitional inversion line. This line is usually slightly sloped due to favored partitioning of the oil-soluble surfactants into the oil phase if a surfactant mixture (polydistributed) is used (Sajjadi *et al.,* 2004). If the formulation of an emulsion system is altered while keeping the composition constant at reasonably balanced amount of water and oil, it will pass through the transitional inversion line and get inverted to emulsion with opposite morphology (Marszall, 1987). For instance, emulsion with average drop size of 40 nm was produced through this manner when the formula system was heated to phase inversion temperature (PIT) to form a bi-continuous *D* phase and gradually cooled

down with gentle stirring (Morales *et al.,* 2003). In contrast, if the system composition is altered to cross the two vertical lines at constant formulation, catastrophic phase inversion will be induced. This type of inversion is called "catastrophic" as it exhibits hysteresis that can be interpreted with a cusp catastrophe model, whereby the phase inversion depends on the hydrodynamic and property of the emulsion system (Silva *et al.,* 1998; Peña & Salager, 2001).

5.4.2 Morphology of mcl-PHA-incorporated emulsion at EIP

5.4.2.1 Fourier transform infrared (FTIR) analysis

From previous chapter, it has been determined that at the optimized condition/formulation, the phase inversion of the standard emulsion system (without incorporation of mcl-PHA) did not involve the formation of multiple emulsion (O/W/O) that would eventually led to drops coalescence and release of internal oil droplets to form O/W emulsion. Instead, it involved the formation of bi-continuous/lamellar phase, which in turn dispersed into submicrometer-sized oil droplets following the EIP. Further elucidation will be discussed in section 5.3.4.

FTIR analysis was conducted and the spectra of the emulsion samples incorporated with mcl-PHA at different amounts and molecular weights (M_w) *viz.* 77435, 7370 and 5130 g mol^{-1} at 30 % of water content (*w/w*) were reported (Figure 5.2*a, b* and *c*, respectively). The different M_ws were obtained through thermal-mediated partial methanolysis of native mcl-PHA. This was achieved by controlling the amount of acidified methanol used (Ishak *et al.,* 2016). The intermolecular interaction among components of emulsion from the functional groups spectra of standard emulsion samples at EIP (Figure 4.3*d*) were used as reference.

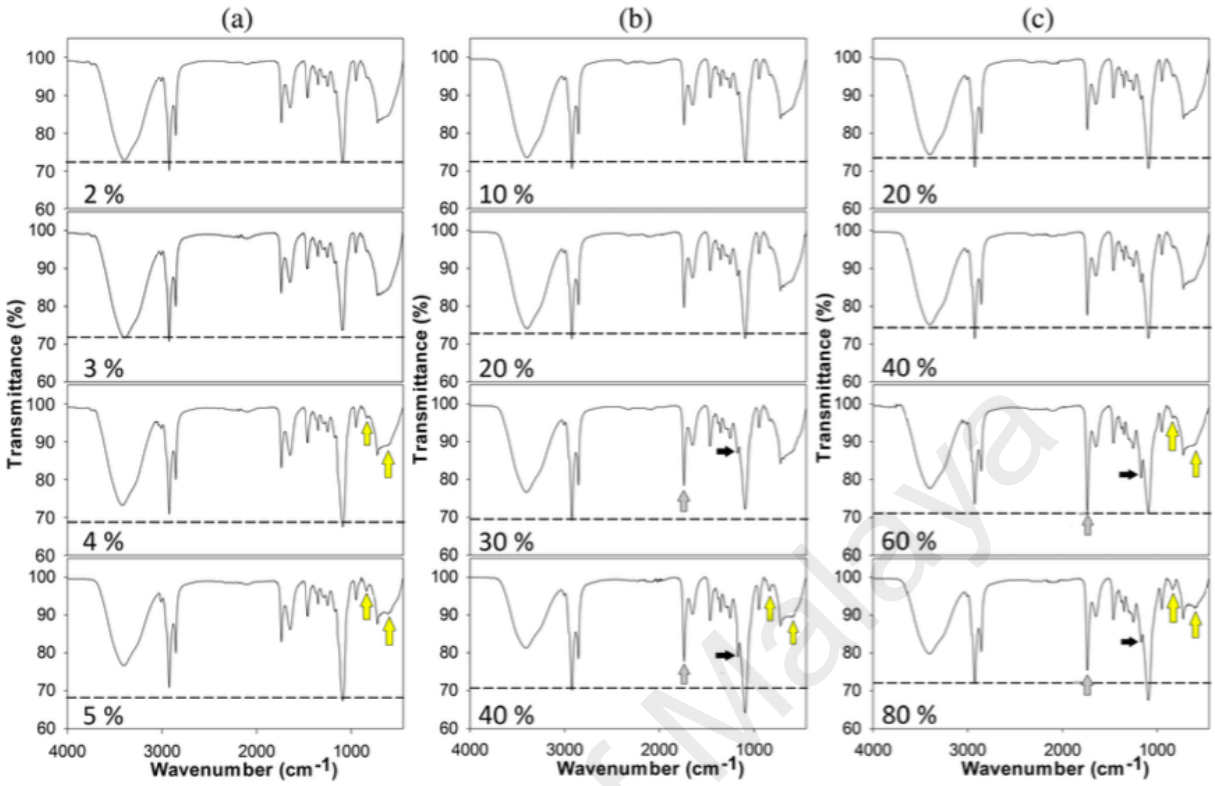

Figure 5.2: FTIR spectra of emulsion sample incorporated with mcl-PHA at different molecular weights M_w, (*a*) 77435, (*b*) 7370, (*c*) 5130 g mol^{-1} at 30 % of water content (*w/w*)

At 2 and 3 % of mcl-PHA amount (*w/w* of total oil fraction) with M_w of 77435 g mol^{-1}, the spectra were similar with the spectra of standard emulsion, indicating similar intermolecular interaction among components within samples. However, when the mcl-PHA amount was increased to 4 and 5 % (*w/w* of total oil fraction), three peaks representing O-H (3450 cm^{-1}), C-H (2925 cm^{-1}) and C-O-C (1100 cm^{-1}) were no longer having the same value of transmittance indicating imbalanced intermolecular interactions among water, oil and surfactants. This suggests that the formation of bi-continuous/lamellar structure phase at EIP was inhibited if more than 4 % (*w/w* of total oil fraction) of mcl-PHA used. Moreover, two peaks at 600 – 850 cm^{-1} (*yellow arrow*) were no longer exist as one broad peak as in the previous spectra, indicating the

Cremophor EL and Span 80 surfactants were not well oriented at the interfacial surface of oil- and water phase.

It was found that more mcl-PHA could be incorporated as additive material when its molecular weight was reduced. For instance, about 20 and 40 % (*w/w* of total oil fraction) of the mcl-PHA amount (7370 and 5130 g mol^{-1}, respectively) can be incorporated without affecting the balance affinity of the surfactants towards oil and water phase i.e. the bi-continuous/lamellar phase formation. However, the balance was disrupted when more than 30 and 60 % (*w/w* of total oil fraction) of mcl-PHA amount (7370 and 5130 g mol^{-1}, respectively) were incorporated in the emulsion systems, concomitantly the observation that three peaks of O-H (3450 cm^{-1}), C-H (2925 cm^{-1}) and C-O-C (1100 cm^{-1}) were no longer having the same value of transmittance.

Two peaks at 1167 cm^{-1} (*black arrow*) 1735 cm^{-1} (*grey arrow*) representing C-O-C of ester bond and C=O of ester bond/carboxylic group of mcl-PHA, respectively, became more prominent as high amount of mcl-PHA was used. Most importantly, peak C=O (1735 cm^{-1}) almost had same value of transmittance with peaks C-H (2925 cm^{-1}) and C-O-C (1100 cm^{-1}) when lower molecular weights of mcl-PHA (5130 g mol^{-1}) was used at high amounts (> 60 % *w/w* of total oil fraction). These were attributed to assemblage of mcl-PHA molecules with the surfactants at the water-oil interface during emulsification. Partial degradation of mcl-PHA may produce short oligomers that could have exhibited surfactant-like properties since they possess terminal hydroxyl groups.

5.4.2.2 SAXS and OPM analysis

The existence of bi-continuous/lamellar structure in emulsion at EIP, as discussed earlier, was also indirectly supported by the interpretation of X-ray scattering pattern produced. Figure 5.3*a*, *b* and *c* show the X-ray spectra of the emulsion samples incorporated with mcl-PHA at different molecular weights (M_w) *viz.* 77435, 7370 and 5130 g mol^{-1}, respectively, at 30 % of water content (*w/w*). It can be seen that samples with 2 and 3 % (*w/w*) of mcl-PHA (77435 g mol^{-1}), 10 and 20 % (*w/w*) of mcl-PHA (7370 g mol^{-1}) as well as 20 and 40 % (*w/w*) of mcl-PHA (5130 g mol^{-1}) show two peaks in their spectra indicating the existence of bi-continuous/lamellar structure phase. These results corroborate the FTIR results whereby the limit of mcl-PHA amount that can be incorporated, without significantly affecting the balance of the three peaks from FTIR earlier *viz.* 3450 cm^{-1}, 2925 cm^{-1} and 1100 cm^{-1}, were 3, 20 and 40 % (*w/w* of total oil fraction) of mcl-PHA with molecular weights of 77435, 7370 and 5130 g mol^{-1}, respectively

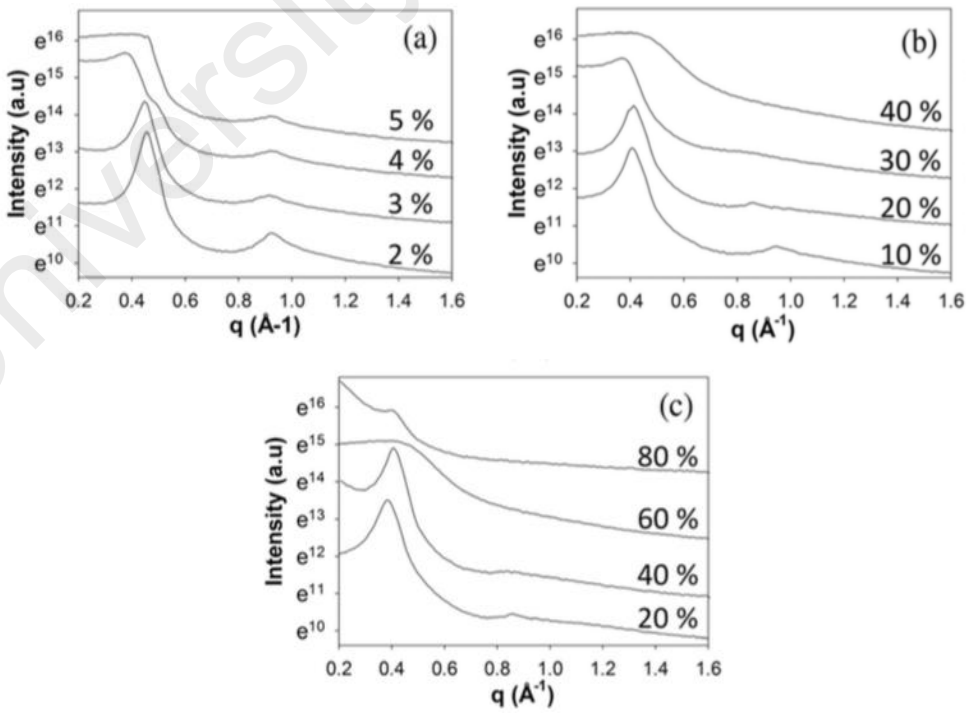

Figure 5.3: X-ray spectra of emulsion sample incorporated with mcl-PHA at different molecular weights M_w, (*a*) 77435, (*b*) 7370, (*c*) 5130 g mol^{-1} at 30 % of water content (*w/w)*

Direct observation of emulsion morphology using OPM is shown in Figure 5.4. It can be seen that formation of bi-continuous/lamellar structure can be induced at EIP in emulsion samples with 2 and 3 % (*w/w*) of mcl-PHA (77435 g mol^{-1}), 10, 20 and 30 % (*w/w*) of mcl-PHA (7370 g mol^{-1}) as well as 20 and 40 % (*w/w*) of mcl-PHA (5130 g mol^{-1}). However, the width of lamellar structure (lattice parameter) for emulsion samples with 30 % (*w/w*) of mcl-PHA (7370 g mol^{-1}) is bigger than other percentages. This could help to explain on why the three peaks representing O-H (3450 cm^{-1}), C-H (2925 cm^{-1}) and C-O-C (1100 cm^{-1}) for this sample were not having the same value of transmittance (Fig. 5.2*b – 30%*) and the two peaks in X-ray spectrum (Fig. 5.3*b – 30%*) were not as prominent as the others due to the failure of surfactants to align along the linear film of water-oil streamline interfaces.

Formation of multiple emulsions can be seen in emulsion samples with 4 and 5 % (*w/w*) of mcl-PHA (77435 g mol^{-1}) as well as 40 % (*w/w*) of mcl-PHA (7370 g mol^{-1}). As for emulsion samples incorporated with 60 and 80 % (*w/w*) of mcl-PHA (5130 g mol^{-1}), W/O emulsion systems were produced at 30 % of water content (*w/w*). Possible reasons for these observations are discussed in section 5.3.4.

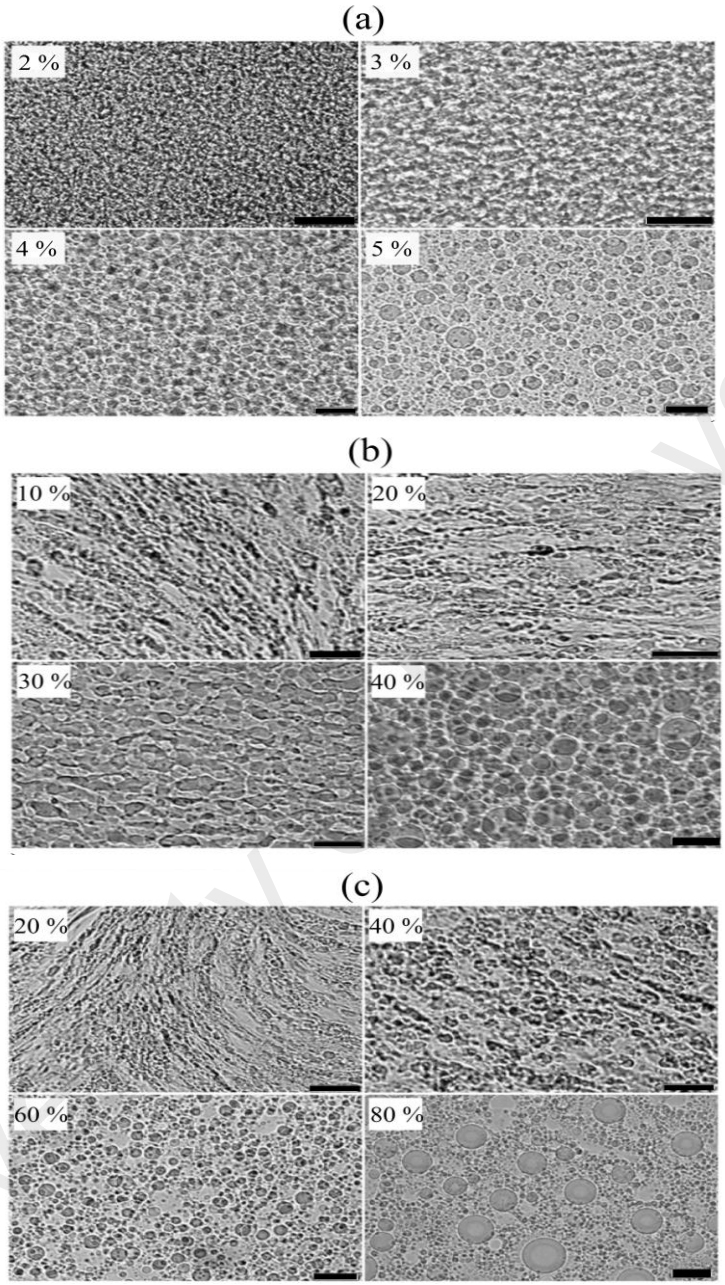

Figure 5.4: OPM images of emulsion sample incorporated with different mcl-PHA molecular weights M_w, (*a*) 77435, (*b*) 7370, (*c*) 5130 g mol^{-1} at 30 % of water content (*w/w*). Scale bars (*white*) represent 50 μm except in (*a-2%*) represents 100 μm

5.4.3 Effects of mcl-PHA molecular weight and amount on final nanoparticle size and distribution

Figure 5.5*a*, *b* and *c* show the viscosity values of the emulsion samples incorporated with mcl-PHA at different molecular weights (M_w) *viz.* 77435, 7370 and 5130 g mol^{-1}, respectively, at 30 % of water content (*w/w*) and their respective final average size of oil droplets produced. Their corresponding particle size distributions and emulsion samples are shown in Figure 5.6.

From the graphs, it can be deduced that only emulsion samples with viscosity below than ~ 85 mPa at 30 % *w/w* of water content result in oil droplets with average size below than 50 nm in diameter. These emulsion samples were able to form bi-continuous/lamellar structure at EIP, as shown in Figure 5.4. The threshold viscosity value is hypothesized to be the maximum for a stable three-phase behavior of surfactant-oil-water system. It may be conjectured that, by incorporating inappropriate amount and molecular weight of mcl-PHA, the formation of bi-continuous/lamellar structure phase would be less efficient at EIP. Instead, the formation of complex morphology of multiple emulsions with close packing conditions occurs at EIP, thus increasing the mixture viscosity.

It is suggested that without proper formation of the surfactant-oil-water system at EIP, gradual dispersion of bulk oil into smaller droplets after inversion could not occur efficiently (elucidated in section 5.3.4). As the result, opaque emulsions with larger particles and high polydispersity index value were produced (Figure 5.6). A study also had suggested that the main requirement for the formation of bluish transparent O/W nanoemulsion is to achieve a complete solubilization of the oil phase in the bi-continuous *D* phase (Morales *et al.,* 2003). FESEM images of polymeric particles at specified formulation are shown in Figure 5.7. Larger particles at submicrometer scale (Fig. 5.7 *d* and *f*) appear denser than smaller particles at nanometer scale.

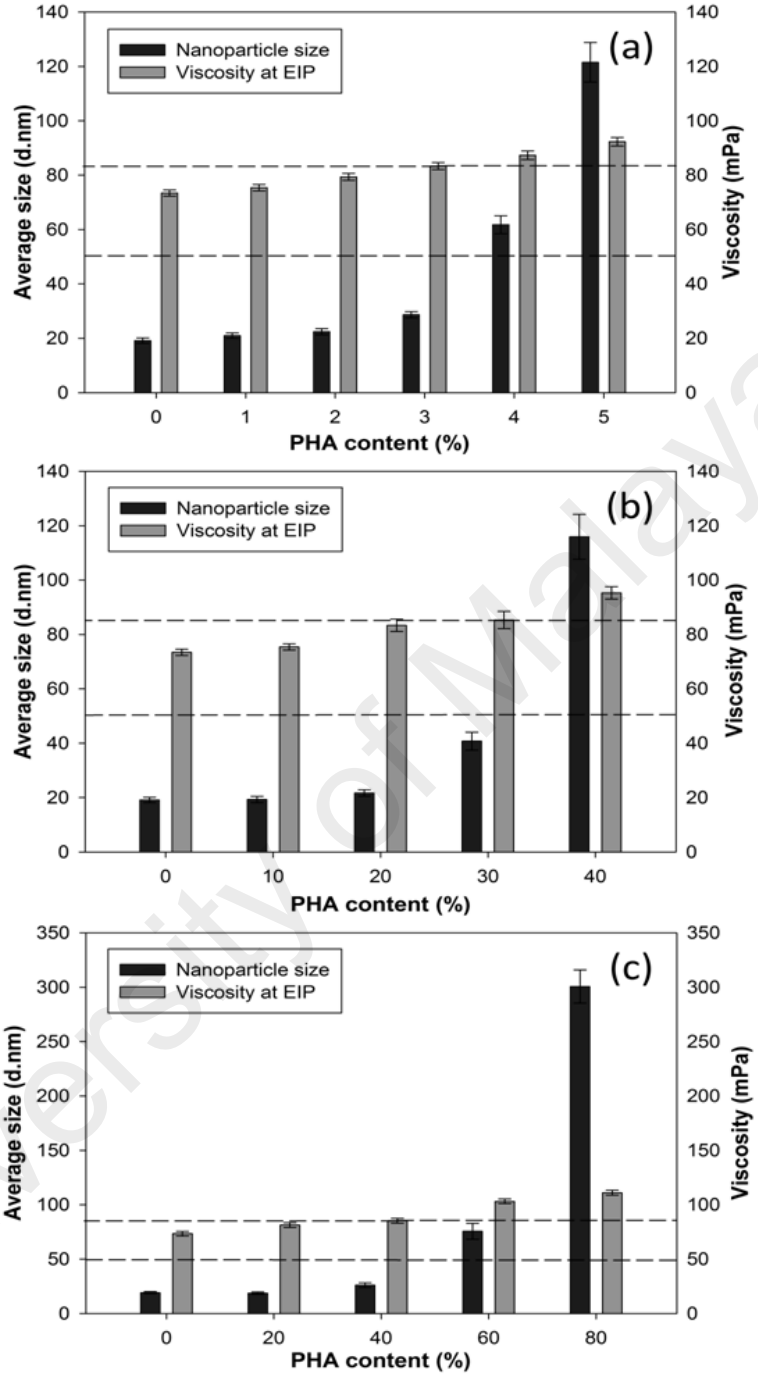

Figure 5.5: Final average nanoparticle sizes when incorporated with different mcl-PHA molecular weights (M_w), (*a*) 77435, (*b*) 7370, (*c*) 5130 g mol^{-1} along with corresponding viscosities of emulsion samples at 30 % of water content (*w/w*); 0 % is standard emulsion

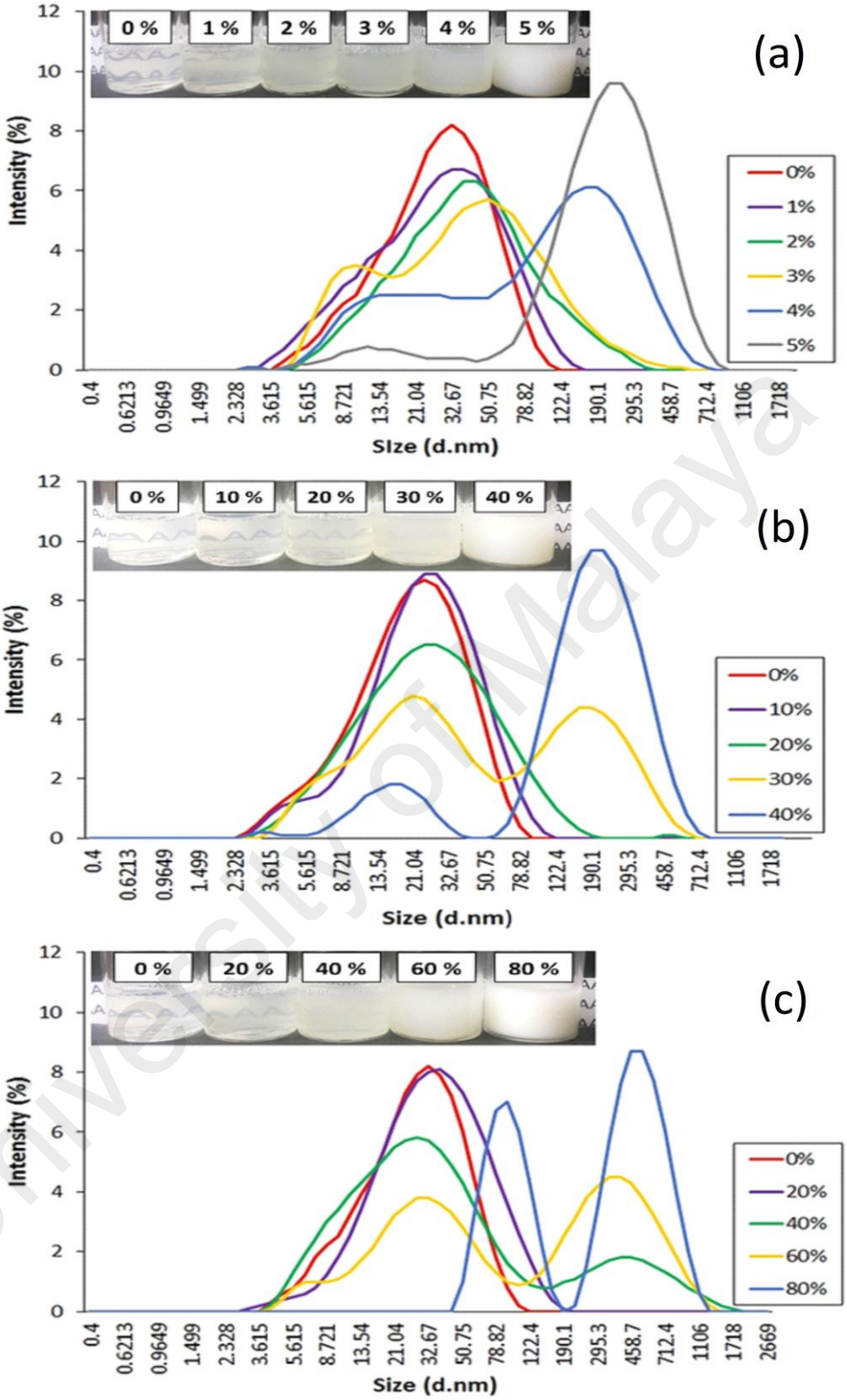

Figure 5.6: Final particle distribution of emulsion sample incorporated with mcl-PHA at different molecular weights M_w, (*a*) 77435, (*b*) 7370, (*c*) 5130 g mol^{-1}; 0 % is standard emulsion

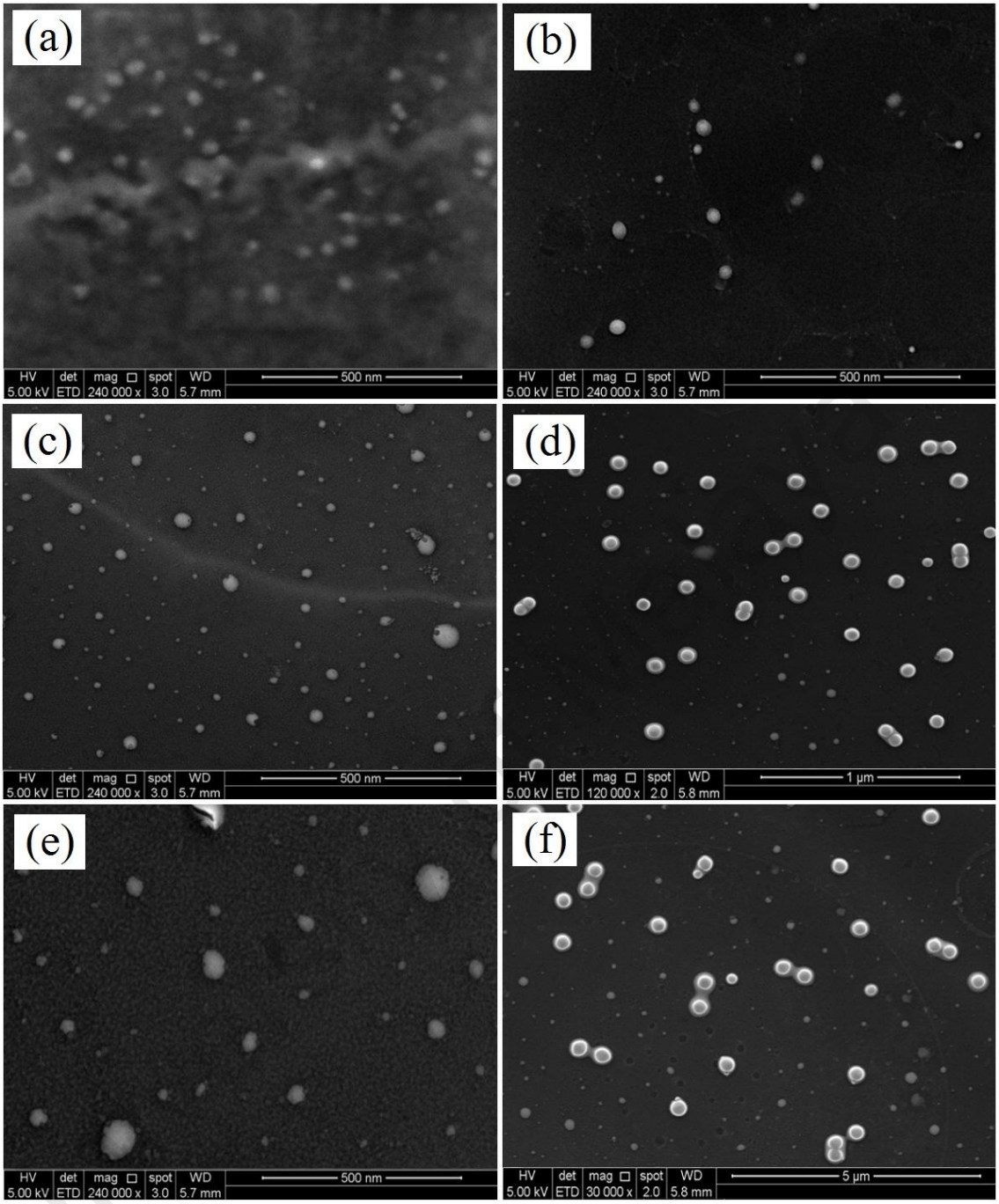

Figure 5.7: FESEM images of (*a*) standard emulsion particles and mcl-PHA-incorporated particles at different mcl-PHA amounts, (*b*) 3 % of 77435, (*c*) 10 % (*d*) 40 % of 7370 and (*e*) 60 % (*f*) 80 % of 5130 g mol^{-1}

5.4.4 Hypothetical inversion mechanism of mcl-PHA-incorporated emulsion

From the results, it is clear that mcl-PHA molecular weight (M_w) and amount significantly affect the system morphology at the emulsion inversion point (EIP) i.e. 30 % of water content (*w/w*). Differences in morphologies at EIP apparently determine the final emulsion appearance, particle size and distribution. Figure 5.8 shows the schematic of two plausible paths of emulsification mechanism (5.8*a* and *b*).

At optimum formulation, the emulsification process of mcl-PHA-incorporated emulsion at appropriate amount and molecular weight is hypothesized to follow similar path as the standard emulsion (emulsion without mcl-PHA) i.e. through the formation of bi-continuous/lamellar structure phase at EIP. The emulsification starts with the formation of water droplets in continuous oil phase (W/O emulsion) that would coalesce and elongate due to mechanical stirring (5.8*a. i*), which eventually results in the formation of bi-continuous/lamellar structure phase at EIP (5.8*a. ii*) as the water content increases. After the continuous oil phase is inverted into dispersed phase (5.8*a. iii*), it is gradually dispersed into smaller droplets (5.8*a. iv*) with the increase in water content. The drops dispersion proceeds until stable nano-sized particles are obtained. The path direction is indicated by *red arrow* on the formulation-composition map (Figure 5.1). This observation is similar to a previous study where high non-ionic surfactant concentration allows for a complete solubilization of the oil phase near the EIP with droplet size distribution primarily controlled by the bi-continuous or lamellar phase during the phase inversion (Fernandez *et al.*, 2004).

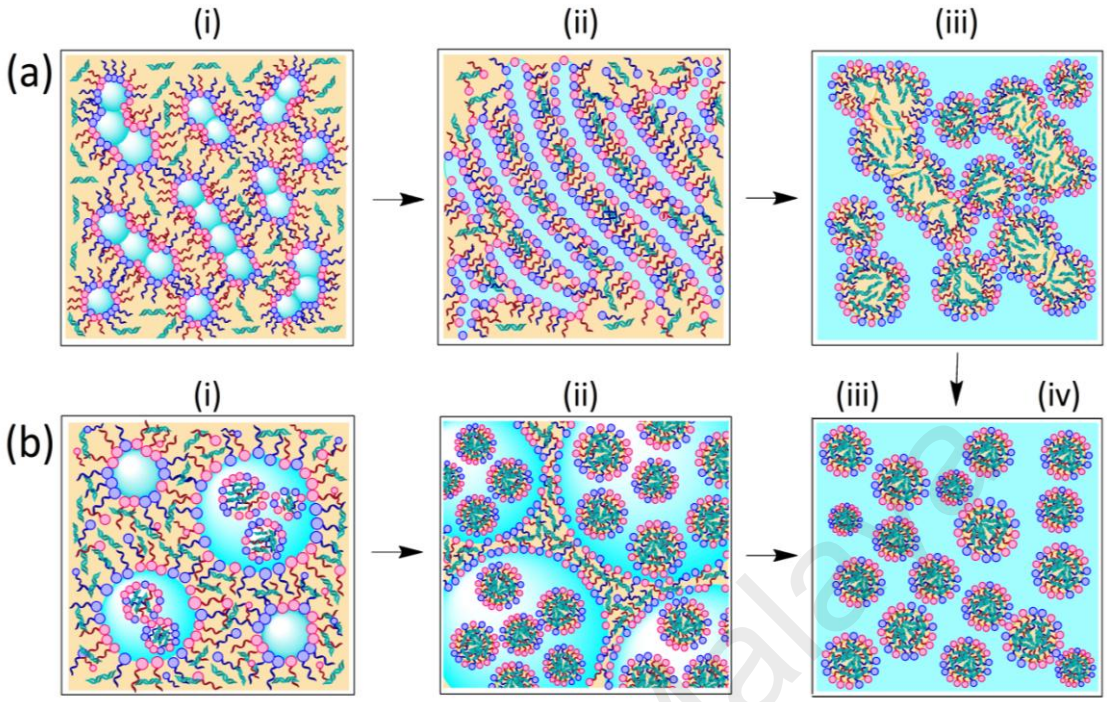

Figure 5.8: Hypothetical inversion mechanism of mcl-PHA-incorporated emulsion at (*a*) optimal condition and (*b*) non-optimal condition

However, the path described above is limited to mcl-PHA at an appropriate molecular weight and amounts. As discussed earlier, more mcl-PHA can be incorporated when its molecular weight was reduced. Nevertheless, incorporating high molecular weight mcl-PHA at inappropriate amounts could cause the samples formulation deviate from the locus of optimum formulation (*HLD* = 0) by increasing the value of *ACN* parameter in Equation 5.1. As the result, the sample is more hydrophilic (*HLD* < 0) at the beginning of emulsification. This formulation adjustment would lead to different path of emulsification than the aforementioned path as shown in Figure 5.8*b*. When water is added into the hydrophilic organic phase, the dispersed water drops will be gradually injected with oil droplets (forming multiple emulsion) as the inner droplets favor the natural interfacial curvature and the outer drops favor the phase in the highest amount as the continuous phase (5.8*b. i*). The dispersed water drops may become swollen with oil droplets that eventually reach close packing conditions of rigid

sphere tessellation at EIP (5.8*b. ii*) and lead to coalescence and release of internal oil droplets to form O/W emulsion (5.8*b. iii*). The path direction is indicated by *blue arrow* on the formulation-composition map (Figure 5.1). The catastrophic phase inversion depends on the hydrodynamic (e.g. stirring and water addition rate) and property (e.g. phase viscosity and surfactant concentration) of the emulsion system. Therefore, the size of injected oil droplets and rate of water drops coalescence are hardly controlled. As a result, opaque O/W emulsion system with large particle size and distribution is produced.

On the other hand, incorporating mcl-PHA with lower molecular weight at higher amount showed different morphology at the same EIP as shown previously (Figure 5.4*c. 60* and *80 %*). As discussed in section 5.3.2.1, partial degradation of mcl-PHA produced short oligomers with surfactant-like properties, as they possess terminal hydroxyl groups. Therefore, incorporating mcl-PHA oligomers could cause deviation of sample formulation from the optimum locus ($HLD = 0$), by increasing the value of A parameter in Equation 5.1. As the result, the sample is more hydrophobic ($HLD > 0$) and produces W/O emulsion instead of multiple emulsions at the beginning of emulsification. It is hypothesized that the emulsification follows the path direction as indicated by *green arrow* on the formulation-composition map (Figure 5.1) and eventually crosses the upper catastrophic inversion line.

5.5 Concluding remarks

Incorporation of inappropriate molecular weight and amount of mcl-PHA affected the final particle size and size distribution of nanoparticle *via* inhibition of bi-continuous/lamellar structure phase formation. Without proper formation of the surfactant-oil-water system at EIP, gradual dispersion of bulk oil into smaller droplets after inversion could not occur efficiently, resulting in opaque emulsions with larger particles and wider size distribution.

Incorporating mcl-PHA at appropriate molecular weight and amount would lead to standard path of normal emulsification by crossing the transitional inversion line. Otherwise, it could cause formulation adjustment that lead to an alternative path of abnormal emulsification subsequently crossing the catastrophic inversion line.

CHAPTER 6: EFFECT OF EMULSIFICATION TEMPERATURE ON THE INVERSION MECHANISM OF PIE

6.1 Summary

The study investigated the effects of temperature on the phase behavior of medium- chain-length poly-3-hydroxyalkanoates (mcl-PHA)-incorporated emulsion system. It is suggested that the three-phase equilibrium consisting of lamellar liquid crystalline (L_a), bi-continuous microemulsion (D) and oil-swollen micelle phases formed in the vicinity of optimal formulation when the combination of phase inversion composition (PIC) and phase inversion temperature (PIT) methods was applied. The interaction effects between temperature and mcl-PHA molecular weight influenced the lamellar/bi-continuous microemulsion formation within the mcl-PHA-incorporated emulsion. It is suggested that the lamellar/bi-continuous microemulsion phase of mcl-PHA-incorporated emulsion can be formed from multiple emulsion system through thermal induction proximately before EIP and its hypothetical formation mechanism is elucidated in this study.

6.2 Introduction and literature review

Emulsification is a process of mixing two immiscible phases (typically water- and oil-based phases) by dispersing one phase (internal) in another continuous phase (external) to form a colloidal dispersion system called emulsion. The process is widely applied in pharmaceutical, food and cosmetic industries (Salager *et al.,* 2004). For instance, emulsification has been used to produce nano-sized emulsions for the delivery of active molecules through oral (Huang *et al.,* 2010), intra-nasal (Kumar *et al.,* 2008), intravenous (Fast & Mecozzi, 2009) and topical (Mou *et al.,* 2008) routes.

Emulsion can be generally classified as water-in-oil (W/O) or oil-in-water (O/W) depending on the dispersed phase. The size of dispersed phase will determine the specific type of emulsion system. Conventional emulsions are made up of droplets with size range from 0.5 to 100 μm. However, these droplets are subjected to significant gravitational influence making the emulsion system prone to sedimentation (Binks, 1998). Nanoemulsions exhibit even smaller droplet size range, typically between 20 – 500 nm. Consequently, they appear as transparent or translucent solution and are stable against sedimentation or creaming (Solans *et al.,* 2002). Due to the kinetic stability and transparency, this type of emulsion is attracting wider practical interests (Solans & Kunieda, 1997).

To generate nanoemulsion using conventional emulsification method will require vigorous agitation of immiscible binary mixture, as substantial energy input is needed to overcome a strong Laplace pressure. Alternatively, the use of surfactants in emulsification can reduce the amount of energy needed to overcome the pressure from interfacial tension of two immiscible liquids. One of the most common low-energy methods to generate emulsion is phase inversion emulsification (PIE). It involves the inversion of two phases i.e. from water-in-oil (W/O) emulsion to oil-in-water (O/W) emulsion or *vice versa* (Maali & Mosavian, 2013; Antón *et al.,* 1986). PIE can be sub-categorized as catastrophic or transitional (Salager *et al.,* 1983; Kumar *et al.,* 2015). Changing the system composition (water-to-oil ratio) through stepwise addition of intended continuous phase induces catastrophic phase inversion (CPI) (Bouchama *et al.,* 2003). This technique is known as phase inversion composition (PIC) or emulsion inversion point (EIP) method (Bouchama *et al.,* 2003). The critical volume fraction that induces this type of inversion is called emulsion inversion point (EIP). On the other hand, altering the system formulation *via* changing the strength of interaction between surfactants and fluid phases induces transitional phase inversion. Applying thermal

effect to modulate the affinity of surfactant(s) toward water- and oil phases is known as phase inversion temperature (PIT) method (Shinoda & Saito, 1968; Sherman & Parkinson, 1978; Anton & Vandamme, 2009). The critical temperature whereby the interfacial tension between oil and water phases at the lowest is called hydrophilic-lipophilic balance temperature (T_{HLB}).

Nanoemulsion templating technique exploiting PIE can be applied to produce polymeric nanoparticle (Vauthier & Bouchemal, 2009; Gaudin & Sintes-Zydowicz, 2008, 2011; Caldero *et al.*, 2011; Fornaguera *et al.*, 2015) with desired properties for delivery applications (Elsabahy & Wooley, 2012). It has been shown that the preparation of medium-chain-length poly-3-hydroxyalkanoates (mcl-PHA)-incorporated polymeric nanoparticle can be produced through the nanoemulsion templating technique (Chapter 3 and 4). It is suggested that mcl-PHA could provide a protective matrix within the nanoparticle to delay premature degradation of encapsulated active compounds (Chapter 4). Mcl-PHA is a biopolyester from microorganism that has melting (T_m) and glass transition (T_g) temperatures ranging from 40 to 65 °C and -50 to -25 °C, respectively (Rai *et al.*, 2011). Therefore, it can be easily dissolved/incorporated within oil phase by elevating and maintaining the solution temperature above its T_m value throughout emulsification to produce polymer-based O/W emulsion. More importantly, the cross-linking initiator and organic solvent that are commonly used to produce polymeric nanoparticle can be circumvented. This temperature-elevated emulsification is similar to the technique of producing solid-lipid particle, whereby the solid lipid is melted at elevated temperature during emulsification (MuÈller *et al.*, 2000).

Phase inversion mechanism of mcl-PHA-incorporated emulsion at 75 °C was found to be significantly influenced by the molecular weight and amount of mcl-PHA (Chapter 5). Inappropriate application of mcl-PHA in terms of molecular weight and

amount inhibits the formation of lamellar/ bi-continuous (*D*) phase at EIP. It is hypothesized that thermal effect would results in similar observation. Therefore, the effect of temperature on the formation of lamellar/bi-continuous (*D*) phase of mcl-PHA-incorporated emulsion system by application of PIC/EIP method was investigated. Formation of the phase structure was also studied by using PIT method. Optical polarizing microscopy (OPM) was employed to investigate the existence of lamellar phase at EIP. Formation mechanism of lamellar/bi-continuous phase structure from multiple emulsions *via* thermal induction is proposed.

6.3 Methodology

6.3.1 Materials

Jojoba oil (Sigma-Aldrich) and mcl-PHA were used as the organic phase the emulsion system. *Pseudomonas putida* Bet001 (Gumel *et al.,* 2012) was used to produce of mcl-PHA by using octanoic acid as carbon source (Ishak *et al.,* 2016). The extracted mcl-PHA showed glass transition, melting and decomposition temperatures at about –37 °C, 52 °C and 250 °C, respectively. Two technical grade surfactants namely Cremophor EL (polyethoxylated castor oil) and Span 80 (sorbitan oleate) were purchased from Sigma-Aldrich. Ultrapure water (Easy, Heal Force, China) was used as aqueous phase to prepare the emulsion system.

6.3.2 Methods

6.3.2.1 Preparation of mcl-PHA-incorporated O/W emulsion

Standard O/W emulsion was used as template to produce mcl-PHA-incorporated nanoparticle. Water-to-organic phase, oil-to-surfactants and Cremophor EL-to-Span 80 ratio were first optimized at 25 °C using response surface methodology (RSM) with the size of oil droplets produced as the response variable. Optimum formulation (*w/w*) of

the aforementioned ratios to obtain nano-sized emulsion (20 – 30 nm) was 86:14, 30:70 and 63:37, respectively. The hydrophile-lipophile balance (*HLB*) value of this surfactant mixture was determined at 10.41 (Chapter 4 and 5).

Incorporation of mcl-PHA into the emulsion system was achieved by elevating the emulsification temperature (Chapter 4 and 5). Two different molecular weights (M_ws) of mcl-PHA (i.e. 77,435 and 7370 g mol^{-1}) were used in this study. The degraded mcl-PHA (7370 g mol^{-1}) was obtained from thermal-mediated partial methanolysis of native mcl-PHA (77,435 g mol^{-1}). This was achieved by controlling the amount of acidified methanol used (Ishak *et al.*, 2016).

6.3.2.2 Study of lamellar and bi-continuous (*D*) phase formation

The phase behavior of emulsion sample was investigated *via* water penetration scan technique under OPM. A small amount of well-mixed sample was placed on the glass slide and covered with coverslip. A drop of ultrapure water was then placed at the edge of coverslip. This resulted in water penetration into the sample layer following water concentration gradient *via* capillary action. Samples were allowed to equilibrate at a given temperature for about 5 minutes. The formation of lamellar phase can be detected by the presence of birefringence in the sample observed under OPM. It was also indirectly indicated through transmittance value, which is measured by detecting the fraction of light that passes through the samples.

6.3.2.3 Analytical instruments

Morphology of the emulsion sample was directly observed using Olympus BX51 microscope fitted with cross-polarizing filters. Observation was done by illuminating emulsion sample layer on a glass slide with polarized light. The slide was heated to a desired temperature using a hot stage (FP82, Mettler-Toledo, Switzerland).

All images were captured using digital camera (DP26, Olympus, Japan) and analyzed using cellSens-standard software.

The size and size distribution of nanoparticles were measured by using Zetasizer-nanoseries (ZEN3600, Malvern Instruments Ltd, UK). The samples were diluted with ultrapure water (0.05 ml of sample in 0.95 ml H_2O) to avoid multiple scattering effects.

The transmittance value of samples was measured by using Litesizer™ 500 (Anton Paar, Austria) at 80 °C.

6.4 Results and discussion

6.4.1 Transitional phase inversion in the vicinity of optimal formulation

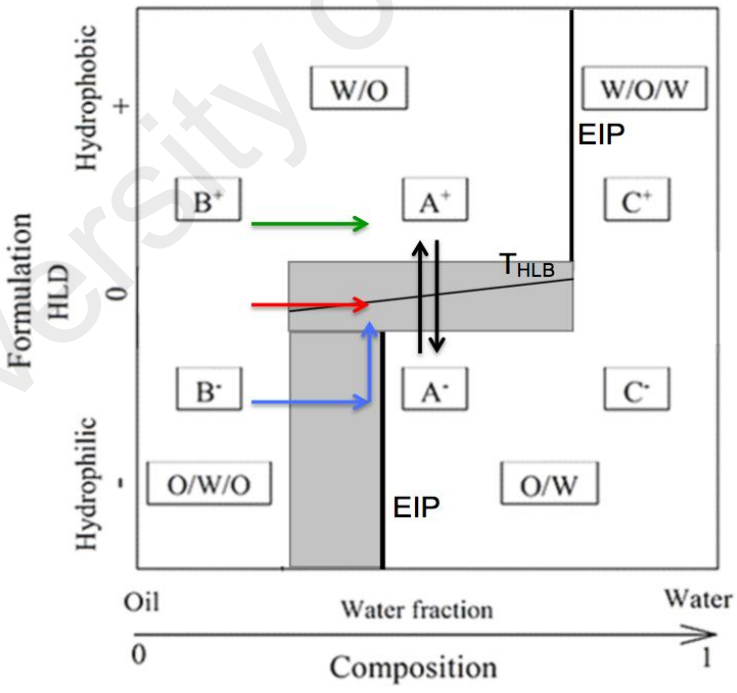

Figure 6.1: Formulation-composition map

Figure 6.1 shows a standard formulation-composition map that has been widely used as guidelines for studying and preparing emulsion through PIE (Tyrode *et al.*, 2003; Sajjadi *et al.,* 2004; Thakur *et al.,* 2007; Paruta-Tuarez *et al.,* 2011). The hydrophilic-lipophilic deviation (*HLD*) can be expressed in mathematical equation as shown below (Salager, 1996; Perazzo *et al.*, 2015):

$$HLD = a - EON - k(ACN) + t(T - 25) + bS + \emptyset(A) \quad \textbf{Eq. 6.1}$$

where α, k and t are surfactant parameters, b and ϕ are constants that characterize type of salt and alcohol/co-surfactant property (respectively), *EON* is the average degree of ethoxylation of the surfactant, *ACN* is the number of carbon atom in the alkane (oil phase), *T* is temperature of the system in °C, while *S* and *A* are salt and alcohol/co-surfactant concentration, respectively. It has been reported that, balanced hydrophilicity and lipophilicity of the surfactant (*HLD* = 0) is attained with a surfactant mixture corresponding to *HLB* value of 10 to 11 (Sajjadi *et al.*, 2004; Zambrano *et al.,* 2003).

System that exists in the vicinity of *HLD* = 0 (horizontal shaded region of the map) is typically associated with the three-phase equilibrium of surfactant-oil-water system (Winsor III equilibrium) (Salager *et al.,* 1982). One definite phase within the system is bi-continuous microemulsion (*D*) phase. The *D* phase typically coexists with other phases in the Winsor III equilibrium. For examples, a rich variety of phase equilibria such as water + bi-continuous *D* phase + oil, water + lamellar liquid crystal + bi-continuous *D* phase, oil + bi-continuous *D* phase + lamellar liquid crystal, etc., occur in the surfactant-oil-water system (Kunieda & Shinoda, 1982). The bilayer geometry of bi-continuous microemulsions is hyperbolic, i.e. the bilayers of surfactant molecules are intertwined everywhere in saddle-shaped and immersed in interconnected water continua (Hyde, 1997). It is formed when lamellar structure phase is swollen/hydrated

with high amount of water following the change in preferred curvature surfactants layer from flat to curved toward oil region (Roger, 2016).

Transitional phase inversion will be induced when an emulsion system traverses the horizontal shaded region and inverts to the opposite morphology following inversion line/point. For instance, nanoemulsion was produced when the course mixture of surfactant, oil and water was heated above its T_{HLB} (indicated by *black arrow* on the formulation-composition map) to form a bi-continuous microemulsion, and gradually cooled down with gentle stirring to form O/W emulsion system (Förster *et al.,* 1992). Apart from varying the temperature, inversion of W/O to O/W emulsion through formation of the bi-continuous microemulsion can also be achieved by PIC/EIP method (indicated by *red arrow* on the formulation-composition map) (Wang *et al.,* 2008). It exploits synergism effect to induce phase inversion where a couple of surfactants are used to lower the interfacial tension with respect to a system having only one type of surfactant (Strey, 1996). A typical progression of the equilibrium phases starts with dispersion of water-swollen micelles, followed by lamellar phase, then a bi-continuous (*D*) phase to a hexagonal phase and eventually a dispersion of oil-swollen micelles (Roger, 2016). Thus, a mechanism analogous to the temperature-induced bi-continuous microemulsion in PIT has been proposed to explain PIC/EIP as well.

6.4.2 Standard emulsion system (without incorporation of mcl-PHA)

It was determined that at optimal formulation, the phase inversion of the standard emulsion system involved the formation of lamellar/ bi-continuous (*D*) phase at EIP (30 % *w/w* of water content), which in turn gradually dispersed into submicrometer-sized oil droplets (*red arrows* in Figure 6.2). Other studies reported the addition of water led to the formation of water droplets that were easily elongated by the action of mixing flow and merged together to form lamellar structures, which

subsequently led to formation of fine oil droplets (De Gennes & Taupin, 1982; Fernandez *et al.*, 2004). Likewise, nano-sized oil droplets were produced through stepwise addition of water (PIC/EIP method) in emulsion system that went through three-phase equilibrium consisting of bi-continuous microemulsion (*D*), lamellar liquid crystalline (L_a) and oil (O) phases (Forgiarini *et al.*, 2001).

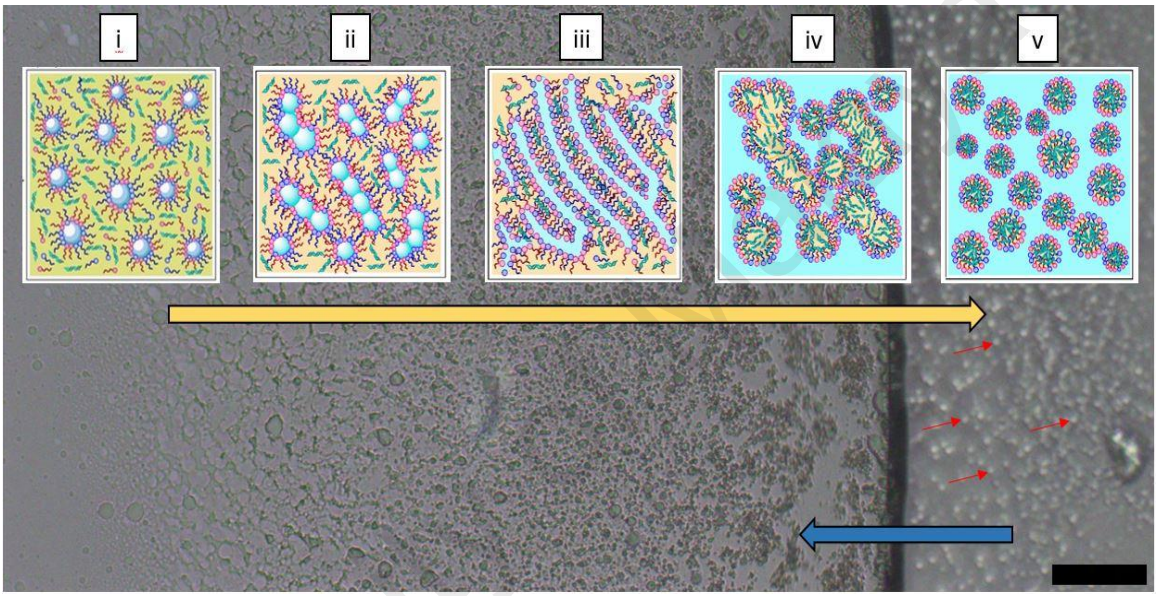

Figure 6.2: OPM images of standard nanoemulsion formation at 35 °C. Initial water content of emulsion sample was 15 % *w/w*. *Yellow arrow* indicates the direction of O/W formation and *blue arrow* the direction of water penetration. Scale bar (*black*) represents 100 µm

According to Equation 6.1, any changes in system properties such as temperature, type of oil phase and surfactant and the presence of salt or alcohol/co-surfactant will result in departure from the optimum formulation (*HLD* = 0). Therefore, increasing the temperature prior to emulsification would change the neutral/optimal formulation (*HLD* = 0) into hydrophobic formulation (*HLD* > 0). Thus, the possible route of emulsification passes through catastrophic inversion line, as indicated by a *green arrow* on the formulation-composition map (Figure 6.1). Deviation from optimum formulation prior to emulsification may cause the absence of lamellar/ bi-

continuous (*D*) phase formation at EIP, as transitional inversion line is not crossed. Consequently, gradual dispersion of oil phase into nano-sized oil droplets cannot occur efficiently and opaque O/W emulsion system with large particle size and size distribution will be easily produced.

In contrast, altering the temperature did not significantly affect the development of standard O/W nanoemulsion through EIP method in this study (Figure 6.3*a*). This probably attributed to the formation of temperature-insensitive bi-continuous microemulsion with high solubilization capacity of Cremophor EL-Span 80 mixture used in this study. Formation of temperature-insensitive microemulsion through mixing of two surfactants in the formulation has been reported in other studies (Antón *et al.,* 1995; Oh *et al.,* 1995). Figure 6.3*b* shows the *in situ* emulsification of standard emulsion at different temperatures. The lamellar structures (indicated by *blue arrows* in Figure 6.3*b*) may swell into bi-continuous microemulsion upon hydration. A few studies suggested that the main requirement for the formation of bluish transparent O/W nanoemulsion is a complete solubilization of the oil phase in the bi-continuous microemulsion (Miñana-perez *et al.,* 1999; Forgiarini *et al.,* 2001; Sajjadi *et al.,* 2004). Similarly, bluish transparent O/W nanoemulsions were formed at final composition of 86 % *w/w* of water content (*see inserts in* Figure 6.3*a*).

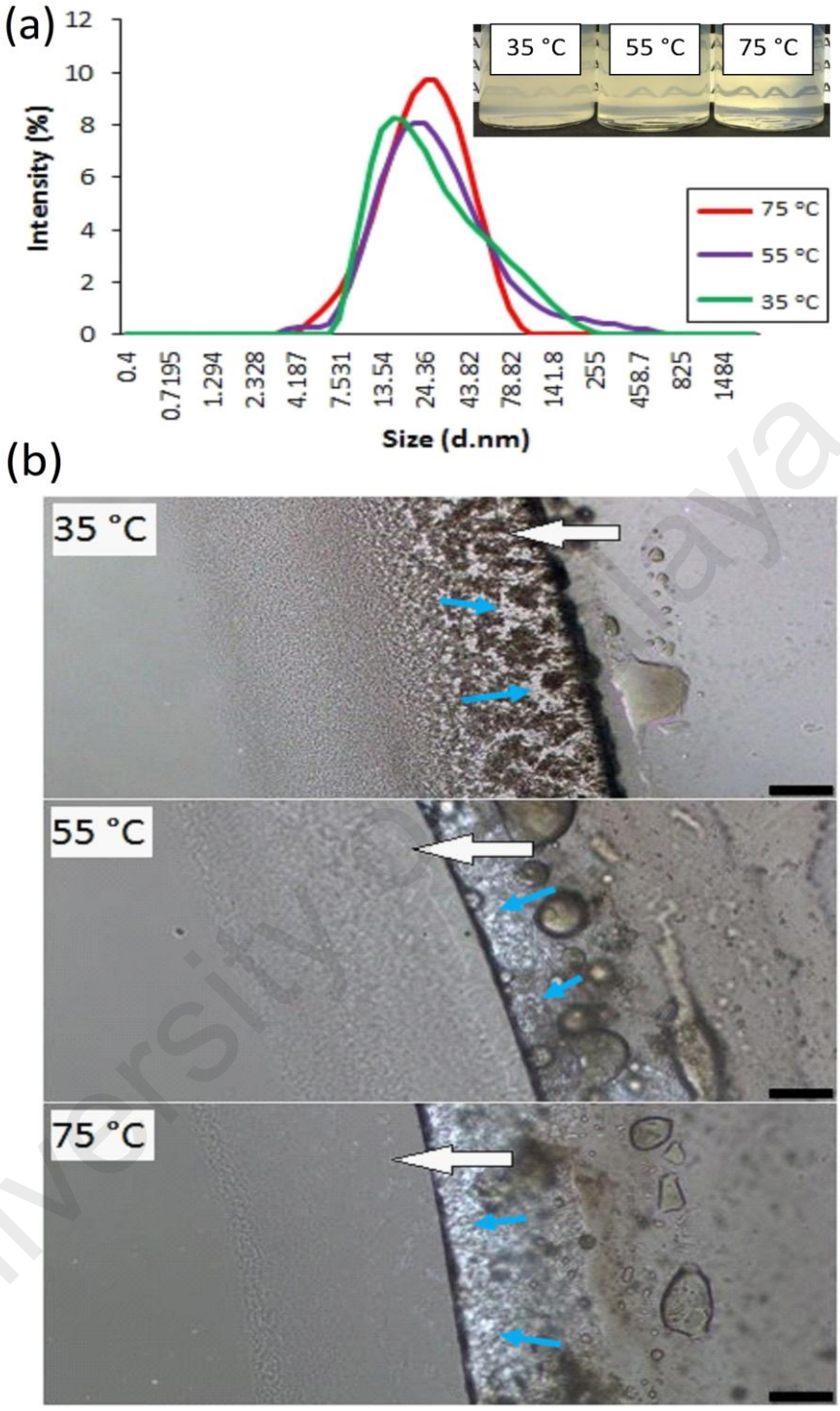

Figure 6.3: (*a*) Final particle size distribution of standard nanoemulsion formed at different temperatures, (*b*) OPM images of lamellar phase (L_a) formation in standard emulsion samples at different temperatures. Initial water content of emulsion samples was 25 % *w/w*. *White arrows* indicate the direction of water penetration. Scale bars (*black*) represent 100

6.4.3 Mcl-PHA-incorporated emulsion system

Formation of standard nanoemulsion using EIP method was used as reference to study the effect of temperature on the formation of mcl-PHA-incorporated nanoemulsion. As mentioned previously, emulsification of the Cremophor EL-Span 80-Oil mixture at optimized ratio is temperature-insensitive. Hence, according to Equation 6.1, the *t* value of surfactant parameter in relation to temperature could be 0. This means that altering the temperature to any degree will not affect the *HLD* value of the emulsion system. In contrast, incorporating mcl-PHA into the system may influence the *k* value of surfactant parameter in relation to alkane/oil phase (*ACN*). It follows that emulsification of mcl-PHA-incorporated emulsion system at any given temperature will always result in deviation from optimum formulation (*HLD* = 0), resulting in the three-phase equilibrium to be absent at EIP.

Figure 6.4 shows the emulsification of mcl-PHA-incorporated system using two different amounts of mcl-PHA (M_w = 77,435 g mol^{-1}). As predicted, at 35 and 55 °C, formation of lamellar (L_a) phase do not occur in emulsion samples incorporated with mcl-PHA at 2 (Figure 6.4*a*) and 5 % (Figure 6.4*b*) *w/w* of oil fraction. However, the presence of birefringence region indicating the formation of lamellar (L_a) phase is detected in emulsion sample incorporated with mcl-PHA at 2 % *w/w* of oil fraction at 75 °C. Increasing the temperature much higher than the mcl-PHA melting point (52 °C) is suggested to aid in complete dissolution of the biopolymer in the organic mixture, resulting in alteration of *k* value of surfactant parameter in relation to alkane/oil phase (*ACN*). Hence, formation of the three-phase equilibrium occurs due to the formulation re-adjustment to *HLD* = 0. Nevertheless, formulation re-adjustment *via* temperature alteration seems interrelated with the amount of incorporated mcl-PHA where it must be below a threshold value. Incorporating mcl-PHA at 5 % (*w/w* of oil fraction) must have

exceeded the value and thus, no formation of lamellar (L_a) phase is observed even at 75 °C (Figure 6.4*b*).

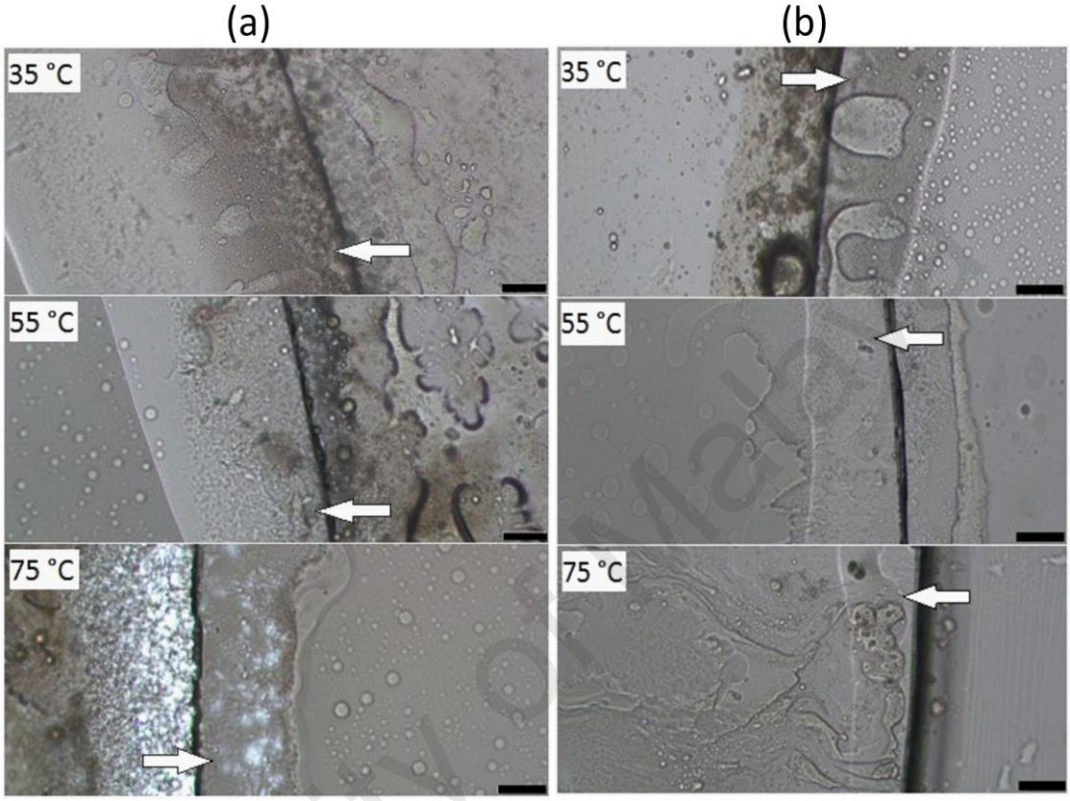

Figure 6.4: OPM images of lamellar phase (L_a) formation of emulsion samples incorporated with mcl-PHA (M_w = 77,435 g mol^{-1}) at (*a*) 2 and (*b*) 5 % *w/w* of oil fraction. Initial water content of emulsion sample was 25 % *w/w*. *White arrows* indicate the direction of water penetration. Scale bars (*black*) represent 100 µm

Figure 6.5 shows the emulsification of mcl-PHA-incorporated system with two different amounts (10 and 20 % *w/w* of oil fraction) of degraded mcl-PHA (M_w = 7370 g mol^{-1}). Melting temperature of this degraded mcl-PHA was determined at 22 °C with broad range of melting enthalpy. The presence of birefringence region indicating the formation of lamellar (L_a) phase is detected in emulsion samples incorporated with 10 and 20 % of mcl-PHA at 55- and 75 °C as shown in Figure 6.5*a* and *b*, respectively, except at 35 °C. A well-dissolved mcl-PHA in organic mixture at 55- and 75 °C is suggested to alter the *k* value of surfactant parameter in relation to the alkane/oil phase

(*ACN*). Hence, 55 °C is practically the T_{HLB} value of the emulsions. According to the definition, *HLD* = 0 is the point of optimum formulation, at which the free energy for transferring the surfactant from the oil to water phase is zero (Salager *et al.*, 1982, 1983). Hence, Cremophor EL and Span 80 are suggested to travel freely to the interface of a well-dissolved mcl-PHA organic solution and water to form lamellar structure phase.

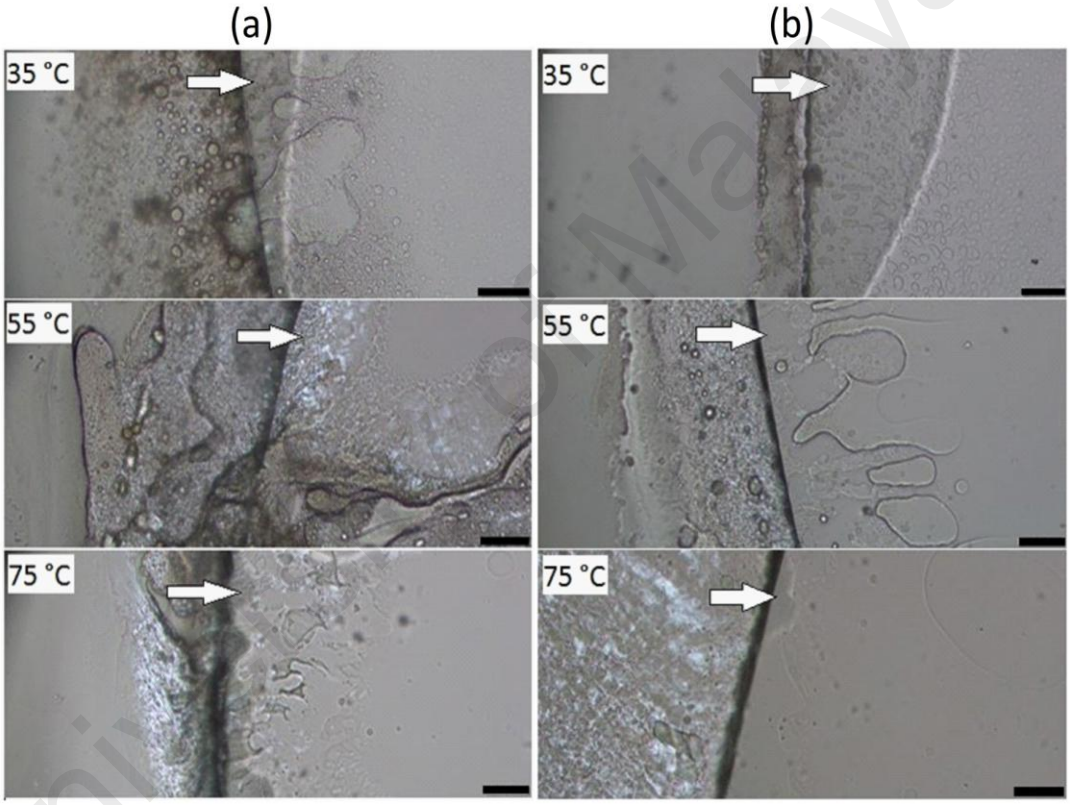

Figure 6.5: OPM images of lamellar phase (L_a) formation of emulsion samples incorporated with mcl-PHA (M_w = 7370 g mol^{-1}) at (*a*) 10 and (*b*) 20 % *w/w* of oil fraction. Initial water content of emulsion sample was 25 % *w/w*. White arrows indicate the direction of water penetration. Scale bars (*black*) represent 100 µm

It has been shown that the amount of incorporated mcl-PHA could be increased further when its molecular weight is reduced (*Chapter 5*). The ceiling amount of degraded mcl-PHA, 7370 and 5130 g mol^{-1}, has been determined at 20 and 40 % *w/w* of oil fraction, respectively. Significant interaction effect between temperature and properties of incorporated mcl-PHA (i.e. molecular weight) is suggested to exist despite the Cremophor EL–Span 80–Oil mixture at optimized ratio is insensitive towards temperature alteration. Nevertheless, the exact nature of interaction between the two parameters on determining the system formulation property (*HLD* value) is yet to be fully elucidated.

6.4.4 Temperature-induced three-phase equilibrium of mcl-PHA-incorporated emulsion system proximately before EIP

In 1990s, an emulsification method, inspired from the original work of Shinoda and Saito 1969, to produce nanoemulsion was conducted by heating a course O/W emulsion above the phase inversion temperature as indicated by *black arrows* on the formulation-composition map (Figure 6.1) (Förster *et al.*, 1992, 1995). The method is described as "emulsification above the inversion temperature" as opposed to "emulsification by the PIT-method" (a few degrees below the PIT). From the studies, the emulsion system was observed to self-assemble at equilibrium into bi-continuous microemulsion, and phase inversion mechanism based on the ultra-low interfacial tension behavior in the vicinity of phase inversion point was put forward (Förster *et al.*, 1992, 1995).

In this study, similar attempt to study the formation of bi-continuous microemulsion through thermal induction was conducted. Figure 6.6 shows the morphology of emulsion systems at 35 % *w/w* of water content, incorporated with 10 % (*w/w* of total oil fraction) of the degraded mcl-PHA at two different temperatures. It can

be seen that at 35 °C (Figure 6.6*a*), many O/W/O multiple emulsions exist in the system. The aforementioned emulsion exists to resolve the incongruity between system formulation and water-oil composition. The formation of dispersed water drops is attributed to higher amount of continuous oil phase, and the inner oil droplets from preferred curvature of the surfactants towards oil region as the result of mcl-PHA incorporation, which caused the system to be more hydrophilic. On the other hand, bi-continuous microemulsion starts to occur when the system is heated to 65 °C as shown in Figure 6.6*b*. The presence of birefringence region (*blue arrows* in Figure 6.6*b*) is detected in the emulsion sample indicating the formation of lamellar (L_a) phase. The observation signifies that the three-phase equilibrium of mcl-PHA-incorporated emulsion system can be induced thermally from multiple emulsions and the possible formation mechanism is discussed in the next section.

In contrast, emulsion systems at 55 % *w/w* of water content, incorporated with similar amount of mcl-PHA do not show any birefringence appearance at any temperature as shown in Figure 6.6*c* and *d*. It is suggested that the three-phase equilibrium is not induced within the system and transitional inversion line is not traversed even though the temperature was elevated above its T_{HLB} value. From the figure, it can be seen that oil-swollen micelles are formed which indicate that the mcl-PHA-incorporated emulsion with 55 % *w/w* of water content already crossed the EIP. By traversing the inversion point, the emulsion system is no longer in the best water-oil composition range to be thermally sensitive. Unlike mcl-PHA-incorporated emulsion with 35 % *w/w* of water content, the system is susceptible to the temperature variation because the inversion point has yet to be traversed, which is indicated by the formation of O/W/O multiple emulsions. The system can persists over a few range of water-oil composition before phase inversion takes place following the EIP and it is called "hysteresis" zone, which is common in catastrophic phase inversion (Mira *et al.,* 2003;

Zambrano *et al.*, 2003; Tyrode *et al.*, 2003, 2005; Rondón-Gonzaléz *et al.*, 2006, 2007, 2008, 2009).

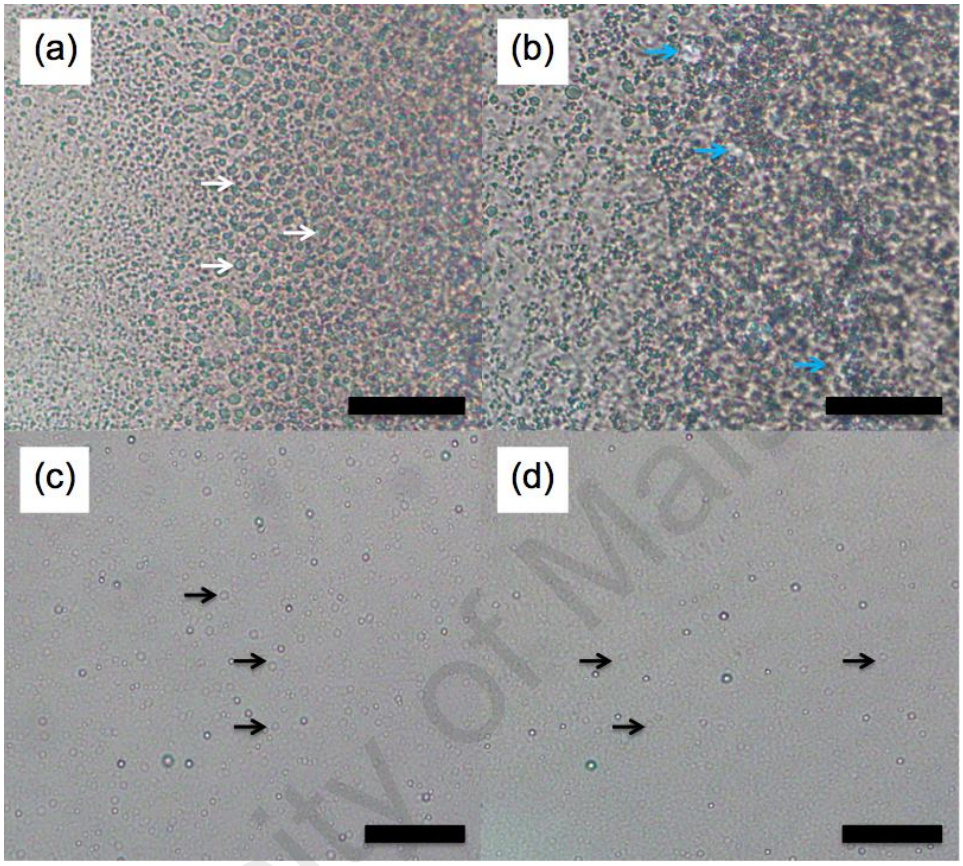

Figure 6.6: (*a*) Multiple emulsions formation (*white arrows*) at 35 °C; (*b*) Bi-continuous microemulsion with lamellar phase (L_a) formation (*blue arrows*) at 65 °C; Oil-swollen micelles (*black arrows*) at (*c*) 35 and (*d*) 65 °C. Scale bars (*black*) represent 100 μm

Litesizer™ 500 (Anton Paar) was used to estimate the hysteresis zone. To this end, emulsification of samples incorporated with 10 % (*w/w* of total oil fraction) of degraded mcl-PHA was carried out at 35 °C to induce multiple emulsion formation with different amount of water (30, 40, 50 and 60 % *w/w*). The samples were heated at 75 °C to aid the dissolution of mcl-PHA, prior to emulsification. The transmittance value of mcl-PHA-incorporated emulsion samples with 30 and 40 % *w/w* of water content increased from 0 to 0.9 ± 0.2 and 0.2 ± 0.1 (%), respectively, when temperature was

raised to 80 °C. However, no light transmittance was detected from samples with 50 and 60 % *w/w* of water content. From the results, it is suggested that the hysteresis zone (vertical shaded region in the formulation-composition map) for the mcl-PHA-incorporated emulsion system is approximately 30 ~ 40 % *w/w* of water content. This range may vary depending on the molecular weight and amount of incorporated mcl-PHA.

Nevertheless, the three-phase equilibrium can only be induced from multiple emulsions when the emulsion system is incorporated with appropriate M_w and amount of mcl-PHA. From Figure 6.7, it can be seen that only emulsion systems incorporated with 2 % (*w/w* of total oil fraction) of original mcl-PHA as well as 10 and 20 % (*w/w* of total oil fraction) of degraded mcl-PHA are able to form bi-continuous microemulsion upon temperature elevation. Unlike mcl-PHA-incorporated emulsion, the phase is formed at any temperature within the standard emulsion samples (without mcl-PHA) demonstrating their temperature-insensitive property (Figure 6.8). The bi-continuous microemulsion formation is indicated by the shear-birefringence appearance at 30 % *w/w* of water content upon viewing in between cross-polarizer sheets and susceptibility to be gradually dispersed into nano-sized oil droplets upon the addition of water (Figure 6.9). Emulsion samples at 6.7*aii*, *aiii*, *bi – iii*, *ciii* and *diii* followed catastrophic phase inversion emulsification (Figure 6.10*a*) while the rest at 6.7*ai*, *ci*, *cii*, *di* and *dii* followed the path that analogous to the transitional phase inversion emulsification (Figure 6.10*b*).

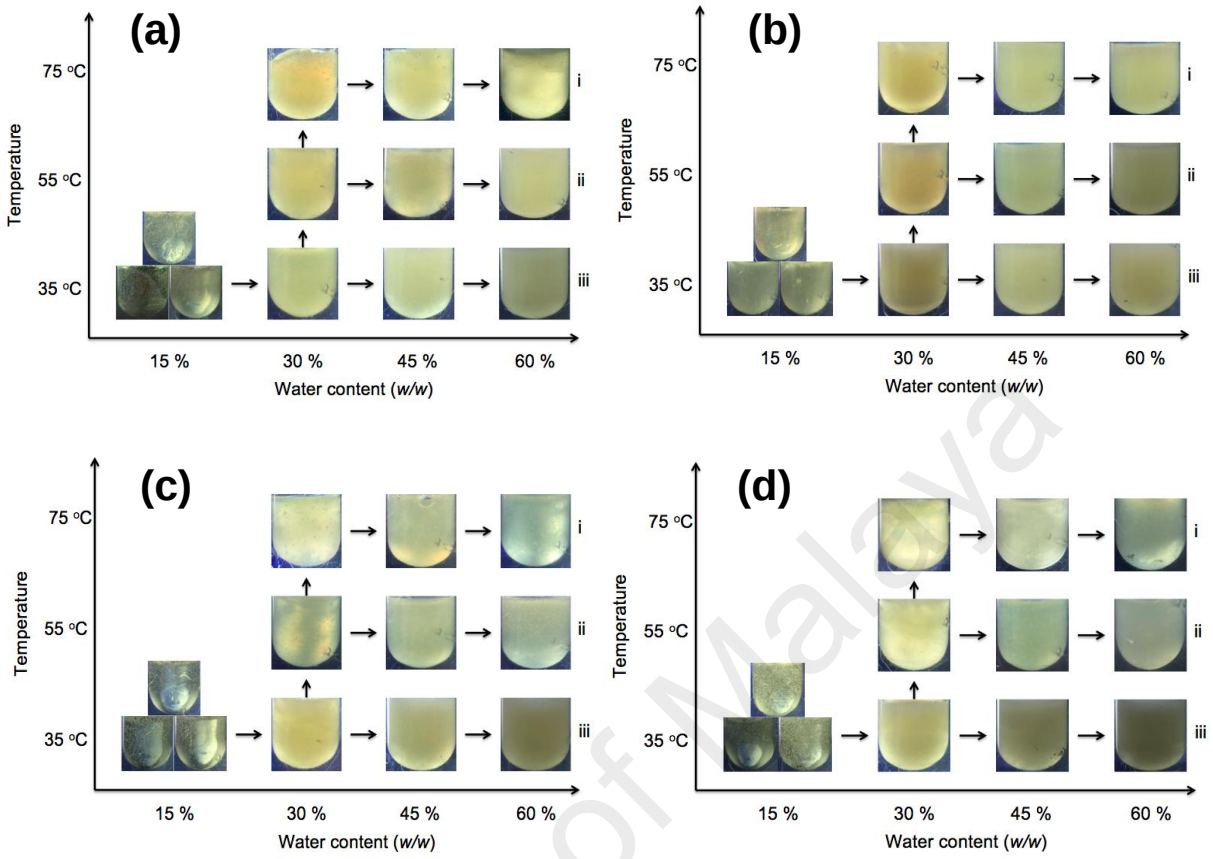

Figure 6.7: Emulsification path through sub-PIC/PIT method of emulsion samples incorporated with mcl-PHA at different amount (*a*) 2, (*b*) 5 % (M_w = 77,435 g mol^{-1}) and (*c*) 10, (*d*) 20 % (M_w = 7370 g mol^{-1}). Samples were viewed in between cross-polarizer sheets

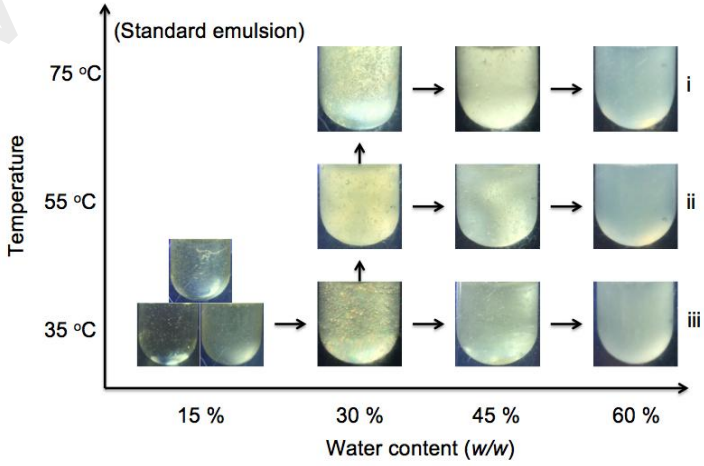

Figure 6.8: Emulsification path of standard emulsion through sub-PIC/PIT method. Samples were viewed in between cross-polarizer sheets

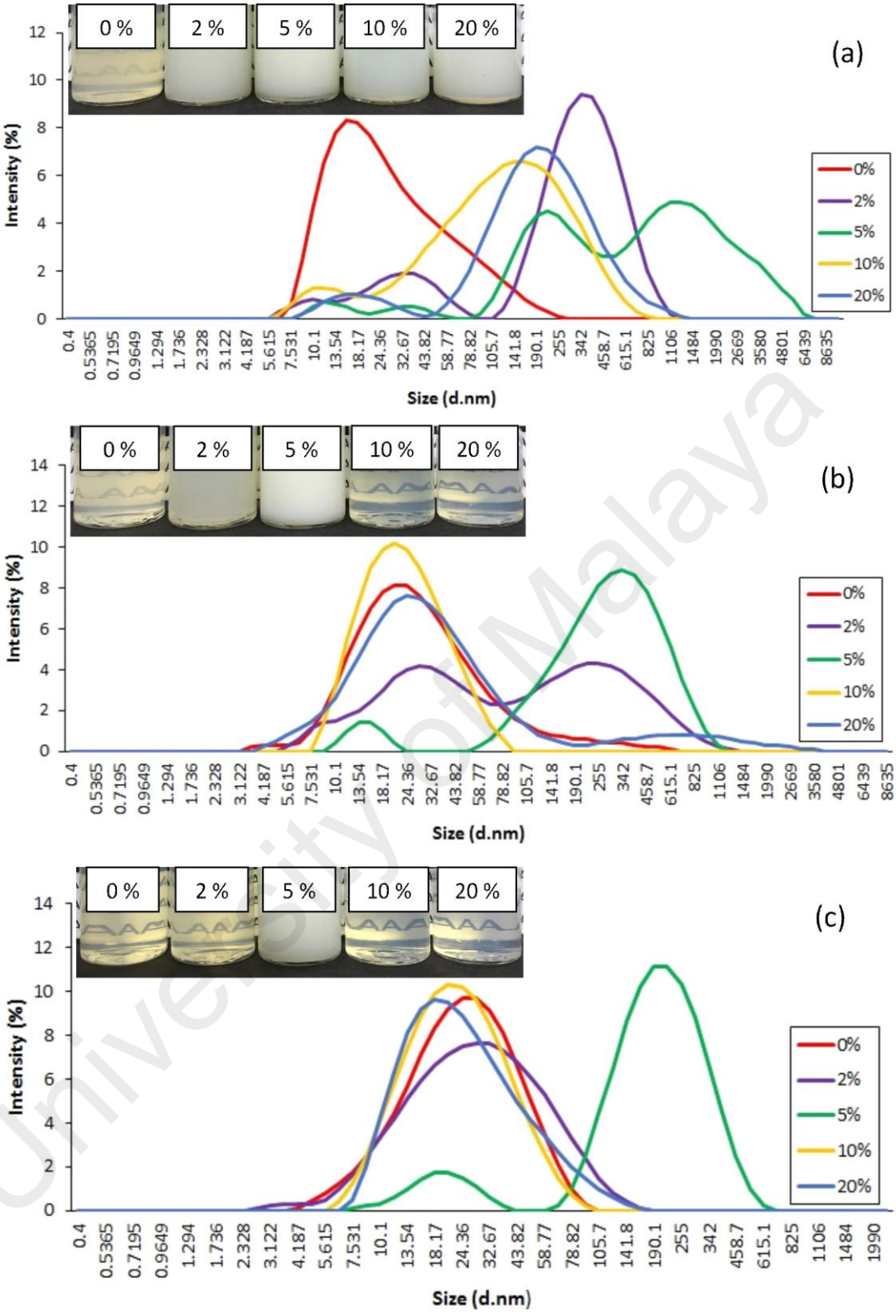

Figure 6.9: Final particle size and size distribution of emulsion samples (86 % *w/w* of water content) incorporated with different molecular weights and amounts of mcl-PHA at (*a*) 35, (*b*) 55 and (*c*) 75 °C. 0 % is standard emulsion and intensity percentage represents the frequency of nanoparticles at a particular size in the solution

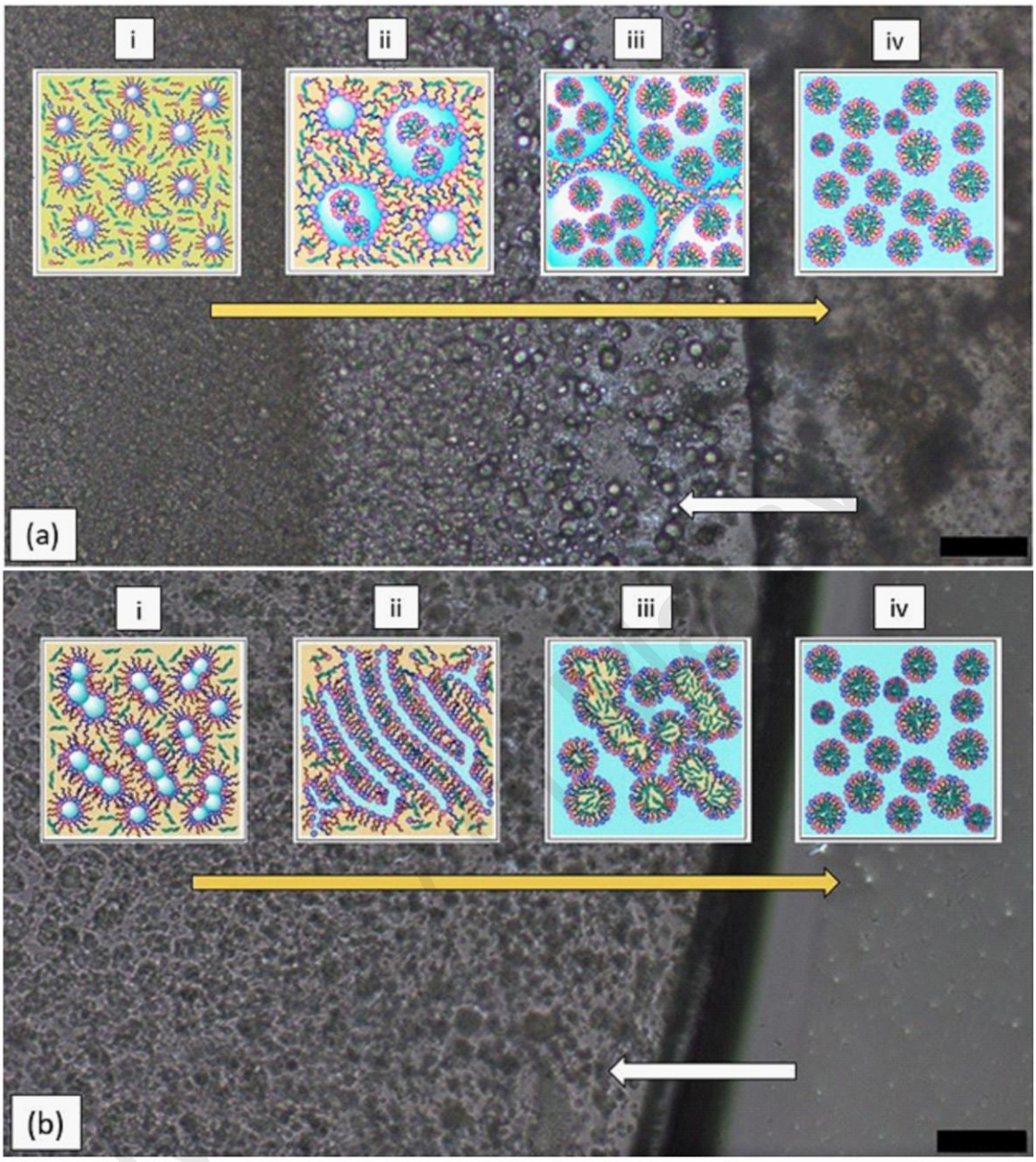

Figure 6.10: Inversion mechanism of mcl-PHA-incorporated emulsion through (*a*) catastrophic phase inversion at 35 °C and (*b*) transitional phase inversion at 75 °C. The emulsion samples contained mcl-PHA (M_w = 7370 g mol^{-1}) at 10 % *w/w* of oil fraction with 29 % *w/w* of initial water content. *Yellow arrows* indicate the direction of O/W formation and *white arrows* the direction of water penetration. Scale bars (*black*) represent 100 μm

6.4.5 Plausible formation mechanism of thermally induced bi-continuous microemulsion from multiple emulsions

From the results, it is clear that three-phase equilibrium that contains bi-continuous emulsion as one of the phases can be induced thermally from multiple emulsions. The formation of bi-continuous emulsion through PIC method occurs in a different way than PIT method. In PIC method, it starts to occurs at 30 % *w/w* of water content in the vicinity of *HLD* = 0 (*Chapter 4*). In contrast, the formation of bi-continuous emulsion from multiple emulsions occurs at a wider range of water content (30 to 40 %) in the vicinity before EIP with PIT method. In a previous study, the formation of lamellar/bi-continuous structure phase was suggested to occur from collision of water droplets leading to drops coalescence and elongation, consequently resulted in phase inversion following the inversion point (*Chapter 4*). The emulsification path is as indicated by *red arrow* in Figure 6.1.

However, it is suggested that the formation of lamellar/bi-continuous structure phase from multiple emulsions occurs differently than the earlier proposed mechanism. Figure 6.11 shows the schematic of the formation mechanism of bi-continuous microemulsion from multiple emulsions. When mcl-PHA-incorporated emulsion system is emulsified through water addition (PIC/EIP method) at lower temperature proximately before EIP as indicated by horizontal *blue arrows* on the formulation-composition map (Figure 6.1), multiple emulsions (6.11*a*) will be formed as a resolution for the incongruity between system formulation and water-oil composition. As the temperature is increased to the neighborhood of optimal formulation (PIT method) as indicated by vertical *blue arrows* on the formulation-composition map (Figure 6.1), the inner oil droplets start to coalesce (6.11*b*) due to the changes in preferred curvature of the surfactant molecules towards the water region as the emulsion system becomes more hydrophobic. The surfactant layer of the inner oil-swollen

micelles will eventually merge with the surfactant layer of the outer water-swollen micelles forming a bi-continuous microemulsion structure (6.11*c*) and it can be further dispersed into nano-sized oil droplets upon addition of water. It is suggested that the bi-continuous microemulsion may co-exist with lamellar structure (L_a) phase and oil-swollen micelles in a three-phase equilibrium system.

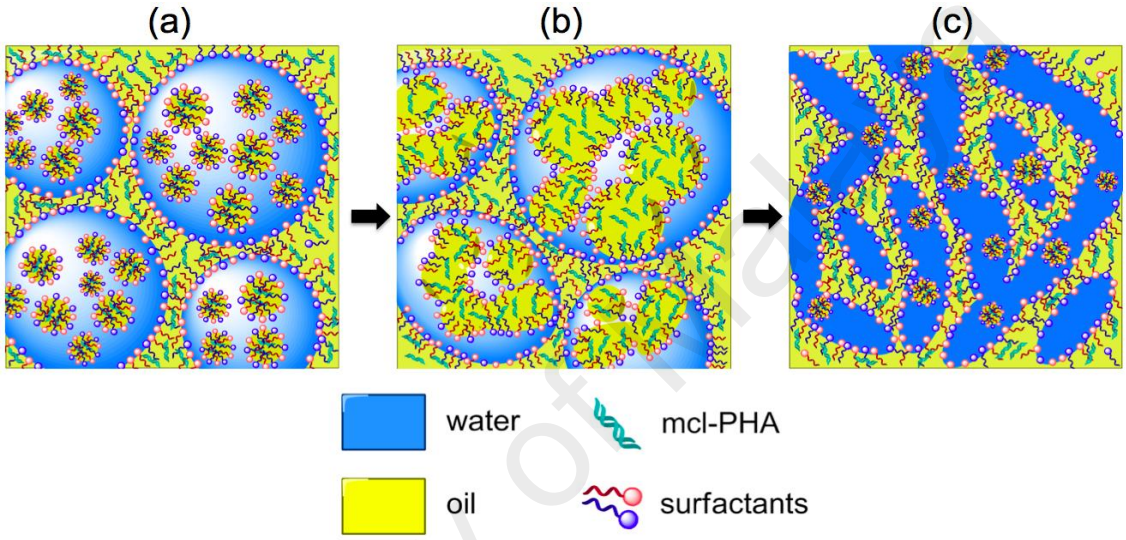

Figure 6.11: Hypothetical formation mechanism of bi-continuous microemulsion from multiple emulsion through thermal induction

Nevertheless, further elevation of the temperature does not alter the bi-continuous microemulsion structure into the water-swollen micelle to form W/O emulsion since the formulation is originally temperature-insensitive. Hence, it is suggested that the phase inversion points (EIP and T_{HLB}) were not traversed by the systems incorporated with appropriate M_w and amount of mcl-PHA during the emulsification to produce nano-sized oil droplets through the sub-PIC/PIT method (Figure 6.7). However, they could pass through the access states that have the same sign of preferred curvature of the surfactant layer as in the final nanoemulsion (Roger, 2016). According to a review, the access states must be traversed by a system to produce nanoemulsion even though without traversing the inversion point (Roger, 2016). It is

proposed that the horizontal shaded region below the T_{HLB} line in the formulation-composition map constitutes the access states region.

6.5 Concluding remarks

It is concluded that the effect of temperature on the establishment of lamellar/bi-continuous (*D*) phase at EIP during emulsification is dependent upon the molecular weight of mcl-PHA. Changing the emulsification temperature of standard emulsion system (without mcl-PHA) did not result in significant deviation from the optimum formulation point (*HLD* = 0), which is attributed to the formation of temperature-insensitive bi-continuous microemulsion.

However, thermal effect exerted significant influence on the emulsification process when hydrophilic-lipophilic balance of the emulsion system was deviated by the incorporation of mcl-PHA. The mcl-PHA-incorporated formulation system could be re-adjusted to its optimal level *via* temperature effect on the [-*k*(ACN)] parameter. It has been shown that the multiple emulsions obtained *via* PIC method at lower temperature before EIP can be thermally induced to form bi-continuous microemulsion. It is suggested that the formation of mcl-PHA-based polymeric nanoparticle through the sub-PIC/PIT method does not involve traversing the inversion points *viz.* EIP and/or T_{HLB}. Hence this could be a clear advantage for up scaling the production of mcl-PHA-based polymeric nanoparticle since the highest viscosity occurring at phase inversion is challenging in term of industrial design.

CHAPTER 7: CONCLUSIONS

From the studies, it can be concluded that, the optimum ratio of water-to-organic phase, oil-to-surfactant and Cremophor EL-to-Span 80 for preparation of mcl-PHA-incorporated nanoparticle through phase inversion emulsification (PIE) was 86:14, 30:70 and 63:37, respectively.

At optimum conditions, phase inversion mechanism of mcl-PHA-incorporated nanoemulsion from W/O to O/W system proceeded *via* the formation of bi-continuous/lamellar structure at EIP resulting in nanometer-sized particles.

The formation of bi-continuous/lamellar structure at EIP was inhibited by relatively high molecular weight and amount of incorporated mcl-PHA. In addition, the interaction effect between temperature and mcl-PHA molecular weight is suggested to influence the formation of the bi-continuous/lamellar structure at EIP as well.

It has been determined that the formation of bi-continuous/lamellar structure can be thermally induced from multiple emulsion system, which suggesting that there is a possible alternative pathway of producing nanometer-sized particles without crossing the transitional and catastrophic inversion line. This could be an advantage for industrial design since the highest viscosity occurring at phase inversion is challenging process-wise.

Overall, it was demonstrated that the production of mcl-PHA-incorporated nanoparticle could be accomplished through standard PIE method at elevated temperature circumventing the usage of organic solvents and cross-linking initiator. Suggestion for the future research/direction of the polymeric nanoparticle is its application for oral delivery of active compounds in nutraceutical and pharmaceutical fields.

REFERENCES

Ahmed, K., Li, Y., McClements, D. J., & Xiao, H. (2012). Nanoemulsion-and emulsion-based delivery systems for curcumin: encapsulation and release properties. *Food Chemistry*, *132*(2), 799-807.

Ahuja, S., & Scypinski, S. (2010). *Handbook of modern pharmaceutical analysis* (Vol. 10). San Diego: Academic Press.

Aillon, K. L., Xie, Y., El-Gendy, N., Berkland, C. J., & Forrest, M. L. (2009). Effects of nanomaterial physicochemical properties on *in vivo* toxicity. *Advanced Drug Delivery Reviews*, *61*(6), 457-466.

Allouche, J., Tyrode, E., Sadtler, V., Choplin, L., & Salager, J. L. (2004). Simultaneous conductivity and viscosity measurements as a technique to track emulsion inversion by the phase-inversion-temperature method. *Langmuir*, *20*(6), 2134-2140.

Alyane, M., Barratt, G., & Lahouel, M. (2015). Remote loading of doxorubicin into liposomes by transmembrane pH gradient to reduce toxicity toward H9c2 cells. *Saudi Pharmaceutical Journal*. *24*(2), 165-175.

Anton, N., & Vandamme, T. F. (2009). The universality of low-energy nano-emulsification. *International Journal of Pharmaceutics*, *377*(1), 142-147.

Anton, R., Mosquera, F., & Oduber, M. (1995). Anionic-nonionic surfactant mixture to attain emulsion insensitivity to temperature. *Progress in Colloid and Polymer Science*, *98*, 85-88.

Antón, R. E., Castillo, P., & Salager, J. L. (1986). Surfactant-oil-water systems near the affinity inversion Part IV: emulsion inversion temperature. *Journal of Dispersion Science and Technology*, *7*(3), 319-329.

Aprahamian, M., Michel, C., Humbert, W., Devissaguet, J. P., & Damge, C. (1987). Transmucosal passage of polyalkylcyanoacrylate nanocapsules as a new drug carrier in the small intestine. *Biology of the Cell*, *61*(1.2), 69-76.

BakoŠ, P. Š. Q. C. D. (2008). From polymer packaging to food–a physicochemical view. *Journal of Food and Nutrition Research*, *47*(3), 105-113.

Ballistreri, A., Giuffrida, M., Guglielmino, S.P., Carnazza, S., Ferreri, A., & Impallomeni, G. (2001). Biosynthesis and structural characterization of medium-chain-length poly (3-hydroxyalkanoates) produced by *Pseudomonas aeruginosa* from fatty acids. *International Journal of Biological Macromolecules, 29*(2), 107-114.

Berthomieu, C., & Hienerwadel, R. (2009). Fourier transform infrared (FTIR) spectroscopy. *Photosynthesis Research, 101*(2-3), 157-170.

Bertrand, N., & Leroux, J. C. (2012). The journey of a drug-carrier in the body: an anatomo-physiological perspective. *Journal of Controlled Release, 161*(2), 152-163.

Bhaskaran, S., & Lakshmi, P. K. (2009). Comparative evaluation of niosome formulations prepared by different techniques. *Acta Pharmaceutica Sciencia, 51*(1), 27-32.

Bisht, S., Feldmann, G., Soni, S., Ravi, R., Karikar, C., Maitra, A., & Maitra, A. (2007). Polymeric nanoparticle-encapsulated curcumin ("nanocurcumin"): a novel strategy for human cancer therapy. *Journal of Nanobiotechnology*, *5*(3), 1-18.

Binks, B. P. (Ed.). (1998). *Modern aspects of emulsion science*. Cambridge: Royal Society of Chemistry.

Borel, T., & Sabliov, C. M. (2014). Nanodelivery of bioactive components for food applications: types of delivery systems, properties, and their effect on ADME profiles and toxicity of nanoparticles. *Annual Review of Food Science and Technology, 5*, 197-213.

Bouchama, F., Van Aken, G. A., Autin, A. J. E., & Koper, G. J. M. (2003). On the mechanism of catastrophic phase inversion in emulsions. *Colloids and Surfaces A: Physicochemical and Engineering Aspects*, *231*(1), 11-17.

Bouwmeester, H., Dekkers, S., Noordam, M. Y., Hagens, W. I., Bulder, A. S., De Heer, C., ..… Sips, A. J. A. M. (2009). Review of health safety aspects of nanotechnologies in food production. *Regulatory Toxicology and Pharmacology*, *53*(1), 52-62.

Braunegg, G., Lefebvre, G., & Genser, K.F. (1998). Polyhydroxyalkanoates, biopolyesters from renewable resources: Physiological and engineering aspects. *Journal of Biotechnology*, *65*(2), 127-161.

Breitenbach, J. (2002). Melt extrusion: from process to drug delivery technology. *European Journal of Pharmaceutics and Biopharmaceutics, 54*(2), 107-117.

Brigelius-Flohé, R. (2006). Bioactivity of vitamin E. *Nutrition Research Reviews, 19*(2), 174-186.

Brooks, B. W., & Richmond, H. N. (1994). Phase inversion in non-ionic surfactant oil-water systems - I. The effect of transitional inversion on emulsion drop sizes. *Chemical Engineering Science*, *49*(7), 1053-1064.

Brown, L., Rosner, B., Willett, W. W., & Sacks, F. M. (1999). Cholesterol-lowering effects of dietary fiber: a meta-analysis. *The American Journal of Clinical Nutrition, 69*(1), 30-42.

Brownlee, I. A., Havler, M. E., Dettmar, P. W., Allen, A., & Pearson, J. P. (2003). Colonic mucus: secretion and turnover in relation to dietary fibre intake. *Proceedings of the Nutrition Society, 62*(1), 245-249.

Brusotti, G., Cesari, I., Dentamaro, A., Caccialanza, G., & Massolini, G. (2014). Isolation and characterization of bioactive compounds from plant resources: The role of analysis in the ethnopharmacological approach. *Journal of Pharmaceutical and Biomedical Analysis, 87*, 218-228.

Budde, C.F., Riedel, S.L., Willis, L.B., Rha, C., & Sinskey, A.J. (2011). Production of poly(3-hydroxybutyrate-*co*-3-hydroxyhexanoate) from plant oil by engineered *Ralstonia eutropha* strains. *Applied and Environmental Microbiology, 77*(9), 2847-2854.

Bunjes, H., Westesen, K., & Koch, M. H. J. (1996). Crystallization tendency and polymorphic transitions in triglyceride nanoparticles. *International Journal of Pharmaceutics, 129*(1), 159-173.

Busolo, M. A., Fernandez, P., Ocio, M. J., & Lagaron, J. M. (2010). Novel silver-based nanoclay as an antimicrobial in polylactic acid food packaging coatings. *Food Additives and Contaminants, 27*(11), 1617-1626.

Calderó, G., García-Celma, M. J., & Solans, C. (2011). Formation of polymeric nano-emulsions by a low-energy method and their use for nanoparticle preparation. *Journal of Colloid and Interface science, 353*(2), 406-411.

Calvo, P., Vila-Jato, J. L., & Alonso, M. a. J. (1997). Evaluation of cationic polymer-coated nanocapsules as ocular drug carriers. *International Journal of Pharmaceutics, 153*(1), 41-50.

Canham, L. T. (2007). Nanoscale semiconducting silicon as a nutritional food additive. *Nanotechnology, 18*(18), 185704.

Carr, K. E., Hazzard, R. A., Reid, S., & Hodges, G. M. (1996). The effect of size on uptake of orally administered latex microparticles in the small intestine and transport to mesenteric lymph nodes. *Pharmaceutical Research, 13*(8), 1205-1209.

Carr, M. E., Wing, R. E., & Doane, W. M. (1991). Encapsulation of atrazine within a starch matrix by extrusion processing. *Cereal Chemistry, 68*(3), 262-266.

Chan, H. K., & Kwok, P. C. L. (2011). Production methods for nanodrug particles using the bottom-up approach. *Advanced Drug Delivery Reviews, 63*(6), 406-416.

Chandrapala, J., Oliver, C., Kentish, S., & Ashokkumar, M. (2012). Ultrasonics in food processing. *Ultrasonics Sonochemistry, 19*(5), 975-983.

Chen, L., & Subirade, M. (2005). Chitosan/β-lactoglobulin core–shell nanoparticles as nutraceutical carriers. *Biomaterials, 26*(30), 6041-6053.

Chen, M. C., Sonaje, K., Chen, K. J., & Sung, H. W. (2011). A review of the prospects for polymeric nanoparticle platforms in oral insulin delivery. *Biomaterials, 32*(36), 9826-9838.

Cho, H. T., Salvia-Trujillo, L., Kim, J., Park, Y., Xiao, H., & McClements, D. J. (2014). Droplet size and composition of nutraceutical nanoemulsions influences bioavailability of long chain fatty acids and Coenzyme Q10. *Food Chemistry, 156*, 117-122.

Choi, C., Chae, S. Y., & Nah, J. W. (2006). Thermosensitive poly (N-isopropylacrylamide)-b-poly (ε-caprolactone) nanoparticles for efficient drug delivery system. *Polymer, 47*(13), 4571-4580.

Clifford, M. N., van der Hooft, J. J. J., & Crozier, A. (2013). Human studies on the absorption, distribution, metabolism, and excretion of tea polyphenols. *The American Journal of Clinical Nutrition, 98*(6), 1619-1630.

Cofrades, S., Antoniou, I., Solas, M. T., Herrero, A. M., & Jiménez-Colmenero, F. (2013). Preparation and impact of multiple (water-in-oil-in-water) emulsions in meat systems. *Food Chemistry*, *141*(1), 338-346.

Couvreur, P. (2013). Nanoparticles in drug delivery: past, present and future. *Advanced Drug Delivery Reviews*, *65*(1), 21-23.

da Silva Malheiros, P., Daroit, D. J., & Brandelli, A. (2010). Food applications of liposome-encapsulated antimicrobial peptides. *Trends in Food Science & Technology*, *21*(6), 284-292.

Das, A. K., Mukesh, D., Swayambunathan, V., Kotkar, D. D., & Ghosh, P. K. (1992). Concentrated emulsions. 3. Studies on the influence of continuous- phase viscosity, volume fraction, droplet size, and temperature on emulsion viscosity. *Langmuir*, *8*(10), 2427-2436.

De Smet, M., Eggink, G., Witholt, B., Kingma, J., & Wynberg, H. (1983). Characterization of intracellular inclusions formed by *Pseudomonas oleovorans* during growth on octane. *Journal of Bacteriology*, *154*(2), 870-878.

De Gennes, P. G., & Taupin, C. (1982). Microemulsions and the flexibility of oil/water interfaces. *The Journal of Physical Chemistry*, *86*(13), 2294-2304.

Devereaux, P.J., Mrkobrada, M., Sessler, D.I., Leslie, K., Alonso-Coello, P., Kurz, A., Villar, J.C., Sigamani, A., Biccard, B.M., Meyhoff, C.S. & Parlow, J.L. (2014) Aspirin in patients undergoing noncardiac surgery. *New England Journal of Medicine*, *370*(16), 1494-1503.

De Vos, P., Faas, M. M., Spasojevic, M., & Sikkema, J. (2010). Encapsulation for preservation of functionality and targeted delivery of bioactive food components. *International Dairy Journal*, *20*(4), 292-302.

Dudhatra, G. B., Mody, S. K., Awale, M. M., Patel, H. B., Modi, C. M., Kumar, A., Kamani, D. R., & Chauhan, B. N. (2012). A comprehensive review on pharmacotherapeutics of herbal bioenhancers. *The Scientific World Journal*, *2012*, 637953.

Eggink, G., van der Wal, H., Huijberts, G.N., & de Waard, P. (1992). Oleic acid as a substrate for poly-3-hydroxyalkanoate formation in *Alcaligenes eutrophus* and *Pseudomonas putida*. *Industrial Crops and Products*, *1*(2), 157-163.

Esposito, E., Fantin, M., Marti, M., Drechsler, M., Paccamiccio, L., Mariani, P., Sivieri, E., Lain, F., Menegatti, E., & Morari, M. (2008). Solid lipid nanoparticles as delivery systems for bromocriptine. *Pharmaceutical Research, 25*(7), 1521-1530.

Falguera, V., Quintero, J. P., Jiménez, A., Muñoz, J. A., & Ibarz, A. (2011). Edible films and coatings: structures, active functions and trends in their use. *Trends in Food Science & Technology, 22*(6), 292-303.

Faraji, A. H., & Wipf, P. (2009). Nanoparticles in cellular drug delivery. *Bioorganic & Medicinal Chemistry, 17*(8), 2950-2962.

Fast, J. P., & Mecozzi, S. (2009). Nanoemulsions for intravenous drug delivery. In M.M. de Villiers, P. Aramwit & G.S. Kwon (Eds.), *Biotechnology: pharmaceutical aspects* (pp. 461-489). New York: Springer.

Fernandez, P., André, V., Rieger, J., & Kühnle, A. (2004). Nano-emulsion formation by emulsion phase inversion. *Colloids and Surfaces A: Physicochemical and Engineering Aspects, 251*(1), 53-58.

Filella, M., Zhang, J., Newman, M. E., & Buffle, J. (1997). Analytical applications of photon correlation spectroscopy for size distribution measurements of natural colloidal suspensions: capabilities and limitations. *Colloids and Surfaces A: Physicochemical and Engineering Aspects, 120*(1), 27-46.

Fitzgerald, C. n., Mora-Soler, L., Gallagher, E., O'Connor, P., Prieto, J., Soler-Vila, A., & Hayes, M. (2012). Isolation and characterization of bioactive pro-peptides with in vitro renin inhibitory activities from the macroalga Palmaria palmata. *Journal of Agricultural and Food Chemistry, 60*(30), 7421-7427.

Fornaguera, C., Dols-Perez, A., Caldero, G., Garcia-Celma, M. J., Camarasa, J., & Solans, C. (2015a). PLGA nanoparticles prepared by nano-emulsion templating using low-energy methods as efficient nanocarriers for drug delivery across the blood–brain barrier. *Journal of Controlled Release, 211*, 134-143.

Fornaguera, C., Feiner-Gracia, N., Calderó, G., García-Celma, M. J., & Solans, C. (2015b). Galantamine-loaded PLGA nanoparticles, from nano-emulsion templating, as novel advanced drug delivery systems to treat neurodegenerative diseases. *Nanoscale, 7*(28), 12076-12084.

Freitas, C., & Müller, R. H. (1998a). Effect of light and temperature on zeta potential and physical stability in solid lipid nanoparticle (SLN™) dispersions. *International Journal of Pharmaceutics, 168*(2), 221-229.

Freitas, C., & Müller, R. H. (1998b). Spray-drying of solid lipid nanoparticles (SLN™). *European Journal of Pharmaceutics and Biopharmaceutics, 46*(2), 145-151.

Ganta, S., & Amiji, M. (2009). Coadministration of paclitaxel and curcumin in nanoemulsion formulations to overcome multidrug resistance in tumor cells. *Molecular Pharmaceutics*, *6*(3), 928-939.

Garti, N., & Benichou, A. (2004). Recent developments in double emulsions for food applications. In S. Friberg, K. Larsson & J. Sjoblom (Eds), *Food emulsions* (pp. 353-412). New York: Marcel Dekker.

Garti, N., & Zour, H. (1997). The effect of surfactants on the crystallization and polymorphic transformation of glutamic acid. *Journal of Crystal Growth, 172*(3), 486-498.

Gaudin, F., & Sintes-Zydowicz, N. (2008). Core–shell biocompatible polyurethane nanocapsules obtained by interfacial step polymerisation in miniemulsion. *Colloids and Surfaces A: Physicochemical and Engineering Aspects, 331*(1), 133-142.

Gaudin, F., & Sintes-Zydowicz, N. (2011). Poly (urethane–urea) nanocapsules prepared by interfacial step polymerisation in miniemulsion: The droplet size: A key- factor for the molecular and thermal characteristics of the polymeric membrane of the nanocapsules? *Colloids and Surfaces A: Physicochemical and Engineering Aspects*, *384*(1), 698-712.

Gibson, G. R., Probert, H. M., Van Loo, J., Rastall, R. A., & Roberfroid, M. B. (2004). Dietary modulation of the human colonic microbiota: updating the concept of prebiotics. *Nutrition Research Reviews, 17*(2), 259-275.

Guinedi, A. S., Mortada, N. D., Mansour, S., & Hathout, R. M. (2005). Preparation and evaluation of reverse-phase evaporation and multilamellar niosomes as ophthalmic carriers of acetazolamide. *International Journal of Pharmaceutics, 306*(1), 71-82.

Gumel, A. M., Annuar, M. S. M., & Heidelberg, T. (2012). Biosynthesis and characterization of polyhydroxyalkanoates copolymers produced by *Pseudomonas putida* Bet001 isolated from palm oil mill effluent. *PLoS One*, *7*(9), e45214.

Guterres, S. S., Fessi, H., Barratt, G., Devissaguet, J. P., & Puisieux, F. (1995). Poly (DL-lactide) nanocapsules containing diclofenac: I. Formulation and stability study. *International Journal of Pharmaceutics*, *113*(1), 57-63.

Hagens, W. I., Oomen, A. G., de Jong, W. H., Cassee, F. R., & Sips, A. J. A. M. (2007). What do we (need to) know about the kinetic properties of nanoparticles in the body? *Regulatory Toxicology and Pharmacology*, *49*(3), 217-229.

Harde, H., Das, M., & Jain, S. (2011). Solid lipid nanoparticles: an oral bioavailability enhancer vehicle. *Expert Opinion on Drug Delivery*, *8*(11), 1407-1424.

Helgason, T., Awad, T. S., Kristbergsson, K., Decker, E. A., McClements, D. J., & Weiss, J. (2009a). Impact of surfactant properties on oxidative stability of β-carotene encapsulated within solid lipid nanoparticles. *Journal of Agricultural and Food Chemistry*, *57*(17), 8033-8040.

Helgason, T., Awad, T. S., Kristbergsson, K., McClements, D. J., & Weiss, J. (2008). Influence of polymorphic transformations on gelation of tripalmitin solid lipid nanoparticle suspensions. *Journal of the American Oil Chemists' Society*, *85*(6), 501-511.

Helgason, T., Awad, T. S., Kristbergsson, K., McClements, D. J., & Weiss, J. (2009b). Effect of surfactant surface coverage on formation of solid lipid nanoparticles (SLN). *Journal of Colloid and Interface Science*, *334*(1), 75-81.

Heurtault, B., Saulnier, P., Pech, B., Proust, J. E., & Benoit, J. P. (2003). Physico-chemical stability of colloidal lipid particles. *Biomaterials*, *24*(23), 4283-4300.

Hinrichs, W. L. J., Mancenido, F. A., Sanders, N. N., Braeckmans, K., De Smedt, S. C., Demeester, J., & Frijlink, H. W. (2006). The choice of a suitable oligosaccharide to prevent aggregation of PEGylated nanoparticles during freeze thawing and freeze drying. *International Journal of Pharmaceutics*, *311*(1), 237-244.

Hoet, P. H. M., Brüske-Hohlfeld, I., & Salata, O. V. (2004). Nanoparticles–known and unknown health risks. *Journal of Nanobiotechnology*, *2*(1), 1-12.

Hommoss, A. (2009). *Nanostructured lipid carriers (NLC) in dermal and personal care formulations.* (Doctoral dissertation) Freie Universität Berlin.

Huang, Q., Yu, H., & Ru, Q. (2010). Bioavailability and delivery of nutraceuticals using nanotechnology. *Journal of Food Science*, *75*(1), 50-57.

Huang, W. Y., Davidge, S. T., & Wu, J. (2013). Bioactive natural constituents from food sources—potential use in hypertension prevention and treatment. *Critical Reviews in Food Science and Nutrition*, *53*(6), 615-630.

Hunter, A. C., Elsom, J., Wibroe, P. P., & Moghimi, S. M. (2012). Polymeric particulate technologies for oral drug delivery and targeting: a pathophysiological perspective. *Nanomedicine: Nanotechnology, Biology and Medicine*, *8*, S5-S20.

Hyde, S. T. (1997). Swelling and structure. Analysis of the topology and geometry of lamellar and sponge lyotropic mesophases. *Langmuir*, *13*(4), 842-851.

Ishak, K. A., Annuar, M. S. M., Heidelberg, T., & Gumel, A. M. (2016). Ultrasound-assisted rapid extraction of bacterial intracellular medium-chain-length Poly(3-Hydroxyalkanoates) (mcl-PHAs) in medium mixture of solvent/marginal non-solvent. *Arabian Journal for Science and Engineering*, *41*(1), 33-44.

Iyer, C., Phillips, M., & Kailasapathy, K. (2005). Release studies of Lactobacillus casei strain Shirota from chitosan-coated alginate-starch microcapsules in ex vivo porcine gastrointestinal contents. *Letters in Applied Microbiology*, *41*(6), 493-497.

Jahanzad, F., Crombie, G., Innes, R., & Sajjadi, S. (2009). Catastrophic phase inversion via formation of multiple emulsions: a prerequisite for formation of fine emulsions. *Chemical Engineering Research and Design*, *87*(4), 492-498.

Jain, R. A. (2000). The manufacturing techniques of various drug loaded biodegradable poly(lactide-co-glycolide)(PLGA) devices. *Biomaterials*, *21*(23), 2475-2490.

Jasiecka, A., Maślanka, T., & Jaroszewski, J. J. (2014). Pharmacological characteristics of metamizole. *Polish Journal of Veterinary Sciences*, *17*(1), 207-214.

Jenning, V., Mäder, K., & Gohla, S. H. (2000). Solid lipid nanoparticles (SLN™) based on binary mixtures of liquid and solid lipids: a ^{1}H-NMR study. *International Journal of Pharmaceutics, 205*(1), 15-21.

Jeong, Y. I., Na, H. S., Seo, D. H., Kim, D. G., Lee, H. C., Jang, M. K., Na, S. K., Roh, S. H., Kim, S. I., & Nah, J. W. (2008). Ciprofloxacin-encapsulated poly (dl-lactide-*co*-glycolide) nanoparticles and its antibacterial activity. *International Journal of Pharmaceutics, 352*(1), 317-323.

Jiang, L., Long, X., & Meng, Q. (2013). Rhamnolipids enhance epithelial permeability in Caco-2 monolayers. *International Journal of Pharmaceutics, 446*(1), 130-135.

Johnson, J., & de Mejia, E. G. (2011). Dietary factors and pancreatic cancer: the role of food bioactive compounds. *Molecular Nutrition & Food Research, 55*(1), 58-73.

Joo, H. H., Lee, H. Y., Guan, Y. S., & Kim, J. C. (2008). Colloidal stability and *in vitro* permeation study of poly (ε -caprolactone) nanocapsules containing hinokitiol. *Journal of Industrial and Engineering Chemistry, 14*(5), 608-613.

Jores, K., Mehnert, W., & Mäder, K. (2003). Physicochemical investigations on solid lipid nanoparticles and on oil-loaded solid lipid nanoparticles: a nuclear magnetic resonance and electron spin resonance study. *Pharmaceutical Research, 20*(8), 1274-1283.

Jores, K., Mehnert, W., Drechsler, M., Bunjes, H., Johann, C., & Mäder, K. (2004). Investigations on the structure of solid lipid nanoparticles (SLN) and oil-loaded solid lipid nanoparticles by photon correlation spectroscopy, field-flow fractionation and transmission electron microscopy. *Journal of Controlled Release, 95*(2), 217-227.

Junghanns, J. U. A. H., & Müller, R. H. (2008). Nanocrystal technology, drug delivery and clinical applications. *International Journal of Nanomedicine, 3*(3), 295.

Kabalnov, A., & Wennerström, H. (1996). Macroemulsion stability: the oriented wedge theory revisited. *Langmuir, 12*(2), 276-292.

Keck, C. M., & Müller, R. H. (2006). Drug nanocrystals of poorly soluble drugs produced by high pressure homogenisation. *European Journal of Pharmaceutics and Biopharmaceutics, 62*(1), 3-16.

Kim, H.W., Chung, M.G., & Rhee, Y.H. (2007). Biosynthesis, modification, and biodegradation of bacterial medium-chain-length polyhydroxyalkanoates. *The Journal of Microbiology*, *45*(2), 87-97.

Kirby, B. J., & Hasselbrink, E. F. (2004). Zeta potential of microfluidic substrates: 1. Theory, experimental techniques, and effects on separations. *Electrophoresis, 25*(2), 187-202.

Kondoh, M., Takahashi, A., & Yagi, K. (2012). Spiral progression in the development of absorption enhancers based on the biology of tight junctions. *Advanced Drug Delivery Reviews, 64*(6), 515-522.

Kosaraju, S. L. (2005). Colon targeted delivery systems: review of polysaccharides for encapsulation and delivery. *Critical Reviews in Food Science and Nutrition, 45*(4), 251-258.

Kris-Etherton, P. M., Harris, W. S., & Appel, L. J. (2002a). Fish consumption, fish oil, omega-3 fatty acids, and cardiovascular disease. *Circulation, 106*(21), 2747-2757.

Kris-Etherton, P. M., Hecker, K. D., Bonanome, A., Coval, S. M., Binkoski, A. E., Hilpert, K. F., ….. Etherton, T. D. (2002b). Bioactive compounds in foods: their role in the prevention of cardiovascular disease and cancer. *The American Journal of Medicine, 113*(9), 71-88.

Kuentz, M. (2012). Lipid-based formulations for oral delivery of lipophilic drugs. *Drug Discovery Today: Technologies, 9*(2), e97-e104.

Kulkarni, C. V. (2012). Lipid crystallization: from self-assembly to hierarchical and biological ordering. *Nanoscale, 4*(19), 5779-5791.

Kulkarni, C. V., Mezzenga, R., & Glatter, O. (2010). Water-in-oil nanostructured emulsions: towards the structural hierarchy of liquid crystalline materials. *Soft Matter, 6*(21), 5615-5624.

Kumar, A., Li, S., Cheng, C. M., & Lee, D. (2015). Recent Developments in Phase Inversion Emulsification. *Industrial & Engineering Chemistry Research, 54*(34), 8375-8396.

Kumar, M., Misra, A., Babbar, A. K., Mishra, A. K., Mishra, P., & Pathak, K. (2008). Intranasal nanoemulsion based brain targeting drug delivery system of risperidone. *International Journal of Pharmaceutics*, *358*(1), 285-291.

Kumari, A., Yadav, S. K., & Yadav, S. C. (2010). Biodegradable polymeric nanoparticles based drug delivery systems. *Colloids and Surfaces B: Biointerfaces*, *75*(1), 1-18.

Kunieda, H., & Shinoda, K. (1982). Phase behavior in systems of nonionic surfactant/water/oil around the hydrophile-lipophile-balance-temperature (HLB-temperature). *Journal of Dispersion Science and Technology*, *3*(3), 233-244.

Lageveen, R.G., Huisman, G.W., Preusting, H., Ketelaar, P., Eggink, G., & Witholt, B. (1988). Formation of polyesters by *Pseudomonas oleovorans*: Effect of substrates on formation and composition of poly-(*r*)-3-hydroxyalkanoates and poly-(*r*)-3-hydroxyalkenoates. *Applied and Environmental Microbiology*, *54*(12), 2924-2932.

Lai, S. K., O'Hanlon, D. E., Harrold, S., Man, S. T., Wang, Y. Y., Cone, R., & Hanes, J. (2007). Rapid transport of large polymeric nanoparticles in fresh undiluted human mucus. *Proceedings of the National Academy of Sciences*, *104*(5), 1482-1487.

Lai, S. K., Wang, Y. Y., & Hanes, J. (2009). Mucus-penetrating nanoparticles for drug and gene delivery to mucosal tissues. *Advanced Drug Delivery Reviews*, *61*(2), 158-171.

Lee, J. M., Shin, H. J., & Lim, K. H. (2003). Morphologies of three-phase emulsions of the ternary nonionic amphiphile/oil/water systems and their determination by electrical method. *Journal of Colloid and Interface Science*, *257*(2), 344-356.

Lertsutthiwong, P., Noomun, K., Jongaroonngamsang, N., Rojsitthisak, P., & Nimmannit, U. (2008). Preparation of alginate nanocapsules containing turmeric oil. *Carbohydrate Polymers*, *74*(2), 209-214.

Lertsutthiwong, P., Rojsitthisak, P., & Nimmannit, U. (2009). Preparation of turmeric oil-loaded chitosan-alginate biopolymeric nanocapsules. *Materials Science and Engineering: C*, *29*(3), 856-860.

Letchford, K., & Burt, H. (2007). A review of the formation and classification of amphiphilic block copolymer nanoparticulate structures: micelles, nanospheres, nanocapsules and polymersomes. *European Journal of Pharmaceutics and Biopharmaceutics, 65*(3), 259-269.

Li, Y., Zheng, J., Xiao, H., & McClements, D. J. (2012). Nanoemulsion-based delivery systems for poorly water-soluble bioactive compounds: Influence of formulation parameters on polymethoxyflavone crystallization. *Food Hydrocolloids, 27*(2), 517-528.

Liang, R., Shoemaker, C. F., Yang, X., Zhong, F., & Huang, Q. (2013). Stability and bioaccessibility of β-carotene in nanoemulsions stabilized by modified starches. *Journal of Agricultural and Food Chemistry, 61*(6), 1249-1257.

Lipinski, C. A. (2002). Poor aqueous solubility-an industry wide problem in ADME screening. *American Pharmaceutical Review*, *5*, 82-85.

Liu, L., Won, Y. J., Cooke, P. H., Coffin, D. R., Fishman, M. L., Hicks, K. B., & Ma, P. X. (2004). Pectin/poly (lactide-co-glycolide) composite matrices for biomedical applications. *Biomaterials, 25*(16), 3201-3210.

Lukowski, G., Kasbohm, J., Pflegel, P., Illing, A., & Wulff, H. (2000). Crystallographic investigation of cetylpalmitate solid lipid nanoparticles. *International Journal of Pharmaceutics, 196*(2), 201-205.

Maali, A., & Mosavian, M. H. (2013). Preparation and application of nanoemulsions in the last decade (2000–2010). *Journal of Dispersion Science and Technology*, *34*(1), 92-105.

Macfarlane, G. T., & Englyst, H. N. (1986). Starch utilization by the human large intestinal microflora. *Journal of Applied Bacteriology*, *60*(3), 195-201.

Madrigal-Carballo, S., Lim, S., Rodriguez, G., Vila, A. O., Krueger, C. G., Gunasekaran, S., & Reed, J. D. (2010). Biopolymer coating of soybean lecithin liposomes via layer-by-layer self-assembly as novel delivery system for ellagic acid. *Journal of Functional Foods, 2*(2), 99-106.

Maestro, A., Solè, I., González, C., Solans, C., & Gutiérrez, J. M. (2008). Influence of the phase behavior on the properties of ionic nanoemulsions prepared by the phase inversion composition method. *Journal of Colloid and Interface Science*, *327*(2), 433-439.

Mahale, N. B., Thakkar, P. D., Mali, R. G., Walunj, D. R., & Chaudhari, S. R. (2012). Niosomes: novel sustained release nonionic stable vesicular systems—an overview. *Advances in Colloid and Interface Science, 183*, 46-54.

Markovsky, E., Baabur-Cohen, H., Eldar-Boock, A., Omer, L., Tiram, G., Ferber, S., ….. Satchi-Fainaro, R. (2012). Administration, distribution, metabolism and elimination of polymer therapeutics. *Journal of Controlled Release, 161*(2), 446-460.

Marsanasco, M., Márquez, A. L., Wagner, J. R., Alonso, S. d. V., & Chiaramoni, N. S. (2011). Liposomes as vehicles for vitamins E and C: An alternative to fortify orange juice and offer vitamin C protection after heat treatment. *Food Research International, 44*(9), 3039-3046.

Marsich, E., Borgogna, M., Donati, I., Mozetic, P., Strand, B. L., Salvador, S. G., Vittur, F., & Paoletti, S. (2008). Alginate/lactose modified chitosan hydrogels: A bioactive biomaterial for chondrocyte encapsulation. *Journal of Biomedical Materials Research Part A, 84*(2), 364-376.

Marszall, L. (1987). HLB of nonionic surfactants: PIT and EIP methods. In M.J. Schick (Ed.), *Nonionic Surfactants, Physical Chemistry* (pp. 493-547). New York: Marcel Dekker

Mayer, S., Weiss, J., & McClements, D. J. (2013). Vitamin E-enriched nanoemulsions formed by emulsion phase inversion: factors influencing droplet size and stability. *Journal of Colloid and Interface Science*, *402*, 122-130.

McClements, D. J. (2004). *Food emulsions: principles, practices, and techniques*. Boca Raton: CRC Press.

McClements, D. J. (2011). Edible nanoemulsions: fabrication, properties, and functional performance. *Soft Matter, 7*(6), 2297-2316.

McClements, D. J., & Li, Y. (2010). Structured emulsion-based delivery systems: Controlling the digestion and release of lipophilic food components. *Advances in Colloid and Interface Science, 159*(2), 213-228.

McClements, D. J., & Rao, J. (2011). Food-grade nanoemulsions: formulation, fabrication, properties, performance, biological fate, and potential toxicity. *Critical Reviews in Food Science and Nutrition, 51*(4), 285-330.

McClements, D. J., & Xiao, H. (2014). Excipient foods: designing food matrices that improve the oral bioavailability of pharmaceuticals and nutraceuticals. *Food & Function, 5*(7), 1320-1333.

McClements, D. J., Decker, E. A., Park, Y., & Weiss, J. (2009). Structural design principles for delivery of bioactive components in nutraceuticals and functional foods. *Critical Reviews in Food Science and Nutrition, 49*(6), 577-606.

McClements, D. J., Li, F., & Xiao, H. (2015). The Nutraceutical Bioavailability Classification Scheme: Classifying Nutraceuticals According to Factors Limiting their Oral Bioavailability. *Annual Review of Food Science and Technology, 6*, 299-327.

Merisko-Liversidge, E., & Liversidge, G. G. (2011). Nanosizing for oral and parenteral drug delivery: a perspective on formulating poorly-water soluble compounds using wet media milling technology. *Advanced Drug Delivery Reviews, 63*(6), 427-440.

Merta, J., Torkkeli, M., Ikonen, T., Serimaa, R., & Stenius, P. (2001). Structure of cationic starch (CS)/anionic surfactant complexes studied by small-angle X-ray scattering (SAXS). *Macromolecules*, *34*(9), 2937-2946.

Mira, I., Zambrano, N., Tyrode, E., Márquez, L., Peña, A. A., Pizzino, A., & Salager, J. L. (2003). Emulsion catastrophic inversion from abnormal to normal morphology. 2. Effect of the stirring intensity on the dynamic inversion frontier. *Industrial & Engineering Chemistry Research*, *42*(1), 57-61.

Mora-Huertas, C. E., Fessi, H., & Elaissari, A. (2010). Polymer-based nanocapsules for drug delivery. *International Journal of Pharmaceutics, 385*(1), 113-142.

Morales, D., Gutiérrez, J. M., Garcia-Celma, M. J., & Solans, Y. C. (2003). A study of the relation between bicontinuous microemulsions and oil/water nano-emulsion formation. *Langmuir, 19*(18), 7196-7200.

Mou, D., Chen, H., Du, D., Mao, C., Wan, J., Xu, H., & Yang, X. (2008). Hydrogel-thickened nanoemulsion system for topical delivery of lipophilic drugs. *International Journal of Pharmaceutics*, *353*(1), 270-276.

MuÈller, R. H., MaÈder, K., & Gohla, S. (2000). Solid lipid nanoparticles (SLN) for controlled drug delivery–a review of the state of the art. *European Journal of Pharmaceutics and Biopharmaceutics, 50*(1), 161-177.

Müller, R. H., & Keck, C. M. (2012). Twenty years of drug nanocrystals: where are we, and where do we go? *European Journal of Pharmaceutics and Biopharmaceutics, 80*(1), 1-3.

Müller, R. H., Radtke, M., & Wissing, S. A. (2002). Solid lipid nanoparticles (SLN) and nanostructured lipid carriers (NLC) in cosmetic and dermatological preparations. *Advanced Drug Delivery Reviews, 54*, S131-S155.

Myers, D. (1990). *Surfaces, Interfaces and Colloids*. New York: Wiley-Vch.

Nagarajan, R. (2002). Molecular packing parameter and surfactant self-assembly: the neglected role of the surfactant tail. *Langmuir, 18*(1), 31-38.

Nakamura, N., Tagawa, T., Kihara, K., Tobita, I., & Kunieda, H. (1997). Phase transition between microemulsion and lamellar liquid crystal. *Langmuir, 13*(7), 2001-2006.

Neethirajan, S., & Jayas, D. S. (2011). Nanotechnology for the food and bioprocessing industries. *Food and Bioprocess Technology, 4*(1), 39-47.

Negi, L. M., Garg, A. K., & Chauhan, M. (2009). Ultradeformable vesicles: concept and execution. *Pharma Times, 41*(9), 11-14.

Neha, B., Ganesh, B., & Preeti, K. (2013). Drug delivery to the brain using polymeric nanoparticles: a review. *International Journal of Pharmaceutical and Life Sciences, 2*(3), 107-132.

Nemmar, A., Hoet, P. H. M., Vanquickenborne, B., Dinsdale, D., Thomeer, M., Hoylaerts, M. F., Vanbilloen, H., Mortelmans, L., & Nemery, B. (2002). Passage of inhaled particles into the blood circulation in humans. *Circulation, 105*(4), 411-414.

Nitschke, M., & Costa, S. (2007). Biosurfactants in food industry. *Trends in Food Science & Technology, 18*(5), 252-259.

Nitta, S. K., & Numata, K. (2013). Biopolymer-based nanoparticles for drug/gene delivery and tissue engineering. *International Journal of Molecular Sciences, 14*(1), 1629-1654.

Norris, D. A., Puri, N., & Sinko, P. J. (1998). The effect of physical barriers and properties on the oral absorption of particulates. *Advanced Drug Delivery Reviews*, *34*(2), 135-154.

Oh, K. H., Baran Jr, J. R., Wade, W. H., & Weerasooriya, V. (1995). Temperature insensitive microemulsion phase behavior with non-ionic surfactants. *Journal of Dispersion Science and Technology*, *16*(2), 165-188.

Omara, A. E., Kam, A., Alqahtania, A., M Li, K., Razmovski-Naumovski, V., Nammi, S., ….. Q Li, G. (2010). Herbal medicines and nutraceuticals for diabetic vascular complications: mechanisms of action and bioactive phytochemicals. *Current Pharmaceutical Design*, *16*(34), 3776-3807.

Oncel, M. Y., Yurttutan, S., Degirmencioglu, H., Uras, N., Altug, N., Erdeve, O., & Dilmen, U. (2012). Intravenous paracetamol treatment in the management of patent ductus arteriosus in extremely low birth weight infants. *Neonatology*, *103*(3), 166-169.

Ostertag, F., Weiss, J., & McClements, D. J. (2012). Low-energy formation of edible nanoemulsions: factors influencing droplet size produced by emulsion phase inversion. *Journal of Colloid and Interface Science*, *388*(1), 95-102.

Paliwal, R., Rai, S., Vaidya, B., Khatri, K., Goyal, A. K., Mishra, N., Mehta, A., & Vyas, S. P. (2009). Effect of lipid core material on characteristics of solid lipid nanoparticles designed for oral lymphatic delivery. *Nanomedicine: Nanotechnology, Biology and Medicine*, *5*(2), 184-191.

Paruta-Tuarez, E., Sadtler, V., Marchal, P., Choplin, L., & Salager, J. L. (2011). Making use of the formulation-composition map to prepare highly concentrated emulsions with particular rheological properties. *Industrial & Engineering Chemistry Research*, *50*(4), 2380-2387.

Peña, A., & Salager, J. L. (2001). Effect of stirring energy upon the dynamic inversion hysteresis of emulsions. *Colloids and Surfaces A: Physicochemical and Engineering Aspects*, *181*(1), 319-323.

Perazzo, A., Preziosi, V., & Guido, S. (2015). Phase inversion emulsification: Current understanding and applications. *Advances in Colloid and Interface Science*, *222*, 581-599.

Philip, S., Keshavarz, T., & Roy, I. (2007). Polyhydroxyalkanoates: Biodegradable polymers with a range of applications. *Journal of Chemical Technology and Biotechnology, 82*(3), 233-247.

Pinto Reis, C., Neufeld, R. J., Ribeiro, A. J., & Veiga, F. (2006). Nanoencapsulation I. Methods for preparation of drug-loaded polymeric nanoparticles. *Nanomedicine: Nanotechnology, Biology and Medicine, 2*(1), 8-21.

Poole Jr, C. P., & Owens, F. J. (2003). *Introduction to nanotechnology*. New Jersey: John Wiley & Sons.

Prabu, P., Chaudhari, A. A., Dharmaraj, N., Khil, M. S., Park, S. Y., & Kim, H. Y. (2009). Preparation, characterization, *in vitro* drug release and cellular uptake of poly (caprolactone) grafted dextran copolymeric nanoparticles loaded with anticancer drug. *Journal of Biomedical Materials Research Part A, 90*(4), 1128-1136.

Prego, C., Fabre, M., Torres, D., & Alonso, M. J. (2006). Efficacy and mechanism of action of chitosan nanocapsules for oral peptide delivery. *Pharmaceutical Research, 23*(3), 549-556.

Qian, C., & McClements, D. J. (2011). Formation of nanoemulsions stabilized by model food-grade emulsifiers using high-pressure homogenization: factors affecting particle size. *Food Hydrocolloids, 25*(5), 1000-1008.

Qian, C., Decker, E. A., Xiao, H., & McClements, D. J. (2012a). Nanoemulsion delivery systems: influence of carrier oil on β-carotene bioaccessibility. *Food Chemistry, 135*(3), 1440-1447.

Qian, C., Decker, E. A., Xiao, H., & McClements, D. J. (2012b). Solid lipid nanoparticles: Effect of carrier oil and emulsifier type on phase behavior and physical stability. *Journal of the American Oil Chemists' Society, 89*(1), 17-28.

Queste, S., Salager, J. L., Strey, R., & Aubry, J. M. (2007). The EACN scale for oil classification revisited thanks to fish diagrams. *Journal of Colloid and Interface Science, 312*(1), 98-107.

Quintanilla-Carvajal, M. X., Camacho-Díaz, B. H., Meraz-Torres, L. S., Chanona-Pérez, J. J., Alamilla-Beltrán, L., Jimenéz-Aparicio, A., & Gutiérrez-López, G. F. (2010). Nanoencapsulation: a new trend in food engineering processing. *Food Engineering Reviews, 2*(1), 39-50.

Rai, R., Keshavarz, T., Roether, J. A., Boccaccini, A. R., & Roy, I. (2011). Medium chain length polyhydroxyalkanoates, promising new biomedical materials for the future. *Materials Science and Engineering: R: Reports*, *72*(3), 29-47.

Rao, J., & McClements, D. J. (2012). Impact of lemon oil composition on formation and stability of model food and beverage emulsions. *Food chemistry, 134*(2), 749-757.

Rastogi, R., Anand, S., & Koul, V. (2009). Flexible polymerosomes—An alternative vehicle for topical delivery. *Colloids and Surfaces B: Biointerfaces*, *72*(1), 161-166.

Razaif, M. R. M., Anis, S. N. S., Harun, H. I., Rashid, K. A., & Annuar, M. S. M. (2016). Unusual poly (3-hydroxyalkanoate)(PHA) biosynthesis behavior of *Pseudomonas putida* Bet001 and *Delftia tsuruhatensis* Bet002 isolated from palm oil mill effluent. *Biotechnology and Applied Biochemistry*, *64*(2), 259-269.

Regev, O., Backov, R., & Faure, C. (2004). Gold nanoparticles spontaneously generated in onion-type multilamellar vesicles. Bilayers-particle coupling imaged by cryo-TEM. *Chemistry of Materials, 16*(25), 5280-5285.

Reis, C. P., Neufeld, R. J., Ribeiro, A. J., & Veiga, F. (2006). Nanoencapsulation I. Methods for preparation of drug-loadedpolymeric nanoparticles. *Nanomedicine: Nanotechnology, Biology and Medicine*, *2*(1), 8-21.

Roger, K. (2016). Nanoemulsification in the vicinity of phase inversion: Disruption of bicontinuous structures in oil/surfactant/water systems. *Current Opinion in Colloid & Interface Science*, *25*, 120-128.

Rondon-Gonzalez, M., Madariaga, L. F., Sadtler, V., Choplin, L., Marquez, L., & Salager, J. L. (2007). Emulsion catastrophic inversion from abnormal to normal morphology. 6. Effect of the phase viscosity on the inversion produced by continuous stirring. *Industrial & Engineering Chemistry Research*, *46*(11), 3595-3601.

Rondón-González, M., Madariaga, L. F., Sadtler, V., Choplin, L., & Salager, J. L. (2009). Emulsion catastrophic inversion from abnormal to normal morphology. 8. Effect of formulation on the inversion produced by continuous stirring. *Industrial & Engineering Chemistry Research*, *48*(6), 2913-2919.

Rondón-Gonzaléz, M., Sadtler, V., Choplin, L., & Salager, J. L. (2006). Emulsion catastrophic inversion from abnormal to normal morphology. 5. Effect of the water-to-oil ratio and surfactant concentration on the inversion produced by continuous stirring. *Industrial & Engineering Chemistry Research*, *45*(9), 3074-3080.

Rondon-Gonzalez, M., Sadtler, V., Marchal, P., Choplin, L., & Salager, J. L. (2008). Emulsion catastrophic inversion from abnormal to normal morphology. 7. Emulsion evolution produced by continuous stirring to generate a very high internal phase ratio emulsion. *Industrial & Engineering Chemistry Research*, *47*(7), 2314-2319.

Ruan, G., & Feng, S. S. (2003). Preparation and characterization of poly (lactic acid)–poly (ethylene glycol)–poly (lactic acid)(PLA–PEG–PLA) microspheres for controlled release of paclitaxel. *Biomaterials, 24*(27), 5037-5044.

Russell-Jones, G. J., Veitch, H., & Arthur, L. (1999). Lectin-mediated transport of nanoparticles across Caco-2 and OK cells. *International Journal of Pharmaceutics, 190*(2), 165-174.

Saberi, A. H., Fang, Y., & McClements, D. J. (2013). Fabrication of vitamin E-enriched nanoemulsions: factors affecting particle size using spontaneous emulsification. *Journal of Colloid and Interface Science*, *391*, 95-102.

Sagalowicz, L., & Leser, M. E. (2010). Delivery systems for liquid food products. *Current Opinion in Colloid & Interface Science, 15*(1), 61-72.

Sahay, G., Alakhova, D. Y., & Kabanov, A. V. (2010). Endocytosis of nanomedicines. *Journal of Controlled Release, 145*(3), 182-195.

Sahin, N. O. (2007). Niosomes as nanocarrier systems. In M.R. Mozafari (Ed), *Nanomaterials and nanosystems for biomedical applications* (pp. 67-81). Netherland: Springer.

Sahni, J. K., Doggui, S., Ali, J., Baboota, S., Dao, L., & Ramassamy, C. (2011). Neurotherapeutic applications of nanoparticles in Alzheimer's disease. *Journal of Controlled Release*, *152*(2), 208-231.

Sajjadi, S., Jahanzad, F., & Yianneskis, M. (2004). Catastrophic phase inversion of abnormal emulsions in the vicinity of the locus of transitional inversion. *Colloids and Surfaces A: Physicochemical and Engineering Aspects*, *240*(1), 149-155.

Salager, J. L. (1996). Quantifying the concept of physico-chemical formulation in surfactant-oil-water systems—state of the art. In C. Solans, M.R. Infante & M.J. Garcia-Celma (Eds), *Trends in Colloid and Interface Science X* (pp. 137-142). Dresden: Steinkopff.

Salager, J. L. (2000). Emulsion properties and related know-how to attain them. *Pharmaceutical Emulsions and Suspensions*, *105*, 73-125.

Salager, J. L., Forgiarini, A., Marquez, L., Pena, A., Pizzino, A., Rodriguez, M. P., & Rondon-Gonzalez, M. (2004). Using emulsion inversion in industrial processes. *Advances in Colloid and Interface Science*, *108*, 259-272.

Salager, J. L., Loaiza-Maldonado, I., Minana-Perez, M., & Silva, F. (1982). Surfactant-oil-water systems near the affinity inversion part I: relationship between equilibrium phase behavior and emulsion type and stability. *Journal of Dispersion Science and Technology*, *3*(3), 279-292.

Salager, J. L., Marquez, N., Graciaa, A., & Lachaise, J. (2000). Partitioning of ethoxylated octylphenol surfactants in microemulsion-oil-water systems: influence of temperature and relation between partitioning coefficient and physicochemical formulation. *Langmuir*, *16*(13), 5534-5539.

Salager, J. L., Minana-Perez, M., Perez-Sanchez, M., Ramfrez-Gouveia, M., & Rojas, C. I. (1983). Surfactant-oil-water systems near the affinity inversion part III: the two kinds of emulsion inversion. *Journal of Dispersion Science and Technology*, *4*(3), 313-329.

Salminen, H., Helgason, T., Kristinsson, B., Kristbergsson, K., & Weiss, J. (2013). Formation of solid shell nanoparticles with liquid ω-3 fatty acid core. *Food Chemistry*, *141*(3), 2934-2943.

Salvia-Trujillo, L., Qian, C., Martín-Belloso, O., & McClements, D. J. (2013). Influence of particle size on lipid digestion and *β*-carotene bioaccessibility in emulsions and nanoemulsions. *Food Chemistry*, *141*(2), 1472-1480.

Sapei, L., Naqvi, M. A., & Rousseau, D. (2012). Stability and release properties of double emulsions for food applications. *Food Hydrocolloids*, *27*(2), 316-323.

Sasidharan, S., Chen, Y., Saravanan, D., Sundram, K. M., & Latha, L. Y. (2011). Extraction, isolation and characterization of bioactive compounds from plants' extracts. *African Journal of Traditional, Complementary and Alternative Medicines*, *8*(1), 1-10.

Sato, K. (2001). Crystallization behaviour of fats and lipids—a review. *Chemical Engineering Science, 56*(7), 2255-2265.

Sheng, Y., Liu, C., Yuan, Y., Tao, X., Yang, F., Shan, X., ….. Xu, F. (2009). Long-circulating polymeric nanoparticles bearing a combinatorial coating of PEG and water-soluble chitosan. *Biomaterials, 30*(12), 2340-2348.

Sherman, P., & Parkinson, C. (1978). Mechanism of temperature induced phase inversion in O/W emulsions stabilised by O/W and W/O emulsifier blends. In A. Weiss (Ed.), *Emulsions* (pp. 10-14). Dresden: Steinkopff.

Shinoda, K., & Saito, H. (1968). The effect of temperature on the phase equilibria and the types of dispersions of the ternary system composed of water, cyclohexane, and nonionic surfactant. *Journal of Colloid and Interface Science*, *26*(1), 70-74.

Siekmann, B., & Westesen, K. (1994). Thermoanalysis of the recrystallization process of melt-homogenized glyceride nanoparticles. *Colloids and Surfaces B: Biointerfaces, 3*(3), 159-175.

Silva, F., Pena, A., Miñana-Pérez, M., & Salager, J. L. (1998). Dynamic inversion hysteresis of emulsions containing anionic surfactants. *Colloids and Surfaces A: Physicochemical and Engineering Aspects*, *132*(2), 221-227.

Silva, W. K., Chicoma, D. L., & Giudici, R. (2011). In-situ real-time monitoring of particle size, polymer, and monomer contents in emulsion polymerization of methyl methacrylate by near infrared spectroscopy. *Polymer Engineering & Science*, *51*(10), 2024-2034.

Simirgiotis, M. J., Schmeda-Hirschmann, G., Bórquez, J., & Kennelly, E. J. (2013). The Passiflora tripartita (Banana Passion) Fruit: A Source of bioactive flavonoid C-glycosides isolated by HSCCC and characterized by HPLC–DAD–ESI/MS/MS. *Molecules*, *18*(2), 1672-1692.

Solaiman, D.K., Ashby, R.D., Hotchkiss Jr, A.T., & Foglia, T.A. (2006). Biosynthesis of medium-chain-length poly (hydroxyalkanoates) from soy molasses. *Biotechnology Letters, 28*(3), 157-162.

Solans, C., Esquena, J., Forgiarini, A. M., Uson, N., Morales, D., Izquierdo, P., Azemar, N., & Garcia-Celma, M. J. (2003). Nano-emulsions: formation, properties, and applications. *Surfactant Science Series, 109*, 525-554.

Solans, C., Izquierdo, P., Nolla, J., Azemar, N., & Garcia-Celma, M. J. (2005). Nano-emulsions. *Current Opinion in Colloid & Interface Science*, *10*(3), 102-110.

Solans, C., & Kunieda, H. (1996). *Industrial applications of microemulsions*. Boca Raton: CRC Press.

Solans, C., & Solé, I. (2012). Nano-emulsions: formation by low-energy methods. *Current Opinion in Colloid & Interface Science*, *17*(5), 246-254.

Soppimath, K. S., Aminabhavi, T. M., Kulkarni, A. R., & Rudzinski, W. E. (2001). Biodegradable polymeric nanoparticles as drug delivery devices. *Journal of Controlled Release*, *70*(1), 1-20.

Sorgi, F. L., & Huang, L. (1996). Large scale production of DC-Chol cationic liposomes by microfluidization. *International Journal of Pharmaceutics*, *144*(2), 131-139.

Sothornvit, R., Rhim, J. W., & Hong, S. I. (2009). Effect of nano-clay type on the physical and antimicrobial properties of whey protein isolate/clay composite films. *Journal of Food Engineering*, *91*(3), 468-473.

Speranza, A., Corradini, M. G., Hartman, T. G., Ribnicky, D., Oren, A., & Rogers, M. A. (2013). Influence of Emulsifier Structure on Lipid Bioaccessibility in Oil–Water Nanoemulsions. *Journal of Agricultural and Food Chemistry*, *61*(26), 6505-6515.

Srinivas, G., Discher, D. E., & Klein, M. L. (2004). Self-assembly and properties of diblock copolymers by coarse-grain molecular dynamics. *Nature Materials*, *3*(9), 638-644.

Stan, S. D., Kar, S., Stoner, G. D., & Singh, S. V. (2008). Bioactive food components and cancer risk reduction. *Journal of Cellular Biochemistry*, *104*(1), 339-356.

Strey, R. (1996). Phase behavior and interfacial curvature in water-oil-surfactant systems. *Current Opinion in Colloid & Interface Science*, *1*(3), 402-410.

Su, J., Flanagan, J., Hemar, Y., & Singh, H. (2006). Synergistic effects of polyglycerol ester of polyricinoleic acid and sodium caseinate on the stabilisation of water–oil–water emulsions. *Food Hydrocolloids*, *20*(2), 261-268.

Su, J., Yang, Q., Teo, J. F., & Chung, T. S. (2010). Cellulose acetate nanofiltration hollow fiber membranes for forward osmosis processes. *Journal of Membrane Science*, *355*(1), 36-44.

Sudesh, K., Abe, H., & Doi, Y. (2000). Synthesis, structure and properties of polyhydroxyalkanoates: Biological polyesters. *Progress in Polymer Science*, *25*(10), 1503-1555.

Sundar, S., Kundu, J., & Kundu, S. C. (2016). Biopolymeric nanoparticles. *Science and Technology of Advanced Materials*, *11*(1), 1-13.

Szentkuti, L. (1997). Light microscopical observations on luminally administered dyes, dextrans, nanospheres and microspheres in the pre-epithelial mucus gel layer of the rat distal colon. *Journal of Controlled Release*, *46*(3), 233-242.

Tamjidi, F., Shahedi, M., Varshosaz, J., & Nasirpour, A. (2013). Nanostructured lipid carriers (NLC), A potential delivery system for bioactive food molecules. *Innovative Food Science & Emerging Technologies*, *19*, 29-43.

Tan, I., Kumar, K.S., Theanmalar, M., Gan, S., & Gordon Iii, B. (1997). Saponified palm kernel oil and its major free fatty acids as carbon substrates for the production of polyhydroxyalkanoates in *Pseudomonas putida* pga1. *Applied Microbiology and Biotechnology*, *47*(3), 207-211.

Thakur, R. K., Villette, C., Aubry, J. M., & Delaplace, G. (2007). Formulation–composition map of a lecithin-based emulsion. *Colloids and Surfaces A: Physicochemical and Engineering Aspects*, *310*(1), 55-61.

Todoroff, J., & Vanbever, R. (2011). Fate of nanomedicines in the lungs. *Current Opinion in Colloid & Interface Science*, *16*(3), 246-254.

Tyrode, E., Allouche, J., Choplin, L., & Salager, J. L. (2005). Emulsion catastrophic inversion from abnormal to normal morphology. 4. Following the emulsion viscosity during three inversion protocols and extending the critical dispersed-phase concept. *Industrial & Engineering Chemistry Research*, *44*(1), 67-74.

Tyrode, E., Mira, I., Zambrano, N., Márquez, L., Rondón-Gonzalez, M., & Salager, J. L. (2003). Emulsion catastrophic inversion from abnormal to normal morphology. 3. Conditions for triggering the dynamic inversion and application to industrial processes. *Industrial & Engineering Chemistry Research*, *42*(19), 4311-4318.

Uchegbu, I. F., & Vyas, S. P. (1998). Non-ionic surfactant based vesicles (niosomes) in drug delivery. *International Journal of Pharmaceutics, 172*(1), 33-70.

Udenigwe, C. C., & Aluko, R. E. (2012). Food Protein-Derived Bioactive Peptides: Production, Processing, and Potential Health Benefits. *Journal of Food Science, 77*(1), 11-24.

Vauthier, C., & Bouchemal, K. (2009). Methods for the preparation and manufacture of polymeric nanoparticles. *Pharmaceutical Research, 26*(5), 1025-1058.

Vieira, R. A., Sayer, C., Lima, E. L., & Pinto, J. C. (2002). In-line and in situ monitoring of semi-batch emulsion copolymerizations using near-infrared spectroscopy. *Journal of Applied Polymer Science, 84*(14), 2670-2682.

Wang, Z., Itoh, Y., Hosaka, Y., Kobayashi, I., Nakano, Y., Maeda, I., Yag, K. (2003). Novel transdermal drug delivery system with polyhydroxyalkanoate and starburst polyamidoamine dendrimer. *Journal of Bioscience and Bioengineering, 95*(5), 541-543.

Weiss, J., Decker, E. A., McClements, D. J., Kristbergsson, K., Helgason, T., & Awad, T. (2008). Solid lipid nanoparticles as delivery systems for bioactive food components. *Food Biophysics, 3*(2), 146-154.

Westesen, K., & Bunjes, H. (1995). Do nanoparticles prepared from lipids solid at room temperature always possess a solid lipid matrix? *International Journal of Pharmaceutics, 115*(1), 129-131.

Westesen, K., Siekmann, B., & Koch, M. H. J. (1993). Investigations on the physical state of lipid nanoparticles by synchrotron radiation X-ray diffraction. *International Journal of Pharmaceutics, 93*(1), 189-199.

Wissing, S. A., Müller, R. H., Manthei, L., & Mayer, C. (2004). Structural characterization of Q10-loaded solid lipid nanoparticles by NMR spectroscopy. *Pharmaceutical Research, 21*(3), 400-405.

Xia, S., & Xu, S. (2005). Ferrous sulfate liposomes: preparation, stability and application in fluid milk. *Food Research International, 38*(3), 289-296.

Xu, J., Zhao, W., Ning, Y., Bashari, M., Wu, F., Chen, H., ….. Zhang, L. (2013). Improved stability and controlled release of ω3/ω6 polyunsaturated fatty acids by spring dextrin encapsulation. *Carbohydrate Polymers, 92*(2), 1633-1640.

Xue, L., & Greisler, H.P. (2003). Biomaterials in the development and future of vascular grafts. *Journal of Vascular Surgery, 37*(2), 472-480.

Yamamoto, A., Katsumi, H., Kusamori, K., & Sakane, T. (2013). Improvement of intestinal absorption of poorly absorbable drugs by various sugar esters., *Yakugaku zasshi: Journal of the Pharmaceutical Society of Japan, 134*(1), 47-53.

Yang, Y., & McClements, D. J. (2013). Vitamin E bioaccessibility: Influence of carrier oil type on digestion and release of emulsified α-tocopherol acetate. *Food Chemistry, 141*(1), 473-481.

Yang, Y., Marshall-Breton, C., Leser, M. E., Sher, A. A., & McClements, D. J. (2012). Fabrication of ultrafine edible emulsions: comparison of high-energy and low-energy homogenization methods. *Food Hydrocolloids, 29*(2), 398-406.

Yao, M., McClements, D. J., & Xiao, H. (2015). Improving oral bioavailability of nutraceuticals by engineered nanoparticle-based delivery systems. *Current Opinion in Food Science, 2*, 14-19.

Yao, M., Xiao, H., & McClements, D. J. (2014). Delivery of lipophilic bioactives: assembly, disassembly, and reassembly of lipid nanoparticles. *Annual Review of Food Science and Technology, 5*, 53-81.

Yu, C. Y., Yin, B. C., Zhang, W., Cheng, S. X., Zhang, X. Z., & Zhuo, R. X. (2009). Composite microparticle drug delivery systems based on chitosan, alginate and pectin with improved pH-sensitive drug release property. *Colloids and Surfaces B: Biointerfaces, 68*(2), 245-249.

Zambrano, N., Tyrode, E., Mira, I., Márquez, L., Rodríguez, M. P., & Salager, J. L. (2003). Emulsion catastrophic inversion from abnormal to normal morphology. 1. Effect of the water-to-oil ratio rate of change on the dynamic inversion frontier. *Industrial & Engineering Chemistry Research, 42*(1), 50-56.

Zhang, L., Gu, F. X., Chan, J. M., Wang, A. Z., Langer, R. S., & Farokhzad, O. C. (2008). Nanoparticles in medicine: therapeutic applications and developments. *Clinical Pharmacology and Therapeutics, 83*(5), 761-769.

Zhang, R., & Somasundaran, P. (2006). Advances in adsorption of surfactants and their mixtures at solid/solution interfaces. *Advances in Colloid and Interface Science*, *123*, 213-229.

Zhao, Y., Mahajan, N., Lu, R., & Fang, J. (2005). Liquid-crystal imaging of molecular-tilt ordering in self-assembled lipid tubules. *Proceedings of the National Academy of Sciences of the United States of America*, *102*(21), 7438-7442.

Zou, L.Q., Peng, S.F., Liu, W., Gan, L., Liu, W.L., Liang, R.H., ….. Chen, X., (2014). Improved in vitro digestion stability of (−)-epigallocatechin gallate through nanoliposome encapsulation. *Food Research International*, *64*, 492-499.

LIST OF PUBLICATIONS AND PAPERS PRESENTED

PUBLICATIONS

Ishak, K.A., Annuar, M.S.M., & Ahmad, N. (2017). Chapter 9: Nano-delivery systems for nutraceutical application In: Nanotechnology Applications. In A. Grumezescu & A. E. Oprea (Eds), *Food: Flavor, Stability, Nutrition, and Safety (1st Edition)* (pp. 179-202). Academic Press, Elsevier

Ishak, K.A., Annuar, M.S.M., & Ahmad, N. (2017). Optimization of Water/Oil/Surfactants System For Preparation of Medium-Chain-Length Poly-3-hydroxyalkanoates (mcl-PHA)-incorporated Nanoparticles via Nanoemulsion Templating Technique. *Applied Biochemistry and Biotechnology*, (10.1007/s12010-017-2492-6)

Ishak, K. A., & Annuar, M. S. M. (2017). Facile formation of medium-chain-length poly-3-hydroxyalkanoates (mcl-PHA)-incorporated nanoparticle using combination of non-ionic surfactants. *Journal of Surfactants and Detergents*, *20*(2): 341-353

Ishak, K. A., & Annuar, M. S. M. (2016). Phase inversion of medium-chain-length poly-3-hydroxyalkanoates (mcl-PHA)-incorporated nanoemulsion: effects of mcl-PHA molecular weight and amount on its mechanism. *Colloid and Polymer Science*, *294*(12): 1969-1981

Ishak, K.A., & Annuar, M.S.M. (2017). Temperature-Induced Three-Phase Equilibrium of Medium-Chain-Length Poly-3-hydroxyalkanoates (mcl-PHA)-Incorporated Emulsion System for Production of Polymeric Nanoparticle. *Journal of Dispersion Science and Technology*, (dx.doi.org/10.1080/01932691.2017.1320563)

PRESENTATIONS

Preparation of medium-chain-length poly-3-hydroxyalkanoates-based polymeric nanoparticle through phase inversion emulsification and its apparent formation mechanism.

Ishak, K.A.,[1] & Annuar, M.S.M.[1]

[1]Institute of Biological Sciences, Faculty of Science, University of Malaya, 50603, Kuala Lumpur.

1) Poster presentation at 17th International Biotechnology Symposium and Exhibition (IBS 2016) - Appendix A

2) Oral presentation at 7th Asian Conference of Colloid and Interface Science (ACCIS 2017) - Appendix B